AUTISM SPECTRUM DISORDERS: ENVIRONMENTAL AND GENETIC RISK

FACTORS ALTER CORTICAL NEUROGENESIS

by

ROBERT JAMES CONNACHER, BS

A dissertation submitted to the

School of Graduate Studies

Rutgers, The State University of New Jersey

For the degree of

Doctor of Philosophy

Graduate Program in Neuroscience

Written under the direction of

Emanuel DiCicco-Bloom,

And approved by

_____

_____

_____

_____

_____

New Brunswick, New Jersey

October, 2017

ABSTRACT OF THE DISSERTATION

AUTISM SPECTRUM DISORDERS: ENVIRONMENTAL AND GENETIC RISK FACTORS ALTER CORTICAL NEUROGENESIS

by ROBERT JAMES CONNACHER, BS

Dissertation Director:

Emanuel DiCicco-Bloom

Cortical Neurogenesis is a highly regulated process which requires neural precursor population expansion followed by migration and subsequent differentiation. Early cortical overgrowth has been observed in individuals with autism spectrum disorder (ASD) and may underpin observed cases of macrocephaly seen within ASD subgroups. To define mechanisms by which this process could be altered, studies have identified environmental and genetic ASD risk factors, including Valproic acid (VPA) and the copy number variant 16p11.2 (16P), respectively.

Valproic acid is a neurotheraputic medicine intended to treat epilepsy, migraines, and bipolar disorder but poses ASD risk to prenatally exposed fetuses when mothers are taking this drug. Prenatal VPA exposure in rodents studies have replicated behavioral and cellular deficits seen in ASD, including alterations in neurogenesis, but convergence of mechanisms remain undefined. Studies suggest VPA may impact development through Histone Deacetylase (HDAC) inhibition, though this enzymatic inhibition has not been directly confirmed in

primary neural cells. The function of HDACs is to epigenetically regulate acetylation sites which can change gene expression. Therefore, I characterized HDAC message and protein in the developing rodent brain, and confirmed that VPA can enzymatically inhibit these proteins. Previously, we found that VPA exposure promotes G1 to S phase transition through rapid increases of G1 cyclins and acetylated Histone H3, suggesting epigenetic regulation of this process. Therefore, I measured mRNA of G1 cyclins after acute VPA exposure, and found upregulation in transcription of these genes, supporting the notion that post-translational modifications of histones may promote proliferation through G1-S phase transition. Additionally, our prior studies found that the increased proliferation resulted in a bigger brain by P21 with more upper layer neurons. Others have also indicated prenatal VPA exposure promotes neurogenesis of upper layer neurons. Therefore with these findings, I characterized the percentage of Pax6 and Tbr2 progenitor cells in S phase, to determine specificity of VPA effect. Interestingly, only the Tbr2 population had more cells in S phase, providing explanation for increased upper layer neurons at P21.

Altered neurogenesis is also observed in the copy number variant 16p11.2, a genetic risk factor for ASD. In the 16p11.2 chromosomal deletion, one copy of 27 genes is missing, including MAPK3, which encodes ERK1. This gene is a central component in the ERK signaling pathway, which is important for regulating cellular growth and proliferation. Therefore, I investigated proliferative changes and signaling alterations in Neural Precursor Cells (NPCs) derived from control and 16p11.2 patients iPSCs. I found that 16p11.2 NPCs had increased

DNA synthesis under control media but exhibited reduced responses to mitogenic stimulation with FGF, a developmental extracellular factor known to activate the ERK pathway. Further characterization of this pathway under control conditions revealed equivalent if not elevated phosphorylation of ERK1, but approximately 50% less Total ERK1. Additionally, as may be predicted, there were elevations in cyclin D1 and P-S6, suggesting mechanisms by which DNA synthesis is increased in these cells. In aggregate, these studies identify cortical neurogenesis as a common target of risk factors that contribute to neuropsychiatric diseases.

Acknowledgements

I wish to express my eternal thanks and gratitude to my advisor Dr Manny DiCicco-Bloom for his patience, support, guidance, and instruction during my graduate career. It certainly has been a long road, and I greatly appreciate everything he has provided so that I can reach this milestone in my life.

Within the Dicicco-Bloom lab I must underscore my appreciation for Xiaofeng Zhou. Her limitless technical skills, patience, and friendship helped me continue to move forward and always feel at home within the lab. My deepest thanks also extend to Smrithi Prem. Words cannot fully express my gratitude for her assistance, encouragement, and unwavering belief in my abilities; I do not know where I would be without her. Furthermore, I wish to thank Smrithi for her collaborative assistance, help, and friendship as she truly is the best person ever. I would also like to extend my sincere appreciation to Madeline Williams, as her collaboration and friendship have been integral to both my project and sanity. Madeline not only generously shared her unaffected control proliferation data but also played a big role in improving my management of data and assisted me with learning additional NPC culture techniques.   Additionally, I wish to thank Dr Madel Durens for countless years of advice, encouragement, support, and friendship. It has been a pleasure to work alongside these exemplar individuals over the years.

At this time I would also like to express my heartfelt thanks to all previous members of the DiCicco-Bloom lab, including but not limited to Drs Genestine-Schmitt, Lunden, Lee, Obiorah, Tascau, and Yan. I am incredibly fortunate to

have known them, and appreciated their countless help, advice, support, and friendship over various stages of my graduate career.

I also wish to thank my committee members Dr Cheryl Dreyfus, Dr Gabriela D'Arcangelo, Dr Mladen-Roko Rasin, and Dr Arnold Rabson, whom have given me numerous suggestions, guidance, and advice. Their help has proved invaluable in my development. Additionally, I wish to express my appreciation for all faculty in the Neuroscience department, which in sum has served as a second family to me. I would also like to highlight my tremendous gratitude for Joan Mordes, Betty Wheeler and Zamina Deen, for all of their guidance and assistance in paperwork, emails and reminders.

Finally, I would like to express my highest gratitude to all other friends, mentors and family. It means so much that everyone has always encouraged and cheered me on. Knowing you all had my back has helped me push through the difficult times and kept me focused on my dreams.

Table of Contents

List of Figures

Chapter 1: Introduction

1.1) Autism Spectrum Disorder

<u>A) Clinical description and prevalence</u>

The Diagnostic and Statistical Manual of Mental Disorders, Fifth Edition (DSM-5) specifies Autism Spectrum Disorders (ASD) as anyone exhibiting the 2 core issues: 1) persistent deficits in social communication and interactions as well as 2) restricted, repetitive behaviors, interests or activities (5). This is in contrast to the DSM-IV which looks for deficits in 3 core symptoms: social interactions, language/communication, and repetitive behaviors/interests (6). Additionally, the DSM-IV specified ASD as Aspergers syndrome, autism and pervasive developmental disorder-not otherwise specified (PDD-NOS) (6). However, the DSM-V now utilizes severity ratings of diagnosis, and can include specifiers to show if patients have medical or genetic co-morbidities(5). The characteristics of these disorders include deficits in social interaction, communication and repetitive behaviors/interests (7).

There is a significant prevalence of ASD, which has been steadily increasing over recent years. According to reports from the CDC, the prevalence of ASD was 1 in 150 in 2000, which increased to 1 in 110 by 2006. Most recent reports indicate 1 in 68 individuals are diagnosed with ASD (CDC 2012) (8) . Although a proportion of this increase is due to increased awareness of ASD and broader diagnosis criterion, it remains unclear how many of these increased cases are due to a true increase in ASD. This is known to be a developmental

disorder, often diagnosed between 2 and 5 years of age. Recent studies have also been able to detect a possible early symptom of ASD in 1 year olds exhibiting motor delay (9). Additionally, within the first 6 months of life, infants with ASD may have a mean decline in eye fixation compared to control (10). Others identified children with lower motor and visual reception scores at 6 months are predictive to develop ASD by 2 years old, while more severe problems were associated with ASD diagnoses as early as one year (11).

B) Genetics of autism

Genetic studies focusing on concordance of monozygotic twins for ASD found 77% concordance for males, and 50% for females (22). The concordance for dizygotic twins is lower with 31% for males and 36% for females (22). These studies show there is a genetic component to developing autism, with females typically being less likely to develop ASD. Autism is also more prevalent in males exhibiting a 4:1 ratio to females (14). This predisposition for males to be affected is also seen through genetic recurrence studies. Boys have a 47% +/- 9.5% increased risk for ASD if they have two or more affected siblings, while girls have 19.8% $\pm$ 6% recurrence risk (14). Additionally, there is a 10% genetic recurrence risk for autism, meaning that a family having one autistic individual has an elevated chance in another child also being diagnosed (11).

Additionally, alterations to chromosomes and genes have been associated with increased risk for ASD. One association of genetics increasing risk for autism is alterations in the 15q11.2-q13 chromosomal region typically through deletions, and altered imprinting from parents genes (12). This chromosomal

region is responsible for Angelmans and Prader Willi syndromes, with duplications often causing increased risk for ASD (12). Angelmans syndrome involves a defect in the maternally inherited ubiquitin E3 gene, UBE3A (13). However Prader Willi syndrome occurs due to paternal chromosomal deletions and imprinting errors which results in altered gene expression (12). Genetic causes of ASD are classified into copy number variants (CNV), and rare single base pair mutation events called single nucleotide polymorphisms (snps) (14). The degree all these genetic factors contribute to causing autism can vary, but they illustrate how genetics play a role in the etiology of autism. Recent studies have identified over 800 different genes that can contribute to developing ASD (14). This becomes problematic as some ASD risk factor genes also contribute to schizophrenia and bipolar disorder (15), therefore, it is hard to understand implications. There are several cases where a single gene mutation can cause autism, including FMR1 (Fragile x), Mecp2 (Rett syndrome), and TSC1 and/or TSC2 (tuberous sclerosis) (14). The penetrance of many monogenic causes such as FMR1, TSC1, and TSC2 is often lower than 50% (16). Approximately 21-50% of Males with Fragile x and up to 60% of patents with Tuberous sclerosis have ASD (17). Mechanisms can be complex, for example Rett syndrome is a genetic disorder causing mutations in the MECP2 gene, which regulates gene expression at methylation sites (14). MECP2 mutation appears to have very high penetrance, but it is highly rare and primarily affects females, making up about 0.5% of ASD cases (16). In addition to monogenetic cases which contribute to approximately 5% of ASD cases (18), copy number variants also play roles in

autism, and involve altering dosage of multiple genes within regions of a chromosome. CNVs overall are observed in 5-10% of ASD individuals screened (19). One such copy number variant is at chromosome 16p11.2 locus, with high penetrance and makes up approximately 1% of all ASD cases (16, 20, 21).

C) Environmental factors contributing to ASD risk

Environmental factors can elicit teratogenic and epigenetic changes during neurogenesis, giving rise to cognitive and behavioral deficits. Maternal ingestion of thalidomide, a drug intended to treat morning sickness was shown to correlate with 4/15 exposed children to develop ASD (23). This prenatal exposure acts as a teratogen on the developing fetus and brought the toxicology community to focus on several compounds that act as teratogens during development in search of possible etiology for neurodevelopmental disorders such as autism. Teratogens are defined as substances that can cause defects during embryological development. This includes studies on heavy metals such as lead and mercury, chemicals including DDT, and BPA, as well as antiepileptic medications (24). Studies have investigated the correlation of environmental factors to developing autism, with concept of three main windows of vulnerability to the developing brain. These windows of neurodevelopmental vulnerability include early and late pregnancy, as well as early postnatal life, where alterations in signaling and neural connections could be severely disrupted (25). Prenatal exposure to Valproic acid (VPA), has shown similar malformations to that of thalidomide exposure, and the children can develop autism (26). Other environmental exposures during pregnancy can come from maternal immune

activation (MIA) as a result of viral infection in mothers, causing increased frequency of ASD in children (27). However, the contribution other environmental factors play in autism risk remain more controversial, often due to confounding variables, thus requiring additional study. When controlling for confounding variables, investigations into studies of lead, mercury, air pollution, or BPAs often resulted in unclear elevation in ASD risk due to variable results among studies (25).

Arguably, the two most compelling pieces of evidence suggesting environmental exposures play roles in developing ASD are twin studies and the discovery of ASD associated disorders which have epigenetic mechanisms. The first piece of evidence is based on the fact that ASD does not arise equally in twins (14). ASD is believed to be a neurodevelopmental disorder, and it has been argued that a fetus developing this disorder can be due to a combination of genes and environment (28). The environment which fetal development occurs is the maternal womb. Because genetically identical fetuses do not always develop the same disorder, there must be differential environmental exposures for each developing brain, causing alterations in gene expression, and neurodevelopmental outcome. Studies investigating monozygotic twins and their methylation sites associated with ASD identified that each twins expressed differential methylation and there was a correlation in autistic traits with this methylation (28). This suggests that genes and environment can both contribute to ASD. Sometimes developmental disorders require insults from genetic mutations and environmental exposures in order to arise (28). This combination

of gene heritability and specific vulnerability to environmental exposures has been suggested to explain why environmental studies often produce inconsistent findings (28). The second piece of evidence, is that several syndromes with elevated ASD have epigenetic mechanisms. For example, Rett syndrome is supportive because it is caused by mutations in the MECP2 gene, which functions as a regulator of gene expression at methylated sites. As described in later paragraphs, epigenetic regulation involves temporary post translational modifications, which can include methylation of DNA. Because autism can occur due to dysregulation of genes which regulate epigenetic sites of DNA, it follows that anything which alters epigenetic signaling, or its regulation could contribute to ASD. Of interest, prenatal exposure to VPA has been established as an ASD risk factor (29). Further, this drug has been proposed to be a Histone deacetylase (HDAC) inhibitor, a class of proteins important in regulating epigenetic modifications on proteins and histones, altering gene expression (30). Therefore, understanding how this ASD risk factor drug regulates epigenetic modifications could further our understanding how environmental factors can give rise to ASD.

D) ASD Neuropathology

In addition to behavior, subsets of ASD individuals exhibit alterations in brain volume. This has been detected by several studies, with observed enlarged head circumference and/or brain volume, especially at young ages (31). Among those diagnosed with autism, 15-20% exhibit macrocephaly and enlarged brain regions defined by head circumference and MRI studies, respectively (32-

34). One region of particular interest is the cerebral cortex, which is enlarged during early development based on MRI and neuropathology studies (33, 35-37). In ASD, enlargement of cortical grey (38) and white matter (38, 39) has been observed. It has been suggested that enlargement of processes from projection neurons could contribute to this phenotype (40). Indeed, many risk factor genes for ASD play roles in regulation of cortical projection neurons, as well as synapse development and function (41). These increases in grey and white matter can be seen at 2.5 years old (38). Measurements detecting increases in head size and brain growth have also specifically been seen in 15% of boys with ASD, and these phenotypes could still be detected by 5 years old using head circumference and MRI measures (34). Abnormally enlarged brain volume between the first and second year of development has become a risk factor for ASD (36). Interestingly, recent studies may suggest that rapid early expansion of the cortex between 6 and 12 months old can be an earlier predictor of ASD (36). By 6 months, cerebellar and callosal white matter phenotypes have shown to be predictive of later sensory abnormalities and repetitive behaviors seen in autism (42).

Others have also identified phenotypes of minicolumnopathy and suggested these increases may explain increases in brain size as well as alterations in grey and white matter (43). Alterations in brain size can be attributed to changes in size of the soma, through alterations in processes, as well as overall changes in density of tissue. Postmortem ASD brains have shown reductions in the soma of neurons in multiple brain regions, with the most

severe region being the nucleus accumbens (44). Additional postmortem

analyses from 7 ASD brains reported a 67% increases in cortical cell number in

the PFC, indicative of this brain overgrowth (45) although this finding has not

been replicated by others. Additional postmortem ASD brains indicated

reductions in neuronal number compared to control (46). Additional growth

abnormalities in ASD include cortical dysplasia, and heterotopia (47). Another

region with growth phenotypes is the cerebellum, with changes in both size and

alterations in Purkinje cell number. Several postmortem studies found reduced

density and number of Purkinje cells, while different MRI studies of living ASD

brains suggest that the size of an ASD cerebellum is enlarged compared to

control brains, and this increase is proportional to total brain volumes (48). This

discrepancy was cautionary however, due to many postmortem studies using

brains of mentally retarded individuals, while MRIs came from high functioning

patients without seizures (48). Stereological analysis of 14 postmortem autistic

brains aged 4- 60 years old revealed common decreases in number and density

of Purkinje cells in the cerebellum as well as reduced density of cells in the

amygdala, and volume for caudate nucleus and nucleus accumbens (44). Of

these 14 ASD individuals, 7 suffered from seizures while a total of 8 also

exhibited mild to severe intellectual deficits (44). Additionally, MRI studies have

indicated that specifically the size of the vermis is often variable, either being

larger or smaller than controls, an indication that ASD causes heterogeneity in its

phenotypes (48). A more detailed investigation of males found that those with

autism and high functioning autism had reduced vermis volume compared to

respective controls (49). All of these alterations in brain regions and size are reflective of growth abnormalities in brain development, and an overarching phenotype in ASD.

It should be noted that autistic individuals have issues with frontal lobe functionality (50). It is also interesting to note that epilepsy can occur between 5 and 46% in ASD individuals, depending on inclusion criteria (51). Having increased seizures suggests that ASD pathology may have both early brain overgrowth and alterations in excitability (52). This feeds into a theory that ASD individuals have several brain regions with hyperactive pyramidal cells such as in the prefrontal cortex, and amygdala (52). Additionally there is reduced connectivity in the amygdala for ASD individuals (53), further suggesting reasons for impaired signaling. Taken together, these data suggest that the ASD phenotype includes regional and global changes in brain growth. Therefore further exploration into proliferation and differentiation of neuronal precursors may elucidate mechanisms and pathophysiology of ASD.

1.2) CNS Development and its regulation

A) Neurogenesis in the Cortex

Cortical neurogenesis, or the generation of new neurons begins with the cells which line the ventricular zone (VZ) of the cerebral wall. All cells which make up the neocortex ultimately come from these cells, which are

Figure 1 Neurogenic gradients in development. Adapted from (3).

identified as the pseudostratified ventricular epithelium (PVE). In the mouse, neurogenesis persists from embryonic day E11 to E17, with a portion of the PVE population leaving the proliferative pool to turn postmitotic and differentiate after each cell cycle. Cells leaving the cycle will then migrate to the cortex and differentiate or undergo cell death (54). Neurogenesis occurs over a transverse gradient starting at the rostrolateral and traveling caudally and medially (3). Observations of additional gradients, includes the increasing length of G1 phase of the cell cycle (TG1) extending rostral to caudal, as well as similarly decreasing expression levels of the homeobox transcription factor (TF) Lhx2, maybe sufficient to inform cells where they orient with respect to others in the PVE (Figure 1).

There are specific TFs expressed during specific stages of neurogenesis and differentiation. The progression goes from Pax6→Tbr2→Tbr1 with the prior TF being downregulated as cells transition between cell types (55). Initially,

neuroepithelial cells, better known as neural stem cells (NSC) residing at the VZ

will expand the progenitor pool with symmetric divisions (FIG. 2). Ultimately,

these divisions give rise to radial glia which will divide asymetrically, creating

more progenitors and neurons (1). Radial glia express the homeobox domain

Pax6 at the ventricular surface, and these cells will ultimately produce neurons

and glia (55).
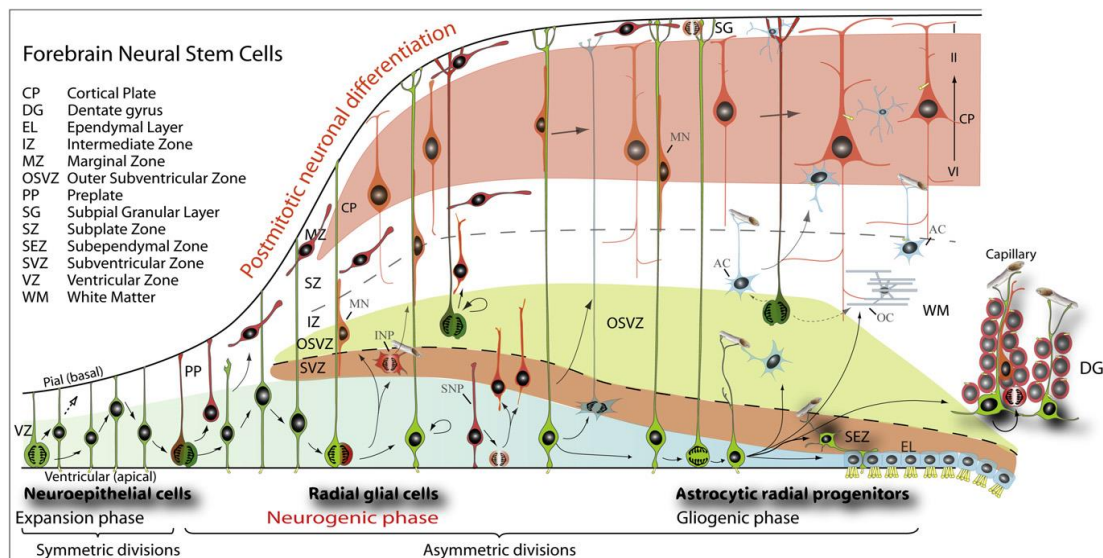
Figure 2 Model for Cortical Neurogenesis (1)

Soon after daughter cells are born, they rapidly move to the subventricular zone

(SVZ) and become specified as intermediate progenitor cells (56). Intermediate

progenitor cells are derived from radial glia and express Tbr2, while early

intermediate progenitors can also express small levels of Pax6 (55).

Intermediate progenitor cells undergo symmetric division and will migrate back

down into the VZ for a period of time (56). When they return to the SVZ, they will

undergo one or two more rounds of division and migrate away towards the

cortical plate where they differentiate and reach their respective cortical layer(1,

56). Finally, as cells become post mitotic, they will express Tbr1 and rapidly downregulate Tbr2 levels. (55).

Altering levels of these factors can influence neurogenesis and differentiation. Artifically increasing Pax6 levels can push stem cells towards neurogenesis rather than maintaining the self renewal pool of progenitors (57) Further, this overexpression increases expression of genes for SVZ cell populations including Eomes/Tbr2 (57). This promotes neurogenesis in cells that would normally expand the progenitor pool, resulting in microcephaly (57). Tbr2 expressing cells help expand glutamatergic neurons at each layer and the Tbr2 mutant cortex has reduced thickness in all cortical layers. (58).

B) The Cell Cycle and its regulation

Development and organogenesis requires the highly regulated process of cell division, which starts immediately after fertilization. This process is known as the cell cycle and is broken into 4 main phases: G1, S, G2 and M. Cells start in G1 or Gap1 phase which precedes the phase of DNA synthesis and is the longest step in the cycle. They then progress to S or the synthesis phase where cells replicate their DNA and continue to grow. This is followed by G2 or Gap2, where cells prepare for mitosis. During mitosis, or M phase, the cell divides to produce two daughter cells. At the end of M phase, cells will either re-enter cell cycle at G1 for another round of division, or continue to the non proliferating state known as G_0 (59). Cells know precisely when to transition from one phase to the next based on the cyclical expression of protein complexes composed of cyclins

and cyclin dependent kinases (cdks), and the downstream signaling cascades
they promote (60). Furthermore, cyclin inhibitory proteins (CKIs) repress
Cyclin/CDK complexes to regulate the progression of cell cycle (61). Mitogens
typically activate extracellular signaling pathways to transcribe cyclins, while
other signaling pathways are capable of inhibiting their expression (62, 63)
(Figure 3).

Progression from G1 to S phase starts with assembly of Cyclin D1 and its
cyclin dependent kinases CDK 4 and 6 to initiate the cell cycle (64). This will
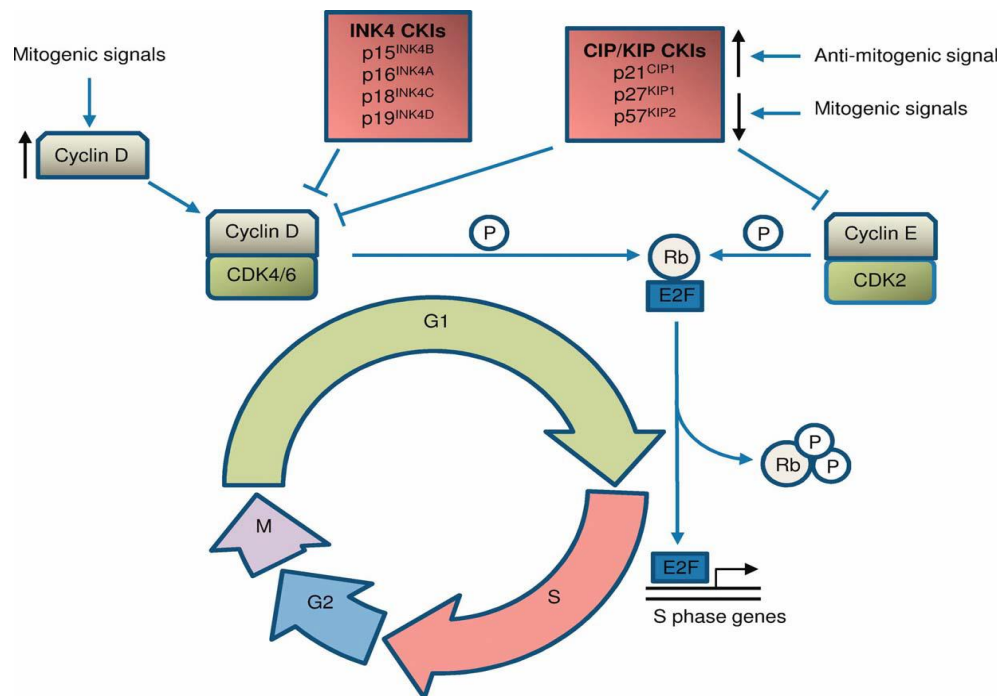
Figure 3 Cell cycle regulation by cyclin/cdk complexes and cyclin
dependent kinase inhibitors (cdki) (2)

elicit phosphorylation of Retinoblastoma protein (Rb) family members (61).
Increasing levels of Rb phosphorylation will decrease its ability to bind and inhibit
E2F transcription factors, promoting E2F activated genes (61). This
phosphorylation disrupts the complex of Rb protein and Histone deacetylase

protein (HDAC) allowing release of E2F1 and DP-1 transcription factors, which in turn increase expression of S phase promoting genes such as cyclin E (59). Cyclin E is transcriptionally activated by E2F1 at its promoter site, and this binding regulates G1 in part through a feedback loop to cyclin E (65). Cyclin E will then complex with Cdk2 to further phosphorylate Rb proteins allowing further release of E2F transcription factors (61). This will promote E2F translocation to the nucleus, causing upregulation of G1 to S phase genes, so cells can transition to S phase. Cell cycle progression can be kept in check by the CDK inhibitory proteins (CKIs) of the CIP/KIP family and INK4, which repress cyclin/ CDK complexes (61). The cyclin dependent kinase inhibitory complexes can be beneficial in that they act as checkpoints for the cell in response to DNA damage, allowing time for DNA repair prior to continuing the cell cycle (59). The INK4 CKI family specifically inhibits cyclin D CDK complexes, while the p21 family of CKIs inhibits both cyclin D and E complexes (2). To further facilitate G1 to S phase transition, accumulation of CDK2-cyclin E complex is able to phosphorylates its CKI, p27, promoting its degradation (59). Notch1 is known to promote radial glia progenitor proliferation by preventing differentiation, and this is done in part through suppression of p27 by degradative mechanisms (3). The CKI p27 is also known to rise in concentration in the PVE after each subsequent cell cycle, and this partially occurs due to the decline in Notch1 tone (3). Ultimately, the concentration of CKIs will eventually rise too high and Notch1 tone decreases enough that cyclin levels cannot facilitate subsequent transitions from G1 to S phase, causing cells to exit the cell cycle (3).

C) Signaling pathways impacting neurogenesis

Many pathways have been implicated in ASD including mTOR and ERK and Wnt signaling (66) (67). Furthermore, these signaling pathways are known to regulate neurogenesis. Mitogen-activated map kinases (MAPK) are typically activated by mitogenic stimulation to initiate signaling cascades, although they have additional intracellular functions and interactions. There are 4 different signaling cascades of MAPK, including 1) Extracellular signal-related kinases (ERK1/2), 2) Jun amino-terminal kinases (JNK 1/2/3), 3) p38-MAPK, and 4) ERK5 (68). Following mitogenic stimulation, MAPK signaling cascades become subsequently activated through phosphorylation, promoting proliferation (69). Activation of most of these signaling cascades start with tyrosine kinase receptor or G protein-coupled receptor activation; however, JNK and p38 are activated mostly by cytokines, osmotic shock and other stressors (70). Overexpressing mutant forms of MAPKs typically reduced proliferation, although proliferation can also be independent of MAPKs (69). Depending on the extracellular signal, this pathway can promote proliferation or differentiation. In PC-12 cells, exposure to EGF or NGF can both stimulate the MAPK pathway, while the former promotes proliferation, the latter induces differentiation (69). Others have suggested that early and late stem cells can differentially respond to mitogens such as EGF and FGF depending on changes in receptor levels over development (71). Studies with undifferentiated embryonic stem cells have also observed high expression of growth factors, while levels were decreased after differentiation by treatment of retinoic acid (72), suggesting that altered regulation of these factors may indicate

differentiation. Relevant to the cell cycle, cyclin D and cyclin E are transcriptionally regulated by several signaling pathways and mitogens (73). Cyclin D1 transcription typically occurs through activation of the Raf > MKK1 > p42/p44MAPK pathway (62).

The protein complex mTOR is a serine/threonine kinase, which plays important roles in neuronal development. The mTOR pathway can either promote stem cell pluripotency or differentiation through transcription factor expression of key genes (74). Extracellularly, activation of a tyrosine kinase receptor causes activation of mTOR and members in its signaling pathway including RAS, AKT, RHEB RAS and TSC1/2. Additionally, mTOR can mediate intracellular signaling such as its phosphorylation of upstream players AKT/PKB, to regulate proliferation and cell survival (74). Hyperactivation of mTOR can disturb neuronal migration, and altering levels of mTORC1 and mTORC2 complexes can have implications in whether a cell remains pluripotent or differentiates (74). Notably, mutations in tumor suppressors of this signaling pathway (PTEN and TSC1/2) are commonly found in neurodevelopmental disorders such as autism, and can exhibit growth phenotypes such as macrocephaly as well as increased risk for pediatric brain tumors (74). Further, in vivo rat experiments have shown that a single VPA injection at E12 can upregulate phospho mTOR and phosphor s6 in the prefrontal cortex of pups by postnatal day 35 (75). Interestingly there are interactions between ERK and mTOR pathways, and inhibition of mTOR can upregulate MAPK through S6K (76). S6K is activated by mTORC1 and interacts with the ribosomal protein S6,

and other TFs that play roles in translation, initiation, and elongation (77).

Additionally, blocking mTOR can cause a negative feedback that hyperactivates

the Ras-Raf-MEK-ERK pathway (76). Recent literature has suggested links

between ERK and AKT pathways, where inhibition of ERK inhibited neural

differentiation and promoted proliferation of VZ/SVZ progenitors, independent of

GSK-3 signaling (78).

The Wnt signaling pathway is also able to regulate neural differentiation by

reducing cortical precursor cells ability to self-renew. This also promotes MAP2

expressing neurons and astrocytes. Activation of Wnt typically causes

extracellular signaling to activate Disheveled which inactivates glycogen

synthase kinase 3-beta (GSK-3B), among other downstream effects.

Furthermore, inhibition of GSK-3beta has been suggested to promote neural

differentiation. On the other hand, Wnt signaling can also promote transcription

of cyclin D1, and studies show Wnt-1 and Wnt-3a molecules can act as

mitogens, stimulating proliferation of dopaminergic neuron precursor populations

(79).

Cyclin E can also be regulated by hedgehog and Wnt signaling, as well as

environmental signals through the Hippo pathway (73). A positive feedback loop

exists to upregulate cyclin E CDK2 proteins through their phosphorylation of Rb

(pRB), promoting further E2F binding [73]. Elevated levels of cyclin E can also

shorten the length of G1 and promote cells to enter into S phase (73).

Alterations in signaling pathways are of interest because increasing or

decreasing their signaling both can lead to autism (66).

Considering alterations in brain growth seems to be a common phenotype in ASD, understanding how these pathways are regulated could explain some of ASD pathophysiology. Therefore, studies using genetic or environmental risk factors for ASD can investigate perturbations in these pathways and may further our understanding of ASD etiology and subpopulations with macrocephaly.

D) Epigenetic regulation of cell cycle

As stated earlier, epigenetic regulation plays roles in development of ASD, through altering gene expression. There are several methods of epigenetic regulation of gene expression which includes histone modifications. DNA is wrapped around clusters of histone proteins composed of H2A, H2B, H3 and H4 (80). Modifications of the amino acid chains on histones can be regulated in various ways, including but not limited to methylation, and acetylation (80). DNA methylation is able to regulate gene expression as histone methyl transferases (HMT) can add methyl groups on arginine and lysines to either promote or silence gene expression (80). Some examples of methylation promoting gene activation are histone H3 trimethylation at lysine residue 4 or 36, while di- and trimethylation on histone 3 lysine 9 are examples for gene silencing (80). Histone acetyl transferases (HATs) are enzymes responsible for acetylating lysine residues, while histone deacetylases (HDACs) remove acetyl groups (80). HDACs consist of 4 classes of enzymes which deacetylate lysine residues on histone cores and specific genes (80). Class I HDACs are ubiquitous but localized in the nucleus, while Class II HDACs shuttle between the nucleus and cytoplasm (80). There is a specific balance of acetylation and deacetylation

which occurs in order to regulate gene expression and control the acetylation state of lysine residues (FIG.4)(4). Typically, the more acetylated a histone is, the more likely transcription
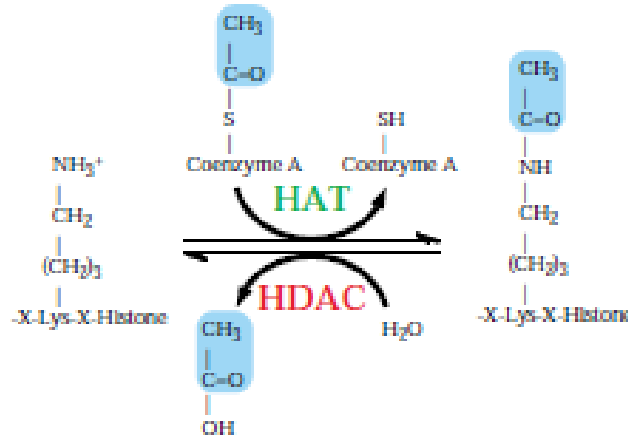
Figure 4 The balance of acetylation and deacetylation is controlled by HATs and HDACs, respectively(4)

factors can interact with DNA to promote gene expression(4). Acetylation of lysine residues can reduce the affinity of Histones to interact with DNA, and hyperacetylation of histones is associated with increased transcription(4). Deacetylation of histones by HDACs increases the histones positive charge (4). Furthermore, HDACs do not directly bind to DNA, rather they are recruited to DNA by their involvement with various transcription factor complexes(81) (82). In addition to inhibiting histone acetylation, HDACs deacetylate more than 50 non histone proteins, implicated in cell proliferation, migration and death (81).

With HDACs being able to regulate a large array of genes and proteins, it is no surprise they can impact the cell cycle. Studies have shown that completely removing HDACs 1 and 2 will halt cell cycle progression at G1, and upregulate expression of CKIs p21 and p57 (83). Further, HDAC 1 and 2 can bind to the promoter regions of p21 and p57 (83), supporting how they can regulate progression of the cell cycle. These two HDACs are also expressed

during cortical development in defined but overlapping populations. HDAC1 is primarily in proliferating cortical progenitors, while HDAC2 is primarily in neurons of the neocortex(84). They are also known to participate in three main complexes known as Sin3, NuRD and CoREST which all regulate gene expression during development (85). Studies of mice lacking HDAC1 or 2 in their neuronal precursors revealed multiple problems including apoptosis, abnormalities in hippocampus, and reduced neuronal differentiation and organization in cortical layering (86). Although there was a reduction in differentiated neurons, there was an increase in BrdU labeling at E14.5 followed by increased cell death at E15.5 (86). These findings suggest that inhibition of HDACs can regulate G1 to S, and also allow for appropriate differentiation, of progenitor cells.

Other proteins relevant to cell cycle such as Rb have been shown to complex with HDACs. Although Rb can block transcriptional activity of E2F regulated genes, addition of a HDAC inhibitor Trichostatin A (TSA) was able to partially prevent this inhibition(87). It was postulated that Rb may not fully sterically block the E2F transactivation domain and therefore suggest HDAC activity may regulate acetylation of E2F sites along with the HAT / E2F1 complex (87). Others have shown that a complex including Rb and HDAC could suppress cyclin E in immortalized MEF cells, and TSA can upregulate cyclin E message in functional RB +/+ cells (88). In HeLa cells, others were able to co-purify the complex that included HDAC1, E2F1 pRB and DNMT1(89). These data suggest

that HDAC inhibitors may alter functionality of specific repressor complexes, promoting E2F mediated transcription of G1 to S phase cyclins.

A wide array of chemicals is capable of inhibiting HDACs. Broad inhibition of HDACs of class I and II can be observed in various cancer cell lines after exposure to hydroxamate compounds including Trichostatin A (TSA), and Vorinostat (SAHA) ,(81). Similar inhibition profiles occur with aliphatic acids such as Valproic acid (VPA), and Phenyl butyrate, while the benzamide MS-275 specifically inhibits HDAC1,2 and 3 (81). Although these drugs are known to inhibit broad ranges of HDACs, their affinity with individual HDACs vary by dose and are often reversible (81).For example, VPAs IC50 for HDACs 1-3 in cell lines ranges from 0.7 to 1 mM, and 1- 1.5mM for HDACs 4,5 and 7 (90).

1.3) Clinical observations related to Valproic acid exposure, and Copy Number Variant 16p11.2

A) VPA's clinical uses in Humans

Valproic acid (VPA) is a short chained branched fatty acid, used to treat migraines, epilepsy, and bipolar disorder (91). The antiepileptic and mood stabilizing effects of VPA are believed to be due to its ability to increase GABA levels and inhibit voltage gated sodium channels (91). VPA enhances GABA production and signaling length by acting on various degradative and biosynthetic enzymes (92). This alteration of excitatory and inhibitory neurotransmitters is one action by which VPA acts, and this has been proposed

to be a hypothesis contributing towards ASD neuropathology(52). In cases of generalized epilepsy, VPA is one of the most effective medications, however this is problematic for pregnant women and their fetus (93-95). Recently, VPA has also generated interest as a potential anticancer therapy due to its histone deacetylase (HDAC) inhibition (96).

B) VPAs effects as a Teratogen and ASD risk factor

Teratogens are defined as developmental insults to the growth of fetal organs, and ultimately give rise to birth defects, often dependent on the dose of the drug, the exposure period and the subsequent populations of cells which are currently dividing and migrating. VPA was identified to be a teratogen in the 1980s with increased risk for myelomeningocele lesion of children who were prenatally exposed (97, 98). Over time, characterization of prenatal VPA exposure revealed several common physical deformations which became known as fetal valproate syndrome (FVS) (99). These deformations include several craniofacial abnormalities such as presence of epicanthic folds on the eye lids, flattened nasal bridge, altered philtrum, and thin upper lip (99). When malformations are seen in external features of the head and face, this suggests that additional growth and development issues could have occurred during brain development. Longitudinal studies have identified prenatal VPA exposure can not only change external craniofacial abnormalities, but also overall shape of skull as evident by an increased cephalic index (100). These developmental issues have also been identified through cerebral deficits in cognitive decline and developmental delay (101) including issues with language delay, repetitive

behaviors and other social impairments (102). Moreover, the behavioral issues

seen in children prenatally exposed to VPA are akin to that of symptoms in ASD.

Indeed, VPA has been established as a risk factor for developing ASD (29, 103-

106). Depending on study and population investigated, the risk for developing

ASD can range from 2.75% to 12% (29, 106). Higher percentage risk could be

conflated due to sample selection coming from antenatal clinics, compared to a

data set coming from the extensive and broadly covered birth registries of

Denmark hospitals. Regardless, the overarching conclusion is that prenatal

exposure to VPA causes altered development in head and brain growth, and

increases risk for developing ASD.

C) The genetic risk factor for ASD, 16p11.2 CNV

As mentioned above, genetics play a substantial role in autism. One

genetic phenotype of interest is the CNV of chromosome 16p11.2. Of those

diagnosed with autism, 1% will also have a deletion or duplication of this region

(107), underscoring its association to ASD. Individuals with this CNV deletion or

duplication often have cognitive impairments as well as speech / language delay,

while the deletion is more strongly associated with ASD (108). The deletion is

also affiliated with a series of phenotypes that overlap with ASD including motor

delay, seizures, as well as behavioral and congenital abnormalities (108).

Notably, individuals with the 16p11.2 deletion often exhibit macrocephaly while

containing a duplication of this CNV leads to microcephaly (108), suggesting that

genes in this region are involved in proliferation and brain development. Indeed,

this region affects one copy of 27 (21) to 29 genes (109, 110), including several

genes which play roles in cell growth. Three of these genes are MAPK3, Major Vault Protein (MVP) (21), and KCD13 (109). MAPK3 encodes for ERK1, which is involved in the ERK pathway. This signaling pathway plays an important role in cortical neurogenesis and regulation of the cell cycle during development (21). Studies have also linked altered ERK signaling to multiple disorders including ASD (21), while altering dosage of KCD13 has been associated with macrocephaly in zebrafish models (109).

D) Converging phenotypes in Genetic and Environmental risk factors for ASD

Multiple risk factor genes for ASD have been linked to proliferation and differentiation. Further, certain genetic alteration risk factors have been linked to macrocephaly such as 16p11.2 deletion, suggesting genes in this CNV directly regulate proliferation and/or differentiation (111). Environmental ASD risk factors can also produce altered brain sizes. The ASD risk factor, maternal immune activation (MIA), causes prenatal exposure to heightened inflammatory responses (27) and may interact with mTOR signaling (112). It also has a correlation for subsets of ASD cases with early brain overgrowth (40). Alternatively, prenatal VPA exposure can also alter head shape through craniofacial abnormalities and a larger cephalic index, suggestive of alterations in brain development (100). VPA has the capacity to impact gene expression and brain development, likely through epigenetic regulation. This can occur through VPAs' ability to inhibit histone deacetylases, which modulate gene expression (111).   Therefore, different risk factors of ASD can either directly or indirectly change brain development. This thesis will examine the theme of altered

neurogenesis focusing on proliferation and differentiation to better understand how environmental and genetic risk factors may cause ASD.

1.4) Models for Environmental and genetic risk factors

A) Rodent models for studying effects of VPA on ASD

To better understand the effects of VPA on development, animal models have been implemented. Founding studies highlight that VPA exposure during a specific time in embryonic rat development can be effective in modeling autism (113, 114). Specifically it may parallel some cases of idiopathic autism as it serves as an environmental and likely epigenetic mechanism as opposed to genetic models of autism impacting single or subsets of genes(115). Animals experiencing prenatal exposure to VPA also show behavioral deficits and loss of neurons in the cerebellum, both characteristics of autism (113, 114). Additional studies utilizing a single injection of VPA at 400 or 600 mg/kg on E12 or E12.5, have examined cell proliferation and brain size showing evidence for enhanced proliferation, reduced cell death and macrocephaly (116-118). Although most studies focused around E12 for the prenatal rat model for ASD, others have been able to recreate some features and behaviors of ASD by early postnatal VPA exposure (52), suggesting that VPAs mechanisms which give rise to ASD neuropathology and behaviors are not necessarily restricted to the specific developmental period during neural tube closure. Therefore, exposure of VPA on the developing brain can give rise to both growth phenotypes and behavioral traits reminiscent of ASD within multiple windows, acting on possibly different

populations of cells. Although VPA injection seems to create a viable ASD model, understanding its proliferative mechanisms which impact brain growth are not fully understood.

In rat cortical glial culture studies from Dr. DiCicco-Bloom's lab, VPA has been shown to cause alterations in neurogenesis, as well as autism like behaviors in rats (119, 120). Acutely exposing cultures to 0.6 mM VPA upregulated G1 cyclins, promoting G1-S phase transition, while 2 mM VPA additionally increased CDK inhibitors (119). This 24 hour culture revealed mitogenic and antimitogenic properties of VPA, underscoring importance of dose dependent responses within a cell population (119). Because previous studies have also demonstrated mitogenic (118, 121) and antimitogenic effects on cortical development (122-124), it is valuable to understand what additional mechanisms could promote these disparate results.

B) Proliferation and differentiation after VPA exposure

Several studies have examined the mitogenic effects of VPA in vitro and in vivo. Data have often been controversial due to contradictory findings in animal models and systems. Contrasting findings from various labs may be a result of disparate culture conditions, as incubation length, and medium components are capable of altering cellular responses. Dose is another confounding variable, as in vitro studies utilize VPA doses from 0.5 mM upwards of 5 mM and in vivo injection paradigms can span from single to multiple doses ranging from 200 mg/kg to 600 mg/kg. With changes to dose and exposure duration, it is no

surprise that researchers have proposed different mechanisms by which VPA

may act during development. In vivo studies from one group found a single 400

mg/kg injection of VPA at E12 resulted in decreased brain weight compared to

control at E18 but macrocephaly from P2 onward, through Gsk3b B catenin

pathway(118). This same group also identified that embryonic neural progenitor

cell survival was also increased due to prenatal VPA exposure through increased

nuclear NF-Kb in culture and *in vivo*(117) suggesting that VPA may regulate

proliferation through multiple pathways. Sensitivity appears to be apparent at

higher doses, as other labs administered a single VPA injection of 500 or 600

mg/kg at E12.5 resulting in reduced offspring body weight and brain mass

compared to saline injected controls (125). Others injected two 200 mg/kg doses

of VPA from E13.5 to E14.5, and argued for reduced proliferation and increased

differentiation, visualized by decreased in PCNA and increased Tuj1 staining at

E15.5 (122), however they did not explain how quantification was determined.

This lab also exposed cortical cultures to 1 mM VPA and 10 ng/ml bFGF, and

argued neural progenitor cells exhibited reduced proliferation and increased

differentiation through the b-catenin Ras ERK p21 pathway (122). Other

researchers identified that in vitro exposure to VPA promoted apoptosis

specifically in differentiating glutamatergic neurons by upregulation of cleaved

caspase 3 protein (126) suggesting cell type specific effects of the drug. The

proposed mechanism was HDAC inhibition, with VPA as well as exposure with

other HDAC inhibitors having correlative increases in acetylated Histone H3,

while valpromide (an inactive chemical analogue of VPA) did not increase

acetylation or apoptosis (126). In contrast, other researchers demonstrated that a single injection of VPA 400 mg/kg at E12.5 can promote glutamatergic differentiation and alter the balance of excitatory and inhibitory neurons with lasting behavioral deficits in pups(127). It is interesting to note that VPA exposure caused an initial upregulation of Pax6 at E14, and then decrease in comparison to control by E18, while subsequent markers in maturation were increased in a time dependent manner (127). Increased Pax6 message was observed after VPA exposure, and by chromatin immunoprecipitation (ChIP) analysis, it was observed that VPA exposure correlated with an increase in acetylated H3 and decrease in HDAC1 at the Pax6 promoter site (127). Others have also observed increases in Pax6 message after 5 mM VPA exposure to embryonic rat cortical cultures (128). Pax6 upregulation is important as it promotes glutamatergic cell type differentiation (127) In neuronal specificity, there is a progression of precursor markers Pax6→Tbr2→NeuroD1→Tbr1 in pyramidal neurons (129) The sequential expression of Pax6, Tbr2, and Tbr1 is seen in the developing neocortex, and gives rise to glutamatergic pyramidal projection neurons (55). VPA also favors upregulation of GABAa receptor involved in epileptogenesis and downregulation of genes involved in developing GABAergic inhibitory neurons as evident by microarray(128). Therefore depending on dose, duration, and progenitor cell type, VPA can regulate differentiation, survival, or proliferation, changing the ratio of neuronal populations of the developing neocortex, and ultimately impacting rodent behavior. In sum, these studies indicate several potential outcomes from VPA

exposure with evidence of altered neurogenesis regardless of time or dose. Because dose, cell type, and conditions can determine if proliferative or antiproliferative effects are seen, it illustrates the sensitivity and degree of complex interactions which can occur due to VPA. These studies help give a better understanding of pathways VPA can activate within specific experimental designs, and thus provide context in framing future experiments and parsing out mechanisms.

C) Epigenetic actions of VPA

Several animal studies have indicated that prenatal exposure to VPA has produced hyperacetylation of histones H3 and H4, and postnatal behavioral issues similar to autism (115). Further, prenatal treatment with an analogue lacking HDAC fails to cause behavioral changes or alterations in acetylation (115). Based on work in cell lines and animal models, VPA has been classified as an HDAC inhibitor(30, 96). However, to date no studies have directly tested enzymatic inhibition of HDAC activity in primary animal tissue. Although confirming this mechanism is still necessary, several studies have put forth supportive evidence characterizing how VPA can interact with HDACs and regulate gene expression. In cell lines, VPA was shown to inhibit HDAC1 at 0.4 mM and can mimic the HDAC inhibitor Trichostatin A (TSA) (30). As evidenced by microarray assay in E17.5 rat cortical neurons, exposure to 5 mM VPA results in 726 upregulated genes and 577 downregulated genes(128). There was also increased acetylation of histone H3 and H4 only at promoters of genes which were up regulated, and similar gene effects were seen by another HDAC

inhibitor, TSA, supporting the notion that VPA regulates gene expression through an HDAC inhibitory mechanism (128). VPA treatment was able to induce Wnt gene expression through this HDAC inhibition mechanism, while also activating transcription of several other promoters (30). In complement to these findings, a single 600mg/kg injection of VPA at E12.5 resulted in demethylation of Wnt1 and Wn2 genes, which are involved in the canonical Wnt/B-Catenin pathway. This demethylation caused an upregulation of their message and protein allowing for enhanced nuclear B-catenin (116). Deregulation of the Wnt/B-catenin pathway and increased stability of B-catenin in neural precursor cells can cause substantial enlargement of brain regions cerebral cortex, amygdala and hippocampus and this overgrowth shows parallels with the overgrowths in a series of autistic patients with brain overgrowth or macrocephalic brain regions(116)

VPA is a neurotherapeutic, as it can stimulate the production of neuroprotectant factors and proteins. Cell survival is another mechanism by which you can get a larger brain. In embryonic rats, VPA exposure can inhibit cell death likely by decreasing IkBa expression to allow more NF-kB nuclear translocation and subsequent up regulation of antiapoptotic proteins (117). VPA as well as other HDAC inhibitors have been shown to up regulate the antiapoptotic heat shock protein 70 (HSP70) in cultured rat neuronal and astrocyte cultures and increase histone 3 lysine 4 di- and trimethylation at the promoter suggesting neurotheraputic effects through epigenetic mechanisms (130). In cortical neurons, treatment of VPA resulted in increased p300, an HAT,

at the HSP70 promoter and HSP70 transcriptional activation(131). Experiments in rat cortical neurons have also suggested HDAC inhibition as a target for the observed elevation of BDNF message from exon IV after VPA treatment (132).

D) Animal models of 16p11.2 CNVs

Although animal models of this genetic deletion have been useful to assay various aspects of the etiology, the model can become discordant when discussing brain growth and neuroatanomy. Fundamentally, mice differ from humans with the chromosomal deletion exhibiting microcephaly, while the duplication produces macrocephaly in mice (21). Additionally, mice do not contain cortical gyri, suggesting some structural and possibly mechanistic results may not parallel the human disorder. Even though there are paradoxical changes in the outcomes of the mouse brain, mechanistic studies have identified relevant changes to signaling pathways including the ERK pathway (21).

Zebrafish have also been used to study this CNV through transfection studies utilizing shRNA of genes within the region and assaying for macrocephaly. Another gene suggested to play a key role within the 16p11.2 CNV is KCTD13, which encodes for polymerase delta interacting protein 1 (PDIP1) (109). This gene interacts with PCNA and experiments in zebrafish showed deletion can yield microcephaly, while overexpression is sufficient for macrocephaly (109). Limitations are that they had to identify their own criteria for macrocephaly by distance across the convex portion of eye cups as an objective

head measurement (109). When trying to recapitulate macrocephaly, additional genes have been uncovered.

E) Using iPSC technology to model genetic forms of Autism

Although animal models provide valuable data for modeling diseases during development, there are limitations. Translation of genes is not always 100% from animal to human, and when studying genetic based disorders, this could possibly confound findings. For example, the animal model of 16p11.2 deletion exhibits microcephaly while humans have macrocephaly (21). Additionally, animal variants of genes may differ in their functions compared to humans, with human genes having more forms.

A newly emerged technology has arisen which allows us to use human samples to study neurogenesis in vitro. This technology requires the creation of induced pluripotent stem cells (iPSCs) from somatic cells, after exposure of reprogramming factors (133). Initially this was conducted by Takahashi and Yamanaka, where expression of concordant expression of Oct4, Sox2, Klf4, and c-Myc transcription factors was able to convert fibroblast cells into embryonic stem cells (134).   In short, this process reprograms dividing human cells into a pluripotent state, and then can be encouraged to terminally differentiate into neurons, glia or other cell types (133). The benefit of using human iPSCs is that they retain genetic diversity of the patients, so they can aid in studying how mutations can cause disease (133). This technique is highly valuable as it allows one to investigate the development of neuronal progenitor cells within the genetic

background of a disease state, and compare that to a normal or control genetic background of healthy individuals. Additional benefits of this technology include being able to study specific neuronal populations with features unique to humans and primates, such as differences seen in corticogenesis (135). Therefore, to understand genetic contributions to a human disease, it is highly beneficial to understand how cellular processes are impacted within the context of a human disease background.

To date, there are no published works that have used human iPSCs containing the 16p11.2 CNV to study etiology of the disorder. However there are several studies which have used iPSC technology to study both genetic (136, 137) and idiopathic forms of autism (138). Using induced neural progenitor cells (NPCs) researchers have modeled idiopathic autism and identified alterations in proliferation indicative of early brain overgrowth compared to control NPCs (138). Others have also used iPSCs to study other genetic autism disorders models as Timothy syndrome, showing aberrant calcium signaling, as well as alterations in gene expression and differentiation (139). Bipolar disorder (140, 141) and schizophrenia (142, 143) have also been examined.

e) Fetal stem cell nature of iPSC NPCs

When studying gene expression profiles of iPSC derived cortical cells, others found they closely resembled primary fetal brain cells using RNA-seq analysis (144) . This highly similar identity was done on single cells, to ensure cell type differences (144). Similarly, many neurons derived from iPSCs have immature synapses, and express markers for immature neurons(133). It has

been suggested that even these differentiated cells exhibit characteristics of young neurons (133). Others looked at gene expression of human iPSCs, NPCs and 6 week old neurons, and determined they all closely resemble human forebrain tissue of the first trimester (142). Gene expression resembling fetal neocortical development was also observed in differentiated iPSCs that were formed into 3D cultures known as human cerebral organoids (145). Therefore the current technology of iPSCs provide a unique ability to model disease states of progenitor cells during early fetal development, highly similar to the first trimester.

Within ASD, there are many alterations in neurogenesis, giving rise to changes in brain growth. As outlined above, I have shown examples of environmental and genetic risk factors for ASD, as well as potential models to study them. To better understand how alterations in neurogenesis could play a role in the etiology of autism, I will now detail methods used to study ASD with a rodent model exposed to the environmental risk factor VPA, as well as an iPSC model to study the genetic risk factor 16p11.2.

Chapter 2: Materials and Methods

2.1) Animal sacrifice

Time-mated, pregnant Sprague Dawley rats were obtained from Hilltop Lab (Philadelphia, PA). They were kept on a 12:12 light:dark cycle, and given ad lib (Purina rat chow) and water. For all subsequent analyses, pregnant dams were sacrificed by CO_2 asphyxiation, followed by cervical dislocation and bilateral pneumothorax to assure death of the mother, as approved by Rutgers IACUC. Following sacrifice, embryonic sac was removed after caesarean section and transferred to a sterile Petri dish containing saline glucose solution. In order to undergo downstream assays, embryonic sacs were opened with forceps, followed by rapid cervical transection of embryos within sterile saline glucose solution.

2.2) Cortical Cell Culture:

For Rat cortical culture, pregnant dams were sacrificed on gestation day 14.5 (E14.5). As described above, embryos were sacrificed by cervical transection followed by removal of fetal skin, skull, and meninges. The dorsolateral cerebral cortices were then dissected from embryos, and transferred to a sterile conical tube. Collected tissue was mechanically dissociated, with a portion reserved to calculate cell number on hemocytometer. Finally, cells were plated on poly-D-lysine (0.1mg/ml) coated 35mm dishes or 24-well plates (Fisher sci) at $1x10^5$ as previously described (146, 147). Culture medium was composed of a 1:1 (vol/vol) mixture of Ham's F-12 (Gibco) and DMEM (Gibco)

supplemented with transferrin (100ug/ml; Calbiochem, La Jolla, CA), putrescine (100uM) **,** progesterone (20nM), selenium (30 nM), glutamine (2 mM), glucose (6 mg/ml), bovine serum albumin (10mg/ml), penicillin (50 U/mL), and streptomycin (50*ug*/ml) as previously reported (146, 147). Culture media was also treated with or without VPA (Sigma, Saint Louis, MO), trichostatin A (TSA) (Calbiochem), suberoylanilide hydroxamic acid (SAHA) (Sigma), basic fibroblast growth factor (bFGF) (10ng/ml media, Peprotech Rocky hill, NJ) or other drugs. All supplementary components were supplied by Sigma unless stated otherwise. Cortical cultures were maintained in a humidified, 5% CO2 incubator at 37^0C until time points for downstream assays.

2.3) Human NPC cell culture:

A) Generation of Human NPCs from iPSCs

Neural induction of iPSCs was conducted with use of the Gibco® PSC Neural induction medium (Thermofisher) using 35mm x 6 well matrigel precoated plates. All inductions followed manufacturers instructions and involved 7 days of exposure to induction medium prior to passaging NPCs into Expansion media. Cells were maintained in a 5% humidified CO2/air incubator at 37° C. Upon reaching 7 days of induction, media was aspirated and NPCs were lifted using accutase (Sigmaaldrich), and plated at 1.5x 10^6 cells/ml into 100% Expansion media on 6 well, 35mm Matrigel (Corning) coated plates containing 5 μM of ROCK inhibitor (STEMCELL technologies).

B) Maintenance of Human NPCs under 100% Expansion Media

NPCs were plated at 1.5x 10^6 cells/ml and grown in 100% Expansion media on 6 well, 35mm Matrigel (Corning) coated plates. Every 48 hrs, spent media was aspirated and cells were fed fresh 100% expansion media until confluent. Culture medium described as 100% Expansion consisted of 1:1 Hams F12 (Gibco) and Neurobasal (Gibco) supplemented with 1x Neural induction supplement (Thermofisher) and 100μg/ml Primocin^{TM}(Invivogen). Cultures were maintained in a 5% humidified CO2/air incubator at 37° C. Upon reaching confluency, cells were lifted for experiments from P3 to P8 with use of 500ul Accutase (Sigmaaldrich) for 10 minutes, followed by pelleting and resuspension for seeding in experiments and subsequent passaging. NPCs were maintained with 5 μM of ROCK inhibitor (STEMCELL technologies) for 24 hrs when thawed and at passage 3 or lower.

C) Passaging of NPCs

When cells reached 100% confluency, media is aspirated, and cells were lifted by addition of 500 uL of Accutase enzyme (Thermofisher) and placed in a 5% humidified CO2/air incubator at 37° C for 10 minutes. After 10 minutes, the cells were washed with 500 uL of room temperature PBS and transferred into a conical tube to be spun down at 300xg for 5 minutes to pellet. Supernatant was then aspirated, and pelleted cells were resuspended with prewarmed DMEM/F12 media, followed by cell counts on a hemocytometer. For passaging, cells were plated at 1.5x 10^6 cells/ml into new 35 mm, 6 well matrigel precoated plates with 100% expansion media.

D) Cell culture of NPCs under Experimental conditions with 30% Expansion Media

Depending on the assay, NPCs were plated at densities ranging from 1x 10^4 to 1x10^6 cells/ml, and grown in 30% Expansion media +/- extracellular factors, on poly-D-Lysine (0.1 mg/mL, Sigma) and Laminin (5 μg/mL, Invitrogen) coated 24 well plates or 35 mm dishes (Corning). Experimental culture medium was made by diluting 100% expansion media by 70% with 1:1 DMEM/F12 and Neurobasal solution supplemented with 100μg/ml Primocin[TM](Invivogen). 100% Expansion culture medium consisted of 1:1 Hams F12 (Gibco) and Neurobasal (Gibco) supplemented with 1x Neural induction supplement (Thermofisher) and 100μg/ml Primocin[TM](Invivogen). All cultures were maintained in a 5% humidified CO2/air incubator at 37° C.

E) Cell culture of NPCs for Total cell numbers assay

NPCs were plated at 5x 10^4 cells/ml and grown in 30% Expansion media +/- extracellular factors, on poly-D-Lysine (0.1 mg/mL, Sigma) and Laminin (5 μg/mL, Invitrogen) coated 1.9 cm^2 x 24 well plates (Corning). Cells were fed fresh media every 48 hours until they were harvested. On days 2, 4 and 6, two 1.9 cm^2 wells for each condition had media removed, followed by addition of accutase for a 10 minute incubation. Subsequently, equal volumes of PBS were added to wells and then transferred to eppindorf tubes. Cells were resuspended and a portion of each suspension was diluted in trypan blue (Gibco), and counted by hemocytometer to estimate total cells in the well.

F) Culturing conditions for NPCs in downstream Immunocytochemistry

NSC marker assay:

NPCs were plated at 1x 10^5 cells/mL into either Matrigel coated 1.9 cm^2 x 24-well plates (Corning) with 450 uL of 100% Expansion media, and incubated in a humidified 5% C02 incubator for 48 hours. After incubation, media was aspirated, and cells were fixed in ice-cold 4% paraformaldehyde for 20 minutes, followed by 3 PBS washes.

NPC differentiation assay:

In order to determine if NPCs can give rise to Neurons, and Oligodendrocytes, NPCs were plated at 2.5x 10^4 cells/mL into Poly-D-Lysine & Laminin coated 1.9 cm^2 x 24-well plates (Corning), while NPCs to be differentiated into Astrocytes were plated at 2.5 x 10^4 cells/mL into Matrigel precoated 1.9 cm^2 x 24-well plates (Corning). Initially, each well contained 450 ul of 100% Expansion media for 24 hrs which was subsequently exchanged with appropriate differentiating media as described in the Gibco Neurobiology Protocol Handbook at Thermofisher Scientific, for differentiating neural stem cells into neurons and glial cells. Neuron differentiation medium was composed of 1x Neurobasal Medium, supplemented with 2% B27, and 2 mM GlutaMAX^{TM}. Astrocyte differentiation medium was composed of 1x D-MEM medium supplemented with 1% N-2, 2 mM GlutaMAX^{TM}, and 1% FBS. Oligodendrocyte differentiation medium was composed of 1x Neurobasal medium supplemented with 2% B-27, 2mM GlutaMAX^{TM}, and 30 ng/ml T3. Cells were grown in 5% C02 humidified

incubators. After 48 hours, 50% of original media was removed, followed by equal addition of appropriate media every two days for a total of 10 days. After differentiation, media was aspirated and cells were fixed with 4% PFA for downstream immunocytochemical analyses.

2.4) DNA Synthesis

A) [^{3}H]dT incorporation in rat cortical culture(*in vitro)*

Incorporation of ^{3}H-deoxythymidine ([^{3}H]dT, 2 uCI/mL), was used to measure DNA synthesis, as described previously (148, 149). Primary Cortical Cells (1x10^5 cells/well) were plated in Poly D lysine precoated 1.9 cm^2 x 24-well plates (Corning) containing same culture components described for rat cortical cell culture and incubated +/- VPA for 20 hours, followed by 4h incubation after pulse of [^{3}H]dT (2uCi/ml). Media was then aspirated, and cells were incubated with 0.25% Trypsin-EDTA (0.5 mM) at 37^{0}C for 20 min, followed by collection onto glass fiber filters using a cell harvester (Skatron, Sterling, VA), using water elution with use of a semiautomatic cell harvester (Skatron, Sterling, VA). Thymidine incorporation was counted by scintillation spectroscopy as described previously (149, 150). Experiments were performed three times or more, each experiment typically included three to four replicates per group.

B) Assaying proliferation of NPCs with 3[H]:

Human NPCs were plated at 1x 10^5 cells/ml and grown in 30% Expansion media +/- extracellular factors, on poly-D-Lysine (0.1 mg/mL, Sigma)

and Laminin (5 μg/mL, Invitrogen) 1.9 cm^2 x 24-well coated plates (Corning)

and cultured in a humidified 5% C02 incubator at 37 ^{0}C . After 46 hrs,

radioactive, tritiated [^{3}H]-thymidine was added to each well (1.5 μCi/mL) and

plates were returned to the incubator. After 2 hrs, radioactive medium was

aspirated and 300 μL of pre-warmed 0.25% Trypsin-EDTA (0.5 mM) was added

to each well and then incubated for 20 minutes. Cells were then collected onto

glass fiber filters using a cell harvester (Skatron, Sterling, VA). DNA

incorporation was counted with a scintillation spectroscopy as described

previously (149, 150)

2.5) *In Vivo* VPA Administration

A) Five injection paradigm:

Time-mated, pregnant E16.5 Sprague Dawley rats received VPA or Saline

control injections twice a day (300mg/kg body weight) subcutaneously for three

days totaling 5 injections. VPA was dissolved in 0.9% saline vehicle at a

concentration of 150mg/ml. All rats were injected with BrdU (50 mg/kg)

subcutaneously 2 hours prior to sacrifice at E18.5. After sacrifice, embryos were

removed by caesarian section, and cervically transected in sterile Saline glucose

on ice. Some embryonic heads were immediately drop fixed in 4% PFA

overnight at 4 ^{0}C, while others were rapidly dissected in Saline Glucose solution

on ice, to extract and then freeze whole cortices at-80 ^{0}C for later protein

analyses.

B) Three injection paradigm:

Time-mated, pregnant E15.5 Sprague Dawley rats received VPA or Saline injections twice a day (300mg/Kg body weight) subcutaneously for a total of 3 injections. VPA was dissolved in 0.9% saline vehicle at a concentration of 150mg/ml. All rats were injected with BrdU (50 mg/kg) subcutaneously 2 hours prior to sacrifice at E16.5. After sacrifice, embryos were extracted, and rapidly cervically transected in sterile Saline glucose on ice. Skull and meninges were removed and some embryonic heads were drop fixed in 4% PFA overnight at 4 ^{0}C, while other embryonic cortices were extracted and frozen in -80 ^{0}C for later protein analyses.

2.6) Protein Collection and Western Blotting

A) Methods for collection, and analysis for in vitro rat cortical precursors

E14.5 rats cerebral cortical precursors were incubated on 35mm poly-D-lysine coated dishes (Corning) at a density of 2 X 10^6 cells/dish containing same culture components described for rat cortical cell culture and exposed +/- VPA for various time points. Most studies harvested protein after 4 or 24 hours, followed by two 1X PBS washes followed by lysis with buffer consisting of 50mM Tris-HCl (pH 7.5), 0.2mM EGTA, 2mM CaCL2, 10ug/ml leupeptin, 10ug/ml aprotinin, 20ug/ml soybean trypsin inhibitor, 1% Triton X-100, 1% 3-[(3-cholamidopropyl) dimethylammonio]-1-propanesulfonate (CHAPS), 0.5% Nonidet P-40, 50mM NaF, 0.5mM microcystin-LR and 1mM PMSF. Unless otherwise stated, all factors were obtained from Sigma. Lysed samples were sonicated using an

Ultrasonics Sonicator (Qsonica, LLC, Newtown CT) on ice and spun down at 4

^{0}C to pellet cell debris. The supernatant was then transferred and measured for

protein levels. Protein concentration was measured with the BCA-protein assay

(Pierce, Rockford, IL) in a Spectrophotometer (Beckman, Indianapolis, IN), and

calculated with comparison to a Bovine serum albumin (BSA) standard curve.

Equivalent protein extracts per lane (10-50 ug) were then separated on 12%

acrylamide gel and transferred to polyvinylidenediflouride (PVDF) membrane

using transfer apparatus at 100V for 1-2 hours. The membranes were blocked

with 5% milk and incubated with primary antibody against cyclin E1 (1:200

Abcam., Boston, MA), acetyl-Histone H3 (1:1000 Milipore., Mahopac, NY), Total

Histone H3 (1:1000, Milipore., Mahopac, NY) and GapdH (1:25000 Meridian Life

Science., Memphis, TN), cyclin D1 (1:200 Santa Cruz., Dallas, TX), HDAC1 and

HDAC2 (1:1000 Gifts from Dr. Karl Herrup), and followed by anti-mouse or anti-

rabbit horseradish peroxidase (HRP)-conjugated secondary overnight at 4^{0}C.

Immune complexes were revealed by using appropriate peroxidase-conjugated

secondary antibodies along with a chemiluminescent reagent (Perkin Elmer,

Waltham, MA) and system (Omega) as previously described (148, 151, 152).

B) Human NPCs

NPCs from passages P3 to P8 were plated in 35mm dishes coated with

poly-D-lysine, and Laminin, in 30% Expansion as described above, at a density

of $1X10^6$ cells/dish, and incubated for 48 hours at 37 ^{0}C with 5% C02.   Cells

were then treated with 10ng/ml bFGF or Vehicle for 10 minutes, and immediately

washed twice in ice-cold PBS followed by addition of lysis buffer consisting of

same components as described above for Rat *in vitro* studies. Protein
quantification, gel electrophoresis, transfer, immunoblotting, and visualization of
protein were also done as described above in western analysis of rat cortical
culture. Primary antibodies utilized for these studies included P-S6 (1:1000, Cell
signaling., Beverly, MA), Total S6 (1:1000, Cell signaling., Beverly, MA), Cyclin
D1 (1:200 Santa Cruz Bio., Santa Cruz, CA), phospho-p44/42 map kinase
(Thr202/Tyr204) (1:1000, Cell signaling Beverly, MA), Total p44/42 map kinase
(1:1000, Cell signaling., Beverly, MA) , total-p44/42 map kinase (1:1000, Cell
signaling., Beverly, MA), GapdH (1:25000, Meridian Life Science., Memphis, TN)

C) *In vivo* Rat protein collection and analysis

As described above, pregnant Sprague Dawley rats were sacrificed four
hours after the last injection of saline or VPA using C02 asphyxiation, followed by
cervical dislocation and bilateral pneumothorax to assure death of the mother.
Subsequently, embryos were harvested, and cortices were collected and stored
in -80 until sample analysis -80^0C. After thawing samples on ice, the tissues
were manually homogenized with 200 ul of lysis buffer and a series of needles,
(25G, 27 ½ G, and 30G) on ice. Samples were further processed by 2x 30
seconds of sonication pulse on ice, followed by centrifugation to remove cellular
debris, and transfer of supernatant to fresh tubes. Subsequent protein
quantification, gel electrophoresis, transfer, immunoblotting, and visualization of
protein was also done as described above in western analysis of rat cortical
culture. Primary antibodies utilized for these studies included cyclin E1 (1:200
Abcam., Boston, MA), Tbr2 (WB 1:1000, 1: 300 IHC, Abcam., Boston, MA), Pax6

(WB 1:750, IHC 1:300 BioLegend., SanDiego, CA), acetyl-Histone H3 (1:1000

Milipore., Mahopac, NY), Total Histone H3 (1:1000, Milipore., Mahopac, NY)

2.7) RNA isolation:

A) *In vitro* isolation *and* extraction of RNA:

Rat cortical cultures were plated (2×10^5 cells/dish) on poly-D-lysine

(0.1mg/ml) coated 35mm dishes (Corning) containing same culture components

described for rat cortical cell culture +/- VPA and +/- cyclohexamide. in

DMEM/F12 media with or without VPA as described above. Dishes were then

incubated in humidified 5% C02 incubators at 37 degrees between 2 and 24

hours before RNA extraction. At point of harvest, media was aspirated and

washed twice with DEPC treated PBS briefly on ice, followed by RNA isolation

with TRIzol reagent (Invitrogen) and downstream treatment with RNase-free

DNase (Qiagen Germantown, MD).

For cyclohexamide experiments, cortical cultures were plated with

treatment of 1 ug/ml cyclohexamide (Gift from Dr. Maduras lab) for one hour to

ensure sufficient inhibition of the elongation phase, followed by addition of 1mM

VPA or DMEM/F12 vehicle to be incubated an additional for 4 hours at 37 ^{0}C. At

point of harvest, procedures followed steps listed within *in vitro* isolation and

extraction of RNA.

B) *In vivo* tissue isolation:

Samples came from adult pregnant Sprague Dawley rats, and their

embryos, sacrificed at E14.5, E16.5, E19.5. Additional tissue came from postnatal day 60 male Sprague Dawley. After sacrifice, brain tissue was removed with DEPC treated scissors and spoonulas. Embryos were first removed by caesarian section and then rapidly dissected in DEPC treated sterile PBS on ice. Extracted tissue was placed in conical tubes and rapidly frozen in liquid nitrogen. RNA was later isolated from tissue with TRIzol reagent (Invitrogen) and subsequently treated with RNase-free DNase (Qiagen Germantown, MD).

C) *In vitro* qRT-PCR and analysis

cDNA was generated using Superscript II reverse transcriptase (Invitrogen) and random primers (Promega). Gene analysis was quantified by qPCR using the following conditions: 25 *ul* samples containing (1 ng) cDNA in a 1x Sybr Green Master mix, Ultra Pure dH20 (Invitrogen), and a final concentration of 20um for each Primer pair. Samples were run in 96 multiwell reaction plates (Applied Biosystems), using the ABI PRISM 7300 Real-Time PCR System (Applied Biosystems). All qPCR reactions were run under the following conditions: 50 C for 2 minutes, 95 C for 10 minutes, then (40 cycles) of 95 C for 15 s and 60 C for 1 minute. Lastly, a dissociation stage was added to provide primer melting points which included the following conditions: 95 C for 15 seconds, 60 C for 1 minute, followed by 95 C for 15 seconds.

Primer sequences for qRT-PCR were as follows: Cyclin E1 forward, 5'-AGC CCC CTG ACC ATT GTG -3', and reverse 5'- TCG TTG ACG TAG GCC ACT TG-3';

Cyclin D1 forward, , 5'- GGC CCA GCA GAA CAT CGA T-3', and reverse 5'-GAC CAG CTT CTT CTT CCA CTT C-3'; Cyclin D3 forward , 5'-CTG TGA TTG CGC ACG ACT TC -3', and reverse 5'-CCG GTC ACT GGG CAG AGA -3'; and a proprietary sequence for rodent GAPDH on exon 1-1 (PrimeTime R qPCR Primers). Analysis of average CT values were normalized to average GapdH to yield ddCT values. Fold change values were calculated in logarithmic base 2 (2^ddCT).

D) *In vivo* RT-PCR and analysis of HDACs

cDNA was generated using Superscript II reverse transcriptase (Invitrogen) and random primers (Promega). Samples for PCR were then prepared using the following conditions: 25 *ul* samples containing (2 ng) cDNA in a Master mix containing the following: Taq man DNA polymerase (Invitrogen), Depc treated H20, 1x nucleotide mix (Promega) and a final concentration of 20um for each Primer pair. Samples were run in .5 ml Eppendorf tubes (Applied biosystems) using Thermocycler (BioRad). PCR reactions were run under the following conditions: 50 C for 2 minutes, 95 C for 10 minutes, then (30 cycles) of 95 C for 15 s and 60 C for 1 minute, finishing at 4 degrees C. cDNA samples were then run in Agarose gels electrophoresis containing Ethidium Bromide (EtBr) and imaged gels (BioRad). Semi-quantitative gene analysis of samples was measured against GapdH using image J.

Primer sequences for RT-PCR were as follows:

HDAC 1 Forward 5'-AGA AGA GAG CGG TGA TGA GG-3';HDAC1 Reverse 5'-

CGC TGG TCC CTA TCT AGT CC-3';HDAC2 Forward 5'-GAC TGT CCA GTG

TTC GAT GG-3';HDAC2 Reverse 5'-GTA GCT CGA GGA CAG CAA GC-

3';HDAC 3 Forward 5'-CTT ACG GGA TGG CAT TGA TG-3';HDAC 3 Reverse

5'-GCA GCC TAA TCG ATC ACA GC-3';HDAC4 Forward 5'-GGA GAA GGG

CAA AGA GAG TG-3';HDAC4 Reverse 5'-GGA TGA AGT CAG AAG CAG GG-

3';HDAC5 Forward 5'-TCG TCCGTG TGT AAC AGT GC-3';HDAC5 Reverse 5'-

GCC CTA GGG AGA TGT TAG GC-3';HDAC6 Forward 5'-CAG ACC ACA GGA

GCT TCA CC-3';HDAC 6 Reverse 5'-TCC TTG TGT CAG CAT CAA-3';HDAC7

Forward 5'-CAG CAG GAG CAA GAA CTT CG-3';HDAC7 Reverse 5'-GGA GGC

AGG AAG CG CTA AG-3';HDAC8 Forward 5'- CGA GTA TGT CAG CAT CTG

CG-3';HDAC8 Reverse 5'-AGG GCA TAT GCT TCG ATC AG-3';HDAC9

Forward 5'-GCA GCT TCC TCC TCT CAG AG-3';HDAC9 Reverse 5'-GCT TAA

CCT CTG TGC TTG CC-3';HDAC10 Forward 5'-CAA GAA GGG TCA GCC TTG

AG-3';HDAC10 Reverse 5'-ACA TCG CTG AAT GAG CAC AC-3';HDAC11

Forward 5'-CAG GAG TCA GGG AAG ACA GC-3';HDAC11 Reverse 5'-GAC

CTA TGG GCA CCA TCA TC-3

2.8) Fluorometric HDAC enzymatic activity assay

Primary cortical cells (1×10^5 cells/well) were plated in Poly D lysine

precoated 0.25 cm^2 x 96-well clear flat bottom plates (Corning) containing same

culture components described for rat cortical cell culture +/- VPA and incubated

for 24 hrs. Following incubation, all wells were incubated with Fluor de Lys®

substrate, followed by developer as per kit instructions (Enzo Life Sciences, Farmingdale, NY). Relative HDAC activity per well was measured in a Microplate fluorimeter, Ex 350 nm Em 460 nm, and signal was determined after subtraction from background in "blank wells" without cortical cells. All conditions were measured in three wells per experiment.

2.9) Immunocytochemistry

A) In vitro studies with Rat cortical precursors:

In vitro cultures of Rat cortical precursors were plated in 35 mm Poly-D-Lysine coated dishes (Corning) and fixed at 24h with 4% paraformaldehyde for 20 minutes, as described by (147). After fixation, cells were washed 2x with phosphate buffered saline (PBS) and then blocked with Normal Goat Serum, followed with staining with antibodies against HDAC1, HDAC2 (1:1000, gifts from Dr. Karl Herrup) in PBS containing 0.3% Triton , and nuclear marker Dapi (1:1000 Sigma-Aldrich, Allentown, PA), or Bromodeoxyuridine (BrdU) (1:100, Dako, CA).

B) Immunocytochemistry with human NPCs:

After designated culture period, media was aspirated, and cells were fixed with 4% ice-cold Paraformaldeyhde for 20 minutes, followed by 3 PBS washes. Cells were then blocked in 5% goat serum + PBS containing 0.3% Tween for 1 hour followed by incubation with primary antibody in PBS 0.3% tween overnight at 4 degrees C. Cells were then washed in PBS, and incubated with secondary antibody in PBS 0.3% Tween for 1 hour at room temperature, followed by PBS

washes. Finally cells were counterstained with Dapi 1:1000 for 10 minutes

followed by two brief PBS washes. Primary antibodies used includes Nestin

(1:2000 EMD Milipore., Billerica, MA), Sox2 (1:1000 Abcam., Boston, MA), GFAP

(1:4000, Sigma., St. Louis, MO), Tuj1 (1:5000, BioLegend., SanDiego, CA), Pax6

(1:500 BioLegend., SanDiego, CA), O4 (1:500, R&D Systems), Oct4 (1:250

SantaCruz., Dallas, TX)), Tau (1:500 SantaCruz., Dallas, TX), Doublecortin

(1:300 SantaCruz., Dallas, TX). All staining was visualized using red and green

Alexa Flour secondary antibodies (1:1000, Molecular probes ThermoFisher.,

Waltham, MA) using fluorescent microscopy (Leica, CA).

2.10) Immunohistochemistry

E18.5 embryos were removed by caesarian section, and rapidly dislocated

in sterile Saline glucose on ice.   Heads were then immediately drop fixed in ice-

cold 4% paraformaldehyde, and stored overnight at 4 degrees C. Fixed heads

were washed 2x with PBS and then placed into a 30% sucrose solution at 4^0C

until settling at bottom of scintillation vials (Wheaton). Brains were then

imbedded in plastic cups containing TissueTek® OCT compound (VWR), frozen

in dry ice and stored at -80^0C until sectioning. Fixed brains derived from the

treatment were then sectioned using a cryostat (Leica, CA) at 14 um thick slices

in a 1:5 series onto positively charged glass slides (Fishersci), and then heated

on slide warmer for 2 hours for improved attachment. Sections were staged

rostral/caudally using landmarks from the 1996 Paxinos atlas (185),

corresponding with Figures 97-99, and then stored at $-20\ ^0$C until later use.

Sections corresponding closest to Figure 97 were selected if they contained at least two of the following anatomical landmarks: Ventral hippocampal commissure (VHC), Anterior commissure (AC), fimbria of hippocampus (Fi), and anterieror transitional promontory (ATP); subsequent sections in series were also chosen until the last section prior to containing the external medullary lamina (eml) and dorsal third ventricle (D3V). Slides containing sections within Figures 97-99 were selected for immunostaining. Immunohistochemistry was conducted as previously described (153, 154).   Antigen retrieval was performed as previously described (153) with modifications. In short, slides were heated in steamer at 92-98^{0}C for 10 minutes during antigen retrieval with citrate buffer. Subsequently, sections were washed in 1xPBS, blocked in 5% goat serum + PBS 0.3% triton, and then incubated with anti-BrdU antibody (1:100) overnight at room temperature. The next day, sections were washed in 1XPBS, incubated with fluorescent antibodies in PBS 0.3% triton at room temperature for 1 hr, followed by three1X PBS washes, and incubated overnight at room temperature in anti Pax-6 (1:300) containing 1% BSA 10% milk + PBS 0.3% triton, or anti Tbr2 (1:300) containing 1% goat serum PBS 0.1% triton. Slides were then washed in 1XPBS, and incubated with fluorescent secondary antibodies at room temperature for one hour in PBS 0.3% triton. Following subsequent washes, slides were stained with Dapi 1:1000 (Sigma) for 10 minutes, followed by brief 1XPBS wash, and cover slipped (Sigma) after addition of fluoromount™ (Sigma-Aldrich). All staining was visualized using red and green Alexa Flour Molecular probes secondary antibodies 1:500 (ThermoFisher).

2.11) **Stereological analyses**

Analysis of E18.5 brains was restricted to the middle third of the ventricle for each section, as determined at 4x using the endpoints of the ventricle at furthest lateral extent and closest to midline. Boundaries were drawn within the region of Pax6 or Tbr2 stain compartments for each section using Stereoinvetigator software and the optical fractionator probe. The counting grid was superimposed over the drawing of each section and the total cell numbers for each population was determined using the optical dissector method, by counting stained cells within green but not red regions of dissector for all sections of the series. The dissector box was defined as 15x 15 x 10um with a 3 um guard zone. For Tbr2 stained sections, the sampling grid size was 35x 35, and 50x50 for Pax6 sections. Immunopositive Pax6 or Tbr2 cells were defined as being stained in over 50% of the nucleus and signal exhibited overlapping nuclear boundaries with Dapi stain. BrdU stain was visibly positive if signal appeared in 40% of the nuclei and overlapped in region with Dapi stain. All Dapi positive cells were also recorded within appropriate areas within dissector box for all sample sites counted. Analysis for each brain ranged from 3 to 5 sections per brain. To ensure sufficient sampling, a coefficient of error value of $\leq.1$ using Gundersen m=1 was utilized for Pax6 and Tbr2 markers.

Experimental Results

Chapter 3: Dysregulation of neurogenesis by Valproic acid exposure

3.1) Previous lab findings and rationale for Valproic acid study

<u>Valproic acid exposure promotes G1-S transition in vitro and in vivo, suggesting an HDAC inhibition mechanism, and leads to more upper layer cerebral cortical neurons</u>

Past experiments in our lab using In vitro and In vivo analyses have established a working paradigm and foundation for the Valproic acid story. The following paragraphs describe these findings in order to present sufficient background and rationale for my experimental design and results.

Initial analyses assayed Valproic acid effects on E14.5 cortical cultures with the expectation that it would be inhibitory on DNA synthesis. Interestingly, 24 hr cortical cultures, incubated with a terminal 4 hr 3[H] pulse prior to harvest, demonstrated that VPA could increase DNA synthesis. A VPA dose response study revealed biphasic effects, with significant peak seen between 0.3 and 1 mM followed by inhibitory responses at 1.5 mM and 3 mM VPA. To determine if diminished responses were a result of toxicity and cell death, cell numbers were analyzed, and this revealed a small but significant decrease at both 1 and 1.5 mM while 3 mM appeared cytotoxic with a 50% reduction in cells respective to

control (Figure 5). Based on minimal cell death and dose response findings, 1

mM VPA was chosen for all subsequent *in vitro* studies of its mitogenic action.
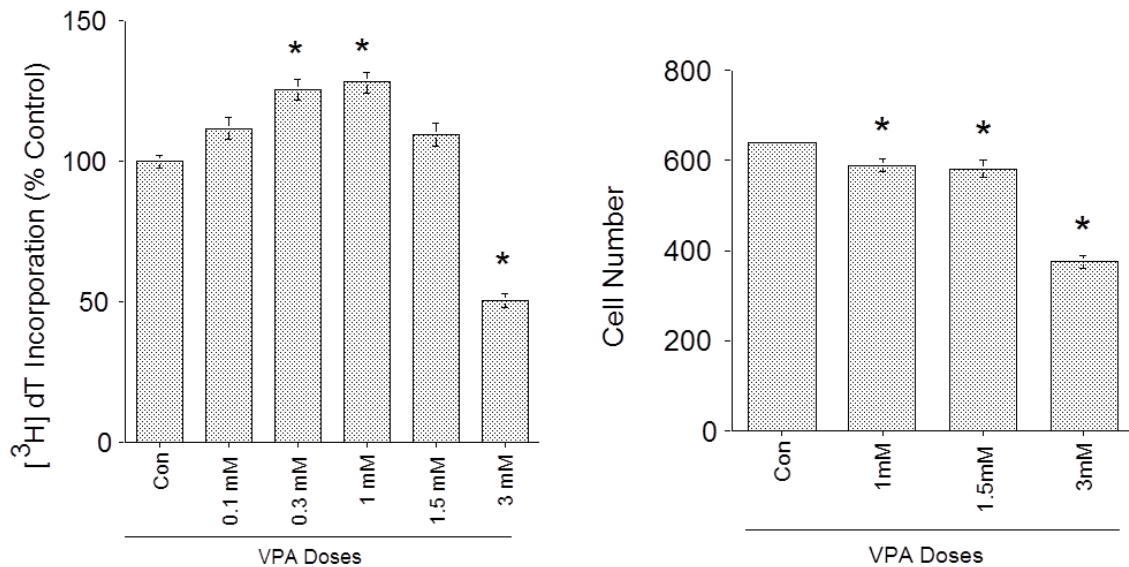
Figure 5 VPA exposure alters DNA synthesis with minimal changes in cell number *in vitro*: VPA exposure to 24 hr primary cortical culture elicits biphasic response in DNA synthesis depending on dose, with slight decrease in cell number at stimulatory, but not inhibitory doses, as visualized by [^{3}H] incorporation. N=4 expts, 4 wells per group. Cell number experiments revealed significant but minimal reductions in total cells after 24 hr exposure to 1 or 1.5 mM VPA, while dramatic reductions were observed after 3 mM exposures indicating significant cytotoxic effects. N=2 expts, 3 dishes per group. Unpublished data by Xiaofeng Zhou

To further understand the increase in DNA synthesis, which could suggest

more cells transitioning from G1 to S phase, the BrdU labeling index was

assessed to measure numbers of cells in S-Phase. Following 22 hours of

culture, a 2 hour pulse of BrdU was given, and the control labeling index of 22%

was increased to 26% with VPA, corroborating the elevated DNA synthesis

finding. Notably with more cells dividing the question would be if cells are

remaining neural precursors or differentiating, and immunohistochemical

quantification of neuronal marker nestin, and differentiated mature marker Tuj1

were analyzed. There was a significant increase in nestin positive cells by over

30% and 15% decrease in Tuj1 positive cells, suggesting that VPA treated cells

remain as precursor cells. With more cells in S phase making DNA, a likely

mechanism to explain this would be increased G1 to S phase transition, through

alterations in cell cycle machinery. Western analyses after 24 hrs revealed

greater than 50% increases in G1 cyclins D3 and E, but no change in D1. (Data

not shown)

Notably, the elevation in cyclin D3 and E protein is rapid, with differences clearly visible after 4 hours of VPA exposure. To define mechanisms VPA mediated signaling pathways were investigated after acute exposure

Figure 6 E14.5 *in vitro* protein analysis +/- VPA: Acute 1mM VPA exposure to primary cortical culture elicits rapid increases in G1 cyclin proteins D3 and E without activation of common mitogenic pathways. Early increases in cyclins is paralleled by increased Acetylated Histone H3. N≥3 expts
Unpublished data by Xiaofeng Zhou

examining P-ERK, GSK-3B, and P-AKT. VPA treated cultures exhibited minimal

changes in all pathways while an established mitogen, IGF1 robustly increased

signaling by 1 and 4 hours. With rapid changes in cyclins observed without

activation of typical mitogenic pathways, investigation of potential epigenetic regulation through acetylated Histone H3 was measured (Figure 6).

Literature has defined VPA as a HDAC inhibitor in cell lines, and our lab was able to visualize increases in acetyl H3 protein as early as 1 hr after VPA exposure, further supporting this claim, and providing correlative evidence that HDAC inhibition could be responsible for the observed G1 to S phase transition. To further test this hypothesis, two other established HDAC inhibitors, Tricostatin A (TSA) and (SAHA) were exposed to cortical culture alone, or in combination with 1 mM VPA. Measuring DNA synthesis revealed that HDAC inhibitors elicited similar increases to that of VPA, while the combination VPA with either drug was not additive, suggesting they act on the same pathway (Figure 7).
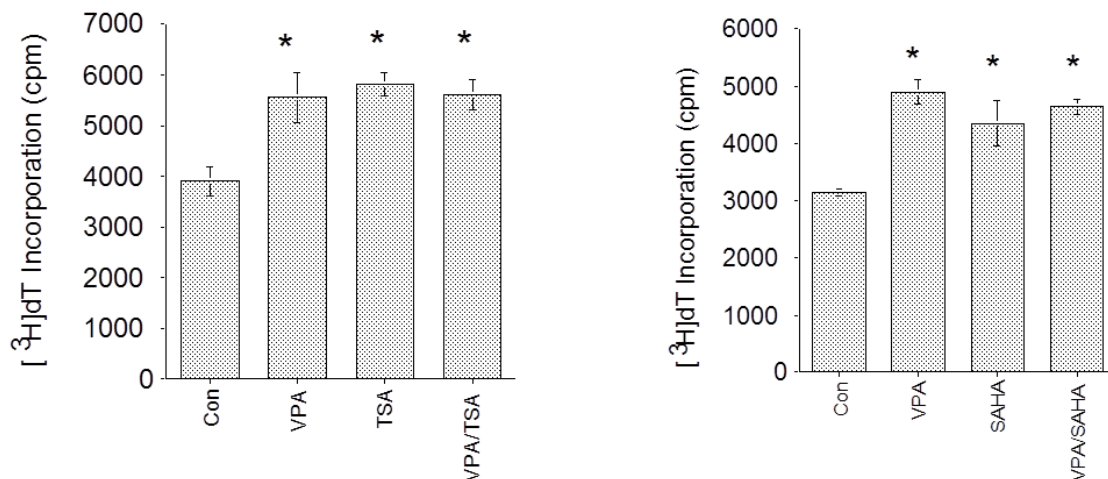
Figure 7 *In vitro* DNA synthesis increases due to HDAC inhibitors +/- VPA: Acute 1mM VPA +/- HDAC inhibitors (5ng) TSA or (0.1 ug) SAHA elicit non additive stimulations in DNA Synthesis. These data suggest that increased DNA synthesis for all these HDAC inhibitors likely occurs through the same mechanism. exposure to primary cortical culture elicits rapid increases in G1 cyclin proteins D3 and E without activation of common mitogenic pathways. Early increases in cyclins is paralleled by increased Acetylated Histone H3. N=1 expt, 4 wells per group. Unpublished data by Xiaofeng Zhou

However, additional studies would be needed to further understand how these

robust changes in cyclins related to the potential mechanism of HDAC inhibition.

To parallel in vitro studies, our lab conducted several in vivo experiments characterizing changes in DNA synthesis and downstream implications of this ASD risk factor on brain development. To focus studies, in vivo injections of saline or VPA were administered to pregnant mothers at various time points ranging from E12.5 to E19.5, analyzing DNA synthesis in the embryonic cortex. A 30% increase in 3[H] labeled thymidine was seen in VPA exposed cortices at E18.5 paralleled with 20% increase in BrdU labeling (Figure 8).
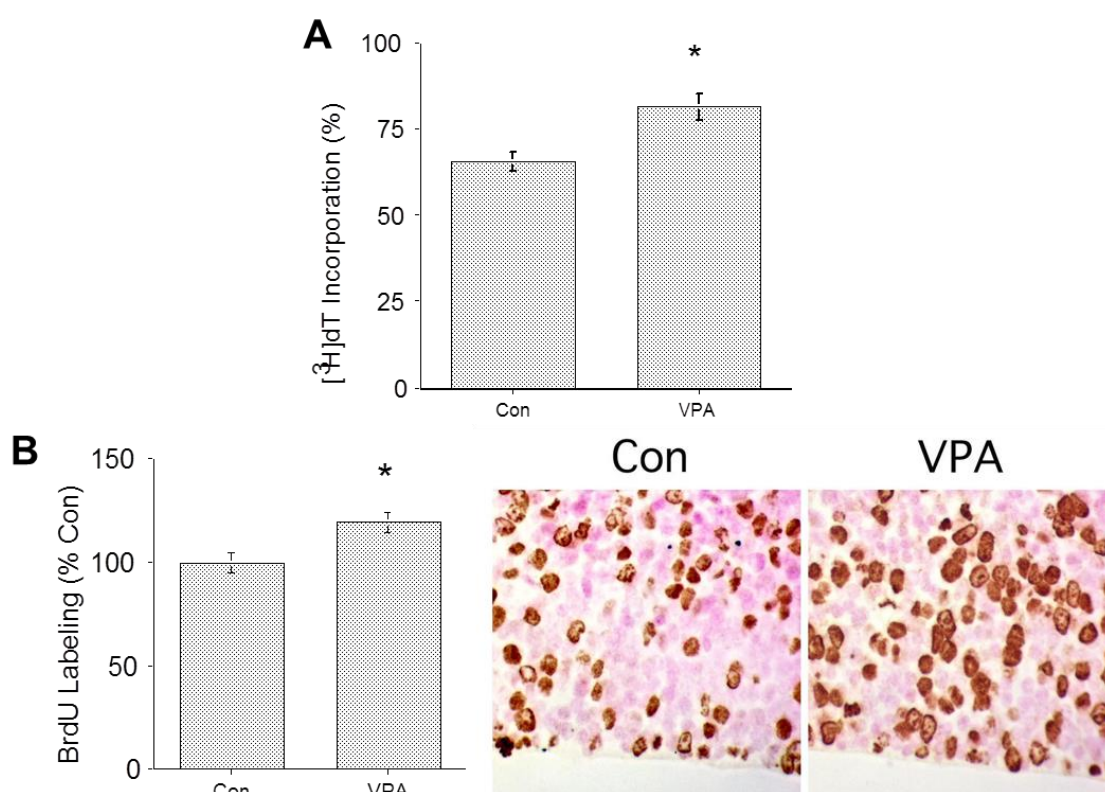
Figure 8 *In vivo* increases in DNA synthesis in E18.5 corticies after VPA exposure: A) 5 injection series of 300 mg/kg VPA or Saline to pregnant dams from E16.5-E18.5 followed by 3[H] pulse elicits increased DNA Synthesis in embryonic cortices. N=3 expts, 6 brains per group. B) 5 injection series followed by pulse with BrdU reveals increases in cortical precursors in S-Phase, as seen by DAB staining. N=2 expts, 3 brains per group. These data suggest that VPA is promoting G1 to S phase transition in the embryonic cortex. Unpublished data by Xiaofeng Zhou

With a defined time point, additional studies investigated changes after a series of 5 injections of VPA or Saline from E16.5 to E18.5. All western analyses seen in vitro were also replicated in vivo, with increased G1 cyclins D3 and E being observed after the 5 injection series. Further, early increases were seen 4 hours after single injection of VPA, a result that was paralleled by increased acetylated Histone H3 but not substantial increases in second messengers ERK GSK-3B or AKT which could explain early robust increases in cyclins (Figure 9).
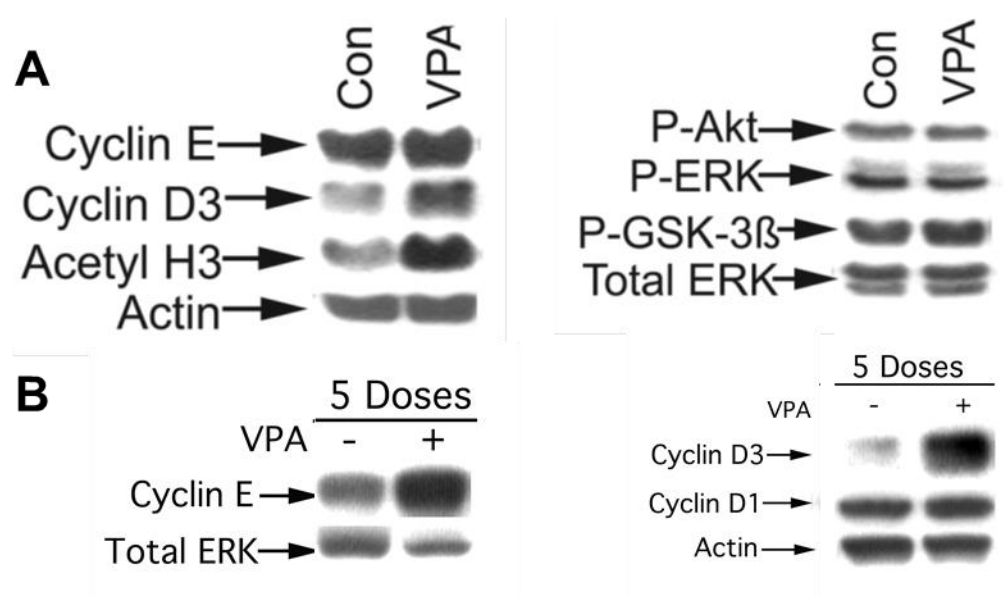
Figure 9 *In vivo* protein analysis +/- VPA: A) 1.5 hrs following a single injection of 300 mg/kg VPA or Saline to pregnant dams at E16.5 elicits rapid increases in G1 cyclins without activation of mitogenic pathways in vivo. B) Following series of 5 Saline or VPA injections from E16.5-E18.5, early changes in G1 cyclins persist. These data suggest that VPA is promoting G1 to S phase transition in embryonic corticies in vivo, replicating in vitro findings. $N \geq 1$ expt, ≥ 3 brains per group. Unpublished data by Xiaofeng Zhou

Considering that VPA injections increased DNA synthesis, numbers of cells in S phase and G1 cyclins, alterations in neurogenesis using stereological analysis were assessed on saline and VPA prenatally exposed embryos, sacrificed by postnatal day 21 (P21) for several neuronal and glial markers.

Stereology revealed a 13.8% increase in total cells within VPA treated cortices, and specific ~15% increases in neuronal type postnatal markers Tbr1 and Neu N. Further, there was a compartment specific 26.4% increase of upper layer neuronal marker Cux1, but no increases in interneuron marker GAD67 or glial marker S100B (Figure 10).

Group	Control	VPA	P-Value	% Increase
Cux1	15,699,036.75	19,849,869.75	0.0014	26.4
Tbr 1	22,920,123.00	26,446,271.75	0.0128	15.4
Neu N	26,249,810.50	29,996,770.75	0.0008	14.3
GAD 67	4,315,718.25	4,692,663.25	0.411	8.7
S100	6,607,790.00	6,707,567.00	0.7882	1.5%
Total cells	43,793,734.75	49,852,581.5	0.0169	13.8

Figure 10 Stereological analysis in postnatal Cortex +/- VPA: Following 5 injections of VPA (300 mg/kg) or Saline to pregnant dams from E16.5-E18.5, embryos were born and then sacrificed at P21. Stereological analysis revealed more total cells in VPA treated brains as well as preferential increases in neuronal specific markers. N$\geq$1 expt, $\geq$3 Brains per group. Unpublished data by Xiaofeng Zhou

These observations support that neuronal specific increases in neurogenesis are occurring that give rise to a bigger brain. However additional experiments remain to understand how VPA is preferentially upregulating upper layer neurons, and if this regulation is within all cortical precursors or a specific compartment of progenitor cells.

Within the following chapter, I will provide evidence and address these questions, to give a greater understanding how this environmental risk factor can alter cortical neurogenesis. Based on the preliminary findings, I hypothesized that VPA is promoting cortical neurogenesis through HDAC inhibition, which allows for G1 cyclin changes in neural precursors, thereby generating more neurons which preferentially reside in upper layers of the cerebral cortex. I expected that the postnatal increase in neuronal populations may be due to increases in radial glial and/or intermediate progenitor proliferation, and VPA may also promote cell cycle re-entry. To address this, I first investigated in vivo protein expression of cyclin E1 and Acetylated H3, to confirm mitogenic effects in cortical tissue seen in previous studies. This was followed by protein analyses of radial glial (Pax6) and intermediate progenitor (Tbr2) markers, in order to determine if gross changes in protein for either compartment could be seen after the VPA injection series. Additional investigations related this to stereological analysis of these two cellular populations, in order to determine estimated numbers of Pax6 and Tbr2 cells within a defined region, as well as their labeling indices. These findings will help identify which cell population(s) could have increased in order to generate more neurons by P21, with preferential increases in Cux1 expressing cells. To further support the proposed epigenetic mechanisms of rapid increases in G1 proteins corresponding with rapid increases in acetylated H3, I also expected to find HDAC expression in cortical precursors which can be enzymatically inhibited by VPA. Furthermore, changes in G1 proteins should correlate with similar alterations in message, so I

measured levels of these cyclin genes by qRT-PCR; any increases would suggest that increases in histone acetylation at this time are promoting transcription of genes followed by translation of protein. In sum, these questions will provide supporting evidence for mechanistic changes to cortical neurogenesis due to prenatal VPA exposure.

These studies will then be followed by complementary studies investigating changes in neurogenesis due to a genetic risk factor for ASD, the CNV 16p11.2. Within the larger picture, these two studies provide a greater understanding in how brain development can be altered by ASD risk factors, and may elucidate ASD etiology corresponding to early brain overgrowth and subgroups which have macrocephaly.

3.2) VPA Rodent Culture model findings

The rodent VPA model of Autism has primarily investigated the effects of the drug after one injection into pregnant dams at embryonic day 12.5, to recapitulate aspects of ASD (114). Others have exposed rodents to Valproic acid both in vitro and in vivo identifying several possible mechanisms which could explain how VPA may act (122, 127) . While most studies focus on single VPA injection at E12.5 to model Autism, additional researchers have investigated impacts of VPA at different developmental windows, also observing some molecular and behavioral aspects of ASD (118, 119, 121, 155). These findings suggest that multiple windows of vulnerability exist, that would be consistent with the usual human exposure during the entire gestation period. Thus, exposure

period in rodents can be catered to study cells of interest. To investigate

potential mechanisms of how VPA can impact cortical neuronal development

within the context of previous lab findings, it was first necessary to replicate key

results to determine rigor and robustness of the model.

A) Rat Cortical precursors exhibit increased proliferation *in vitro*

In addition to previous lab findings, others have suggested 0.2-0.5 mM

VPA exposure can increase NPC proliferation in rat cortical cultures when

exposed from E12 to E18 (118). With previous results from our lab finding rapid

increases in G1 cyclins and acetylated H3, but not activation of common

mitogenic signaling pathways, epigenetic modifications could be a potential

mechanism for this change. Recent literature identified VPA doses between .4

and 1 mM could inhibit by 50% many of the HDAC s in cell lines (30, 90),

although this mechanism has not been investigated in cerebral cortical

precursors. Therefore, I assayed DNA synthesis in primary rat E14.5 cortical

precursors including exposures of .03, 0.1, 0.3, 0.5, 1, and 1.5mM VPA for 24

hour incubation. I was able to replicate similar biphasic results observed in our

lab, with DNA Synthesis being significantly increased after exposure to VPA

doses between 0.3 mM and 1mM, with declining non significant increases by

1.5mM (0.3 mM VPA P=0.005, 0.5 mM VPA P=0.025, 1 mM VPA P=0.015, 1.5

mM VPA P=0.659). Analysis was conducted by experiment as percent control,

with maximal stimulations of these doses with increases from 147 to 172% from

control (Control=100% $\pm$15% SEM N=18 expts, 0.03 VPA =126% $\pm$12.84% SEM

N=3 expts, 0.1 mM VPA=134 +7.02% SEM N=3 expts, 0.3 mM VPA= 172% +

14% SEM N=7 expts, 0.5 mM VPA=147% +7% SEM N=15 expts, 1mM

VPA=161% +14% SEM N=8 expts, 1.5 mM VPA=131 +22.23% SEM N=4 expts)

(Figure 11). Additionally, the three maximal doses were not significantly different

from each other (P=0.2465), suggesting any of these doses may also elicit

increases in G1 cyclins paralleling our previous findings at 1 mM exposures.

Reports using cancer cell lines indicate VPA can inhibit HDACs within the

stimulatory doses used in my assay. Thus, it is possible that VPA may be

inhibiting HDACs within cortical precursors to increase DNA synthesis. However

additional studies must first confirm if lower doses of VPA can also stimulate G1

cyclins, providing similar mechanism to that seen in previous studies in our lab.
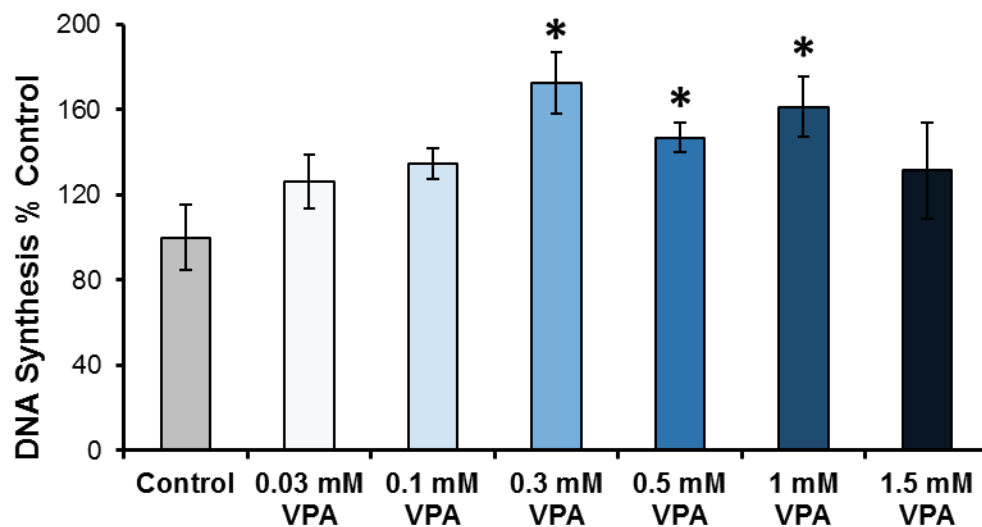
Figure 11 VPA dose response curve of DNA synthesis in E14.5 cortical
precursors: Exposing rat E14.5 cortical precursors to various VPA doses for
24h culture elicited biphasic changes to DNA synthesis, with maximal
stimulations between 0.3 and 1 mM VPA. This effectively replicates
previous lab findings and identifies 0.5 mM as another responsive dose. All
conditions were N≥3 experiments, 4 wells per group ; Control N=18, 0.03
mM VPA N=3, 0.1 mM VPA N=3, 0.3 mM VPA N=7, 0.5 mM VPA N=15, 1
mM VPA N=8, 1.5 mM VPA N=4

Exposure of cortical precursors to 0.5 mM VPA replicated previously observed increases in DNA synthesis after 24 hrs and this could suggest cells are transitioning from G1 to S phase. To examine this further and replicate previous protein results, a preliminary approach was taken. Preliminary studies looked at cyclins which regulate the G1 to S phase transition. Considering previous dose response had no significant difference between 0.3, 0.5 and 1mM I assayed if the middle dose of 0.5 mM VPA could impact G1 cyclin proteins, and acetylated histone H3 after 4 hours of culture. Preliminary observations replicated previous findings with a 67% increase in Cyclin E1 (Fold Change VPA= 1.67 $\pm$0.05 SEM, N=2 expts). Additionally, Cyclin D1 was not observably changed compared to control (N=1). Preliminary analysis of acetylated Histone H3 protein also replicated with a 31% increase (Fold Change VPA=1.31 $\pm$0.04 SEM, N=2 expts). These findings support previous data, indicating that the G1 to S phase regulator Cyclin E is rapidly increased in response to VPA exposure, and this increase is paralleled with elevated acetylated Histone H3, supporting the notion that epigenetic modifications could be responsible for this mechanism (Figure 12). Because of this and previous lab findings of increased DNA synthesis after exposure to HDAC inhibitors TSA or SAHA, I hypothesized that HDAC message and protein would be present in developing rat cortical cells.
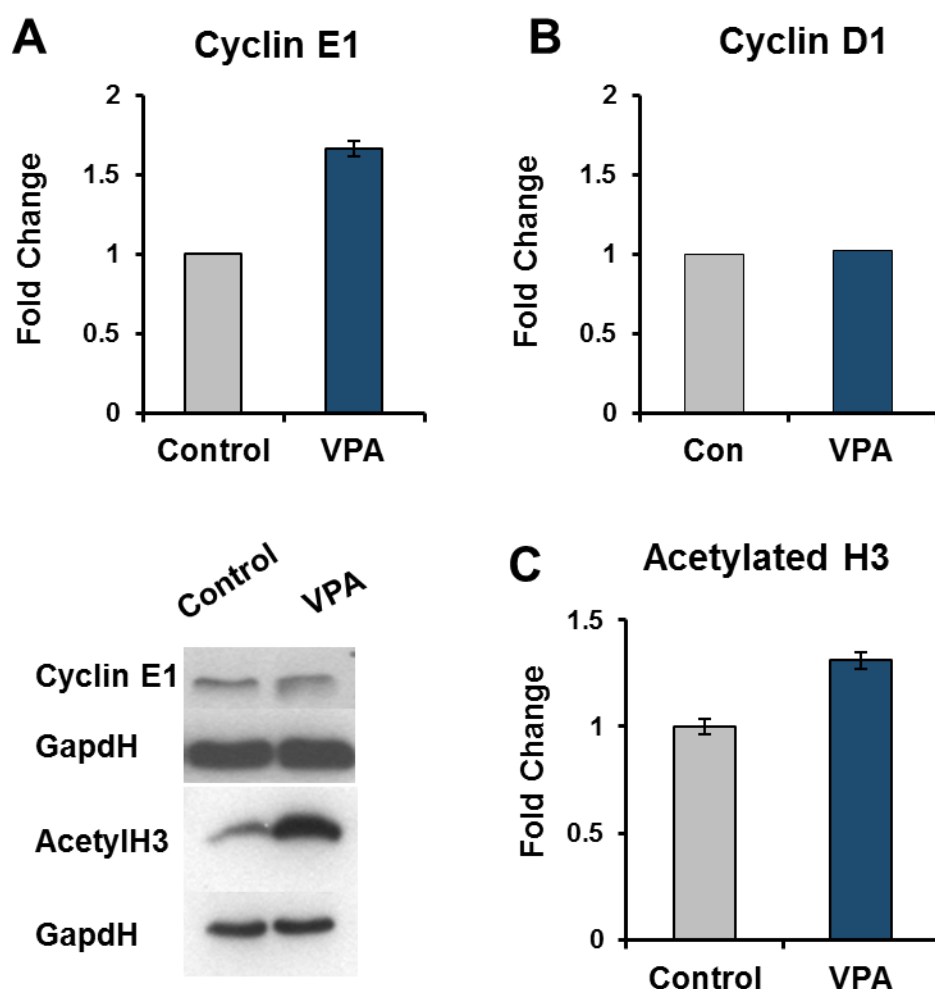
Figure 12 Preliminary replications of *in vitro* results +/- VPA: Following 4h exposure with 0.5 mM VPA, E14.5 cortical precursors increased acetylated Histone H3 and Cyclin E1 proteins, suggesting epigenetic mechanisms may regulate G1 to S phase transition. (A) Cyclin E1, N=2 expts, 1 dish per group (B) Cyclin D1, N=1 expt, 1 dish per group (C) Acetylated H3, N=2 expts, 1 dish per group

To further elucidate putative HDAC targets of VPA during cortical development, I designed intron spanning primers for all HDAC classes using Primer3 (www.primer3.com) and conducted semi quantitative analysis on cDNA derived from key developmental time points E14.5, E16.5 E19.5 and Adulthood. Preliminary results identified that all HDACs were observed in the cortex throughout development (Figure 13a). It was noted that HDACs 4, 6 and 11 had

multiple bands, suggesting alternate splicing may be occurring for these genes.
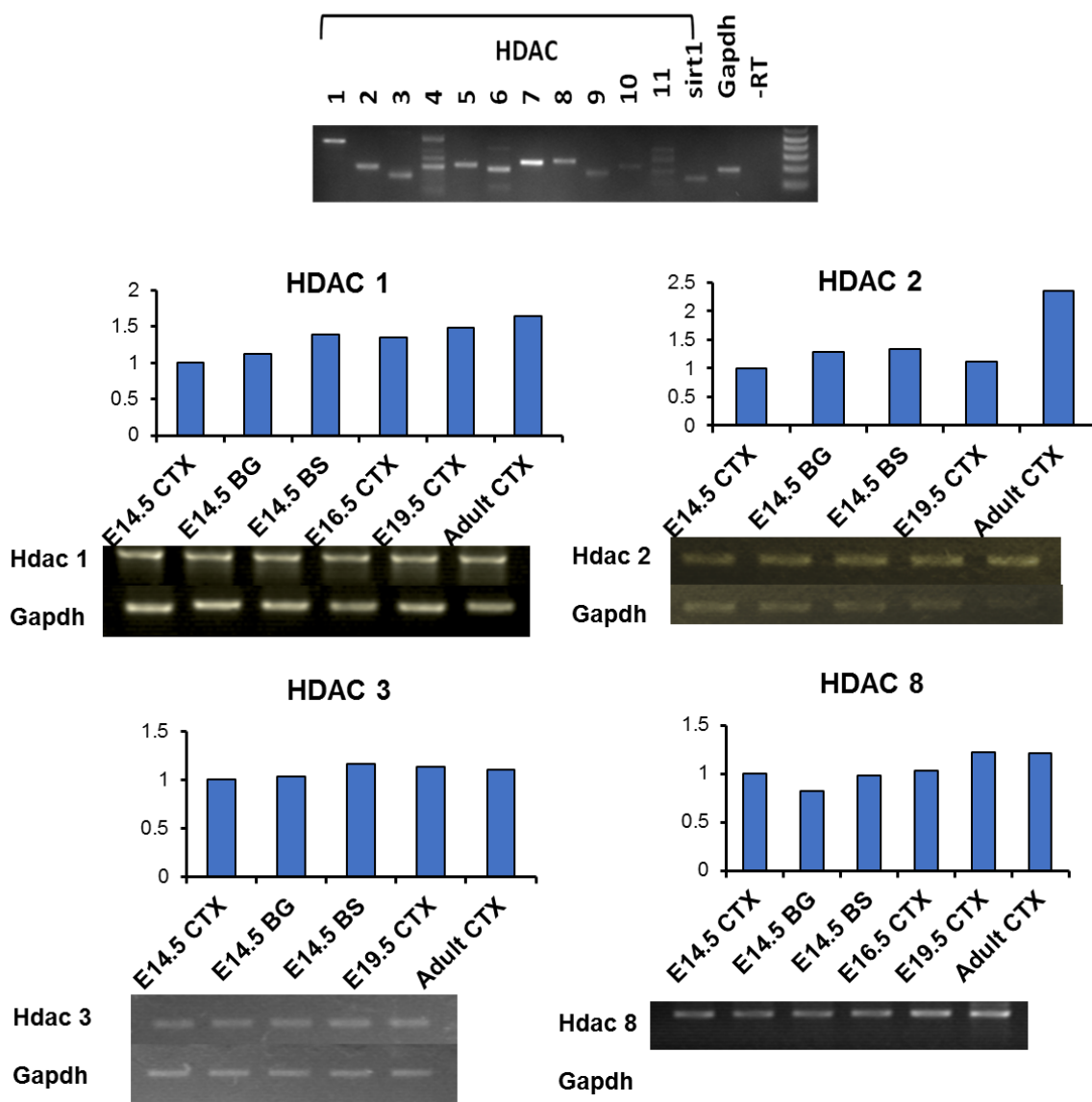
Figure 13 RT-PCR analyses of HDACs during development: A) Broad expression of HDAC cDNA in the E14.5 cortex B) Preliminary comparison of class I HDAC expression across E14.5 tissues and comparison of cortical message over development N=1 expt, 1 brain per age/region. All cDNA was detected after 30 cycles, with visualization by gel electrophoresis. CTX=cortex, BG=basal ganglia, BS=brain stem.

Next, I determined if there were tissue specific changes in individual HDAC message. Comparing cDNA from the cortex, basal ganglia and brain stem to GapdH for individual HDACs would identify if any class I HDACs were

differentially expressed. Preliminary results for HDACs 1,2,3, and 8 indicated

there were only subtle differences across tissues, suggesting HDAC message

appears to be expressed uniformly in these regions (Figure 13b). Although

certain HDACs had trending elevations, they all exhibited similar levels of

expression during cortical development. Given relatively uniform expression of

message, I decided to take a more limited approach with HDAC protein analyses.

Literature has

suggested that VPA

primarily inhibits

class I and II HDACs

with HDAC 1 being

most strongly

inhibited at an IC50

of .7 mM, followed

by HDAC2 at 0.8

mM (90). To

establish expression

of these HDACs in

cortical rat

precursors,
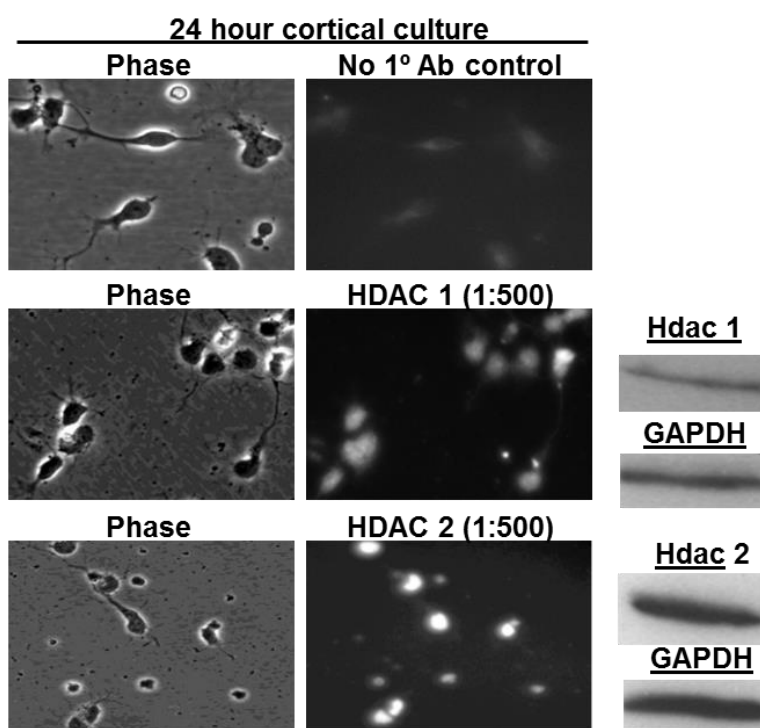
Figure 14 IHC and WB visualizations of HDAC 1 and 2 proteins in E14.5 Rat cortical culture: Analyses indicate HDAC expression after 24 hr culture. IHC N=1 expt, 3 dishes per group, WB N=1 expt, 1 dish

preliminary immunocytochemical and western analyses were conducted. Both

HDAC 1 and 2 were visualized by western and primarily within the nucleus of

cortical precursors (Figure 14).

To date, VPA has only been shown to enzymatically inhibit HDACs in cell lines (30, 90). Given the expression of HDAC protein and message in rat cortical cells, and previous evidence that VPA exposure to cortical precursors elicits increases in acetylated Histone H3, I hypothesized that rat cortical precursors have HDAC activity which can be enzymatically inhibited by VPA. To test this I measured HDAC enzymatic activity in rat cortical precursors with and without VPA doses able to increase DNA synthesis for these cells.
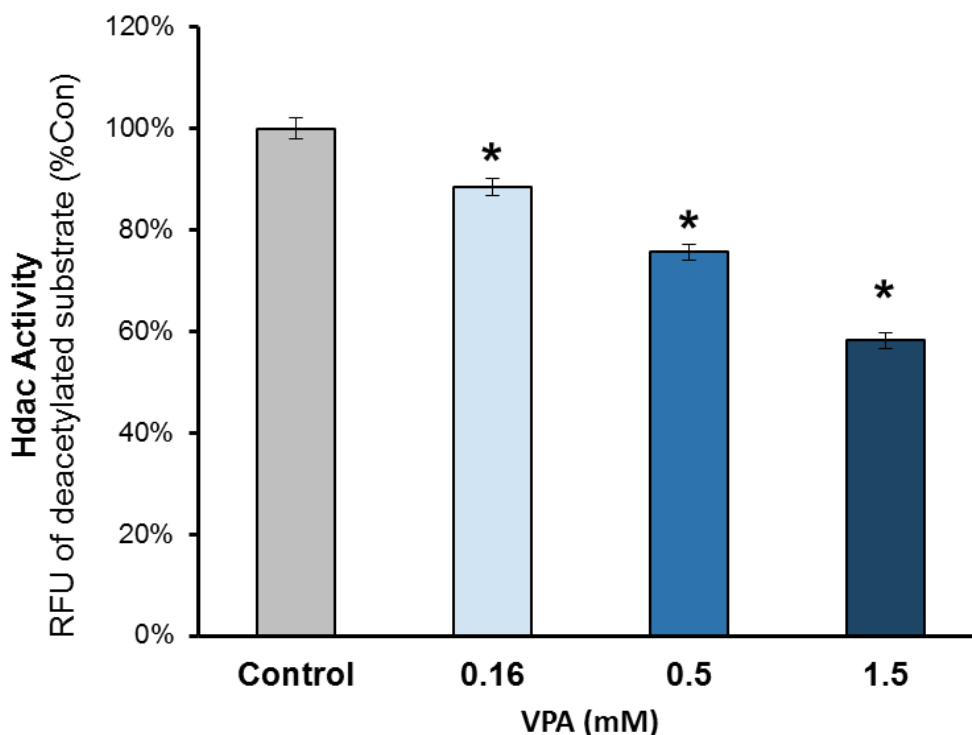
Figure 15 HDAC enzymatic activity +/- VPA in E14.5 cortical culture: E14.5 Rat cortical cells exhibit endogenous HDAC activity, as visualized by deacetylation of fluorescent substrate. VPA exposure is able to inhibit HDACs in a dose dependent manner. Fluorescence was measured in a fluorometer, Ex 350 nm Em 460 nm. This data suggests HDAC inhibition could occur from VPA doses that can increase G1 cyclins and DNA Synthesis. N=2 expts, 3 wells per group

Cortical precursors exhibited endogenous HDAC activity, and this was inhibited in a dose dependent manner by VPA (HDAC Activity Control= 100% $\pm$0.02% SEM, VPA 0.16mM= 89% $\pm$0.018% SEM, VPA 0.5mM= 76% $\pm$ 0.016% SEM, VPA 1.5mM=58% $\pm$0.015% SEM P<0.006) (Figure 15). These data suggest that VPA can significantly inhibit enzymatic HDAC activity in cortical precursors at doses able to increase DNA synthesis and G1 proteins, and therefore could allow for alterations in gene expression.

<u>B) VPA exposure rapidly upregulates cyclin D3 and E1, while downregulating cyclin D1 message</u>

The G1 to S phase transition of cortical precursors observed after VPA exposure in vitro and in vivo is supported by rapid early increases in G1 cyclin D3 and E protein. Notably, these increases occur before activation of messenger pathways commonly activated by mitogenic stimulation. In addition, the upregulation of cyclin protein is paralleled with early robust increases in acetylated H3 and VPA is able to enzymatically inhibit HDACs at doses which can elicit all the aforementioned effects. This suggests it may epigenetically regulate cyclin genes. To investigate if this regulation is due to post-transcriptional modifications, rat cortical cultures were acutely exposed to 1mM VPA, and then expression of mRNA of several G1 cyclins was measured.

Initially, cultures were exposed to 1 mM VPA for 4 hr followed by qRT-PCR. This time was chosen because cyclin proteins were already elevated, without significant second messenger pathway stimulation, and elevated

message at this time would support post-translational regulation of cyclin

transcription by histone acetylation. Elevated cDNA was observed for both cyclin

D3 (1.88 fold $\pm$0.22 SEM P=.007 N=4) and Cyclin E1 at 4hrs (1.82 fold $\pm$ 0.13

SEM, P$\leq$.0001 N=4). These data suggest that VPA may be directly increasing

transcription through post translational modifications of the histones regulating

cyclin genes.   Next I measured cyclin D1 gene expression. Previous in vitro and

in vivo analyses indicated that cyclin D1 protein was not significantly changed

after VPA exposure for any time point. However, after 4 hr VPA exposure, cyclin

D1 message was actually decreased (0.65 fold $\pm$0.04 SEM P= 0.0002 N=4).

This may suggest post transcriptional and translational modifications could be

impacting the observed cyclin D1 levels. I next conducted preliminary studies to

characterize the duration of altered cyclin E1 message over time. Preliminary

results for 8 and 17hr exposures of VPA revealed similar increases in cyclin E1

message to previous time points (VPA 8hr=1.86 fold $\pm$0.08 SEM P=0.008 N=2 ,

VPA 17hr=1.95 fold N=1). These data support that upregulation of translation is

persistent, allowing for maintained increases in protein over time. To investigate

if mRNA is altered at an earlier time point, preliminary analysis measured cyclins

after 2 hr VPA exposure. At this earlier time point, cyclin E1 cDNA was still

increased (1.71 fold $\pm$0.01 SEM P=0.0004 N=2), as well as a trending increase in

cyclin D3 (1.79 fold $\pm$0.19 SEM P=.054 N=2). These data suggest that early

increases in message could contribute to the rapid increases in cyclin proteins

seen after acute VPA exposure. Further, it suggests that HDAC inhibition may

allow for increased acetylation at histones regulating the promoter site of these

genes. Analysis of cyclin D1 at 2 hrs was also reflective of its respective 4hr

changes (0.8 fold +0.04 SEM P=0.032, N=2) (Figure 16).
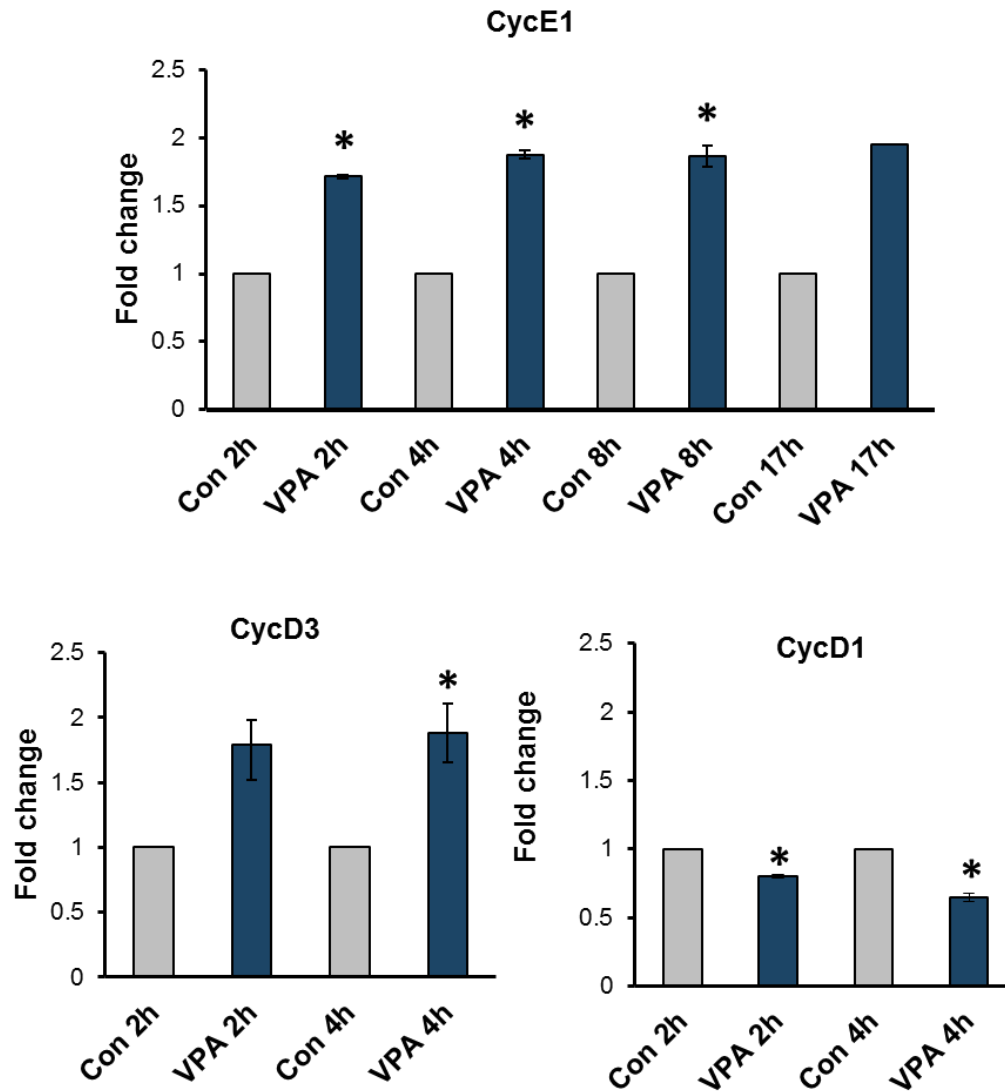
Figure 16 *In vitro* qRT-PCR analysis of G1 cyclins from E14.5 cortical precursors +/- VPA:
These data suggest that VPA exposure causes rapid upregulation of cyclin mRNA, likely due
to post transcriptional modifications of Histone acetylation. All qRT-PCR experiments were
done in triplicate wells per condition, with the following culture replicates (A) 2h N=2, 4h
N=4,8h N=2, 17h N=1. (B) 2h N=2, 4h N=4N=2 and N=4, (C) 2h N=2, 4h N=4

Altered message suggest that VPA be post translationally modifying

histone acetylation to reduce transcription of this gene, while unaltered protein

expression suggests it may also reduce D1 protein degradation. In sum, these rapid changes in message support that VPA epigenetically regulates these promoters, possibly through HDAC inhibition to alter levels of histone acetylation.

Therefore this epigenetic regulation of promoters is supportive of post translational modifications of the regulatory/epigenetic system, while unaltered cyclin D1 protein with decreased message also suggests VPA may post transcriptionally modify some proteins. Thus, VPA may enzymatically inhibit HDACs, altering acetylation of histone, causing changes in transcription at the promoters of cyclin genes.

Although the expectation is that VPA is increasing transcription of cyclin D3 and E1, likely through HDAC inhibition, one less likely mechanism would be increased transcription due to other proteins which in turn could regulate cyclin transcription or increase stability of existing proteins responsible for cyclin transcription. Cyclin E mRNA has been shown to be relatively stable through the cell cycle but exhibits minor expression changes during the cell cycle when using HeLa cells (156). However, treatment with actinomycin determined no alterations in cyclin E mRNA stability, yet cyclin E exhibits a half life of 3.3 hrs during G1-S phase transition (156). To investigate potential protein changes contributing to altered stability of cyclin E mRNA, I pretreated cortical cultures with cyclohexamide (CHX) to block protein synthesis at the elongation step, freezing message in the polyribosome, and then added VPA or vehicle 1 hour later, followed by 4 hr incubation. An observed increase of cyclin E1 message was seen after VPA treatment (VPA&CHX=2.41 fold $\pm$0.02 P<0.00001 N=3)

(Figure 17). This increase however is not statistically different from average fold increases of VPA under normal conditions (VPA -CHX= 2.1 Fold +0.47 SEM, P=0.5445 N=3) suggesting newly synthesized proteins are not significantly altering cyclin E1 proteins to stimulate this increased message.

CycE1
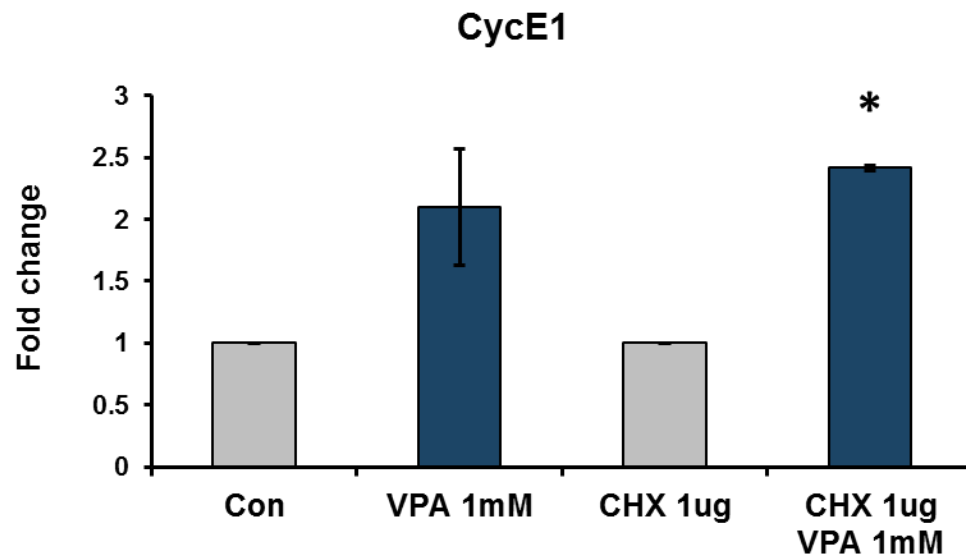
Figure 17 *In vitro* qRT-PCR analysis of cyclin E1 +/- VPA and cyclohexamide: E14.5 cortical precursors in control media or pretreated 1 hr with 1 ug cyclohexamide (CHX), followed by 4 hr culture +/- VPA. These data suggest that newly transcribed proteins do not contribute to increased transcription of cyclinE1 N=3 expts/ with 3 wells per condition.

In summary, cortical precursors exposed to VPA have increased transcription of cyclins D3 and E1 supporting that post transcriptional modification of histones is the primary mechanism to regulate these cyclin genes. Further, these modifications are likely due to HDAC inhibition, thereby allowing for subsequent increases in cyclin proteins to promote G1 –S phase transition, altering neurogenesis.

3.3) VPA proliferative effects *in vivo*

The most prevalent VPA animal model of autism originated by creating a model of human thalidomide studies, where prenatal exposure during days 20-24 of the first trimester resulted in 5/15 children to develop ASD (113). This model relies on a single injection of VPA at E12.5 to mimic exposure during the first trimester of human gestation, and has produced behavioral and anatomical abnormalities consistent with ASD. Macrocephaly has also been an observed outcome after a single VPA injection to rodent at E12, indicating VPA can impact neurogenesis (118). However, altering the time of VPA injection has also indicated there can be increases in glial precursors(119). Recently, chronic exposure of VPA throughout murine pregnancy has also revealed cortical dysgenesis in embryos, increasing numbers of their upper layer cortical projection neurons (121). Previous in vivo studies from our lab (unpublished) have also indicated proliferative increases, and greater upper layer neurons using a distinct injection paradigm. Taking all this information together would indicate VPA can promote proliferation of various progenitors.

In an initial attempt for the in vivo studies to closely model our in vitro exposure age of E14.5 precursors, litters were injected from E15.5 to E16.5 for 3 injections, followed by a BrdU injection 2 hrs prior to sacrifice. Subsets of embryos were dissected for protein analysis while remaining brains were reserved for stereology analyses. It was found by western that cyclin E1 levels did not significantly change (Saline=1 $\pm$0.09 SEM N=9, VPA=1.12 $\pm$12 SEM N=9,

P=0.25). Because VPA exposure had increased cyclin E1 protein and message

in vitro, supporting increased DNA synthesis changes, this in vivo result suggests

analyses at E16.5 may not be ideal to observe changes. Examination of

acetylated H3 levels also showed a non significant increase (Saline=1 ±0.12

SEM N=9, VPA=1.23 ±13 SEM N=9, P=0.23).
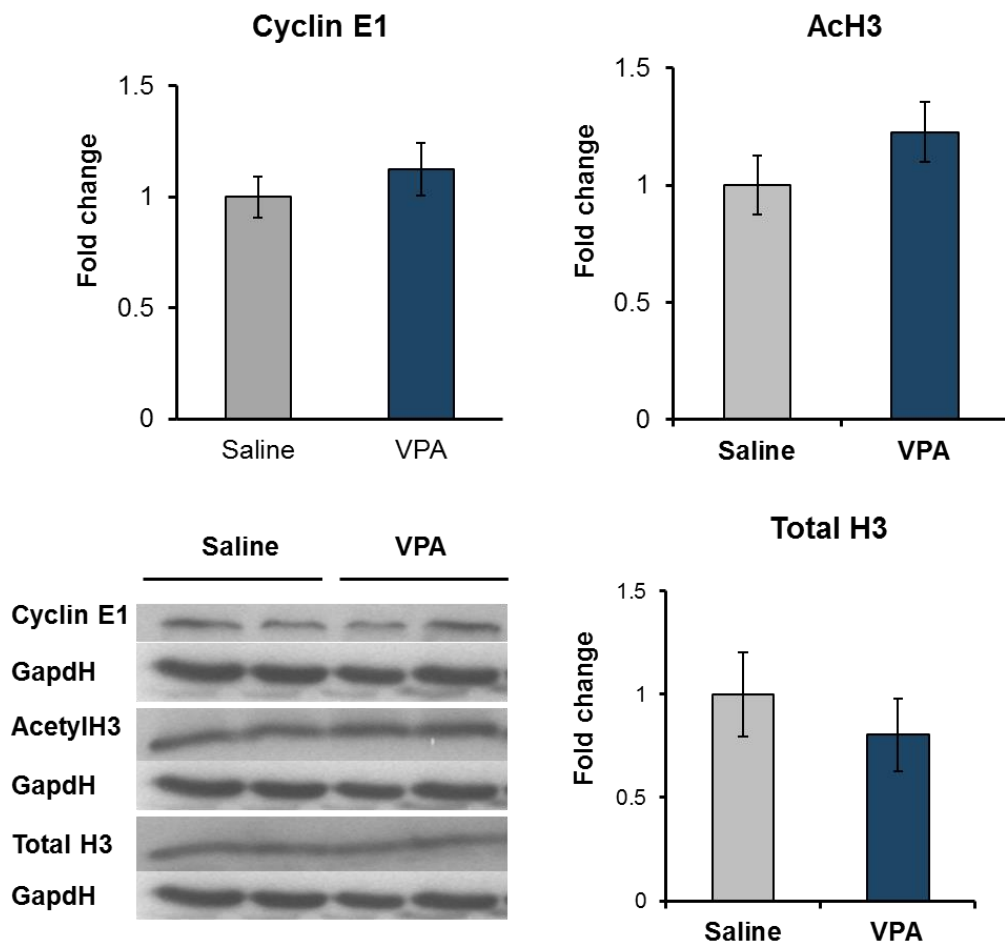
Figure 18 *In vivo* protein analysis at E16.5 +/- VPA: Pregnant dams were injected twice a day for a total of three Saline or VPA (300mg/kg) injections from E15.5 to E16.5, followed by sacrifice. No significant changes were observed in embryonic cortices, suggesting VPA is not robustly altering neurogenesis during this window. N=3 expts, 3 brains per group for CycE1 and AcH3. Analysis for Total H3 included N=1 expt, with 2 saline, and 3 VPA brains.

To investigate if total histone H3 protein was being altered due to VPA treatment,

I measured levels of total H3 normalized to GapdH for Saline and VPA brains,

which revealed no significant differences (Saline=1 ±0.2 SEM N=2, VPA=0.8

$\pm$0.17 SEM, P=0.52 N=3) (Figure 18). These studies at E16.5 are close to the

peak time of cortical neurogenesis, however results suggest it is not a robust

time to observe changes in cyclin E1. A possible explanation could be that too

many cells are still cycling during this higher period of cortical development to

observe robust increases in cyclin E1. This can be conceptualized by the

progressively increasing length of G1 over neurogenesis, which increases from

11.8hr at E15.5 to 12.8 hr E17 when the last rounds of cell cycle occur (3). Thus

this time period of exposure was not employed in further studies.

To investigate how VPA can give rise to a bigger brain in later

neurogenesis, I conducted our labs established series of 5 injections of saline or

VPA to pregnant rat mothers from E16.5 to E18.5, and then measured protein of

embryonic cortices.   There was a significant increase in cyclin E1 protein

observed in the VPA treated whole cortices (Saline=1 $\pm$0.021 SEM, VPA=1.58

fold $\pm$0.05 SEM P$\leq$0.00001 N=16). To ensure consistency of VPA effect and

putative mechanism with in vitro studies and other literature, acetylated Histone

H3 was measured. VPA treated embryos had a modest but significant increase

in Acetylated histone H3 (Saline=1 $\pm$0.02 SEM, VPA=1.07 fold $\pm$0.22 SEM

P=0.014 N=16) (Figure 19).
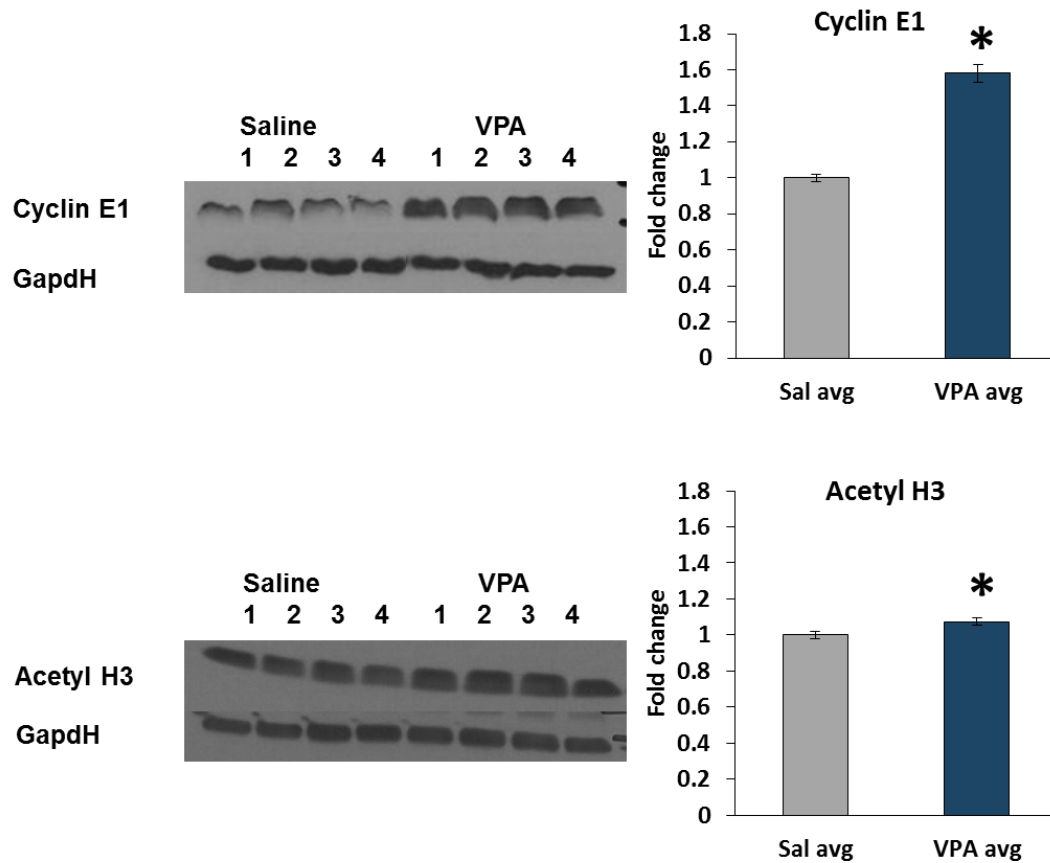
Figure 19 *In vivo* cyclin E and acetylated H3 protein expression in E18.5 cortices +/- VPA: Pregnant dams were injected twice/ day for a total of five Saline or VPA (300mg/kg) exposures from E16.5 to E18.5, followed by 2h BrdU pulse and then sacrifice. Embryonic cortices exhibited increases in Cyclin E1 and Acetylated H3 proteins suggesting VPA is stimulating neurogenesis during this window. N=3 expts, 4 brains per group, yielding a total of 12 brains per condition.

Because increases in cyclin E1 after VPA injection corresponds with our labs in vivo stimulation of DNA synthesis and BrdU labeling in embryonic cortices, I wondered whether specific precursor cell subsets were preferentially entering S phase. As described previously, cortical progenitor cells initially divide symmetrically as radial glia at the ventricular zone, and express the transcription factor Pax6. As these cells begin to mature, they transition to intermediate progenitor cells primarily within the SVZ with expression of the transcription factor Tbr2. To examine these compartment specific populations, I measured

protein levels of Pax6 and Tbr2. Expression of Pax6 was not visibly changed in embryonic cortices after prenatal VPA exposure (Saline=1 $\pm$0.016 SEM, VPA=1.02 fold $\pm$0.026 SEM P$\leq$0.59 N=12). However, Tbr2 was significantly increased in VPA exposed embryos (Saline=1 $\pm$0.11 SEM N=16, VPA=2.21 fold $\pm$0.28 SEM P$\leq$0.0008 N=17) (Figure 20).
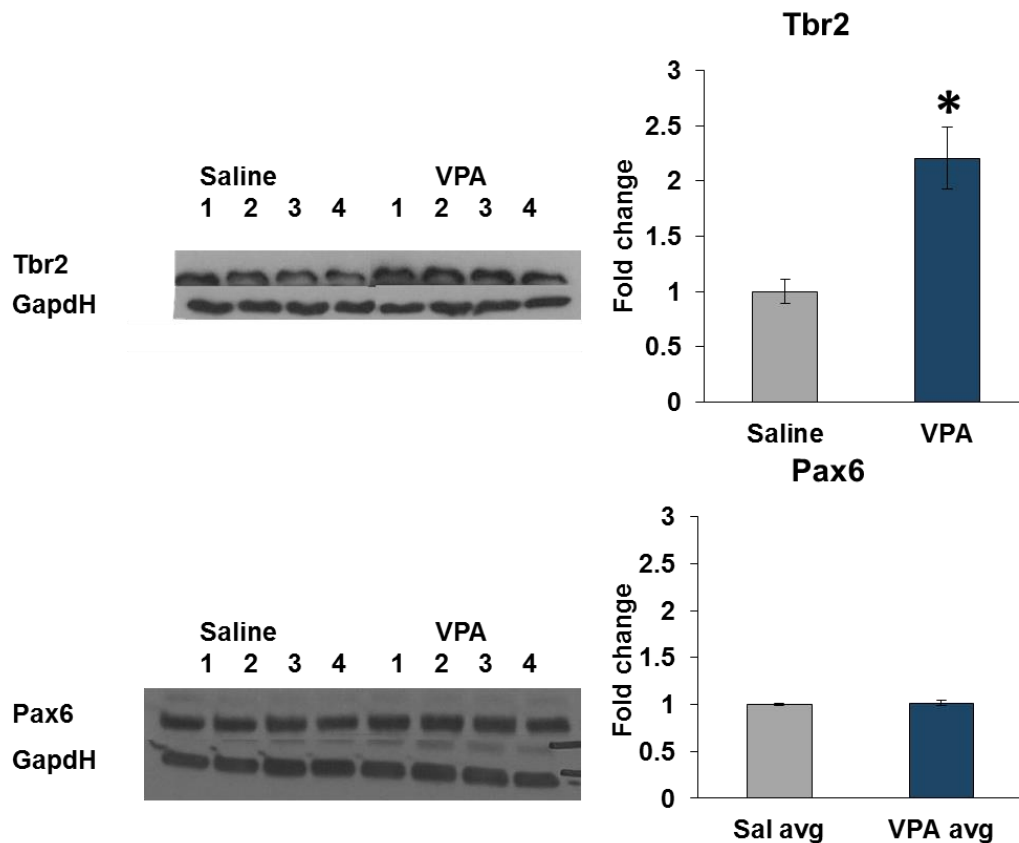
Figure 20 *In vivo* cyclin E and acetylated H3 protein expression in E18.5 cortices +/- VPA: Pregnant dams were injected twice/ day for a total of five Saline or VPA (300mg/kg) exposures from E16.5 to E18.5, followed by 2h BrdU pulse and then sacrifice. Embryonic cortices exhibited increases in Tbr2 but not Pax6 proteins, suggesting VPA may preferentially stimulate neurogenesis in the Tbr2 compartment. Pax6 N=3 expts, 4 brains per group, yielding 12 brains per condition. Tbr2 N=3 expts, $\geq$4 brains per group, yielding a total of 12 saline and 13 VPA brains per condition.

Therefore, in addition to increasing cyclin E1 and acetylated H3, prenatal exposure to VPA can also preferentially increase Tbr2 protein levels. Therefore

with evidence of increased Tbr2 protein, and previous findings in our lab that

VPA increases the BrdU labeling index in the embryonic cortex, I hypothesized

that VPA could be altering the labeling index of the Tbr2 specific population. To

address this, I used non biased stereology to examine if this VPA injection series

altered the percentage of TBR2 and/or PAX6 cells with BrdU, using a defined

region of the embryonic cortex (Figure 21a). This rostral and "dorsomedial"

region of the lateral ventricle was chosen as Pax6 is expressed along a gradient

rostral to caudal as well as medial to lateral (157, 158). Furthermore, Pax6, and

other homeodomain protein gradients are believed to regulate regional

development of neurons (159) and Tbr2 has been shown to have high rostral

expression, playing roles in neuronal specification (160). These overlapping but

distinct TFs were counted under high magnification revealing compartment

specific changes. Initially, the labeling index was counted for Pax 6 + BrdU+

cells within the pax6 dorsomedial region (Figure 21b,c). Analysis of the Pax6

labeling index revealed no significant difference between saline and VPA treated

brains (Saline=28.75% $\pm$0.014% SEM N=7, VPA=29.02% $\pm$0.013 SEM P$\leq$0.89

N=6) (Figure 21 d). However, the labeling index for TBR2 was significantly

increased in VPA treated embryos (Saline=20.3% $\pm$0.006% SEM N=7, VPA=23.6

$\pm$0.013% SEM P=0.006 N=6) (Figure 22 d).
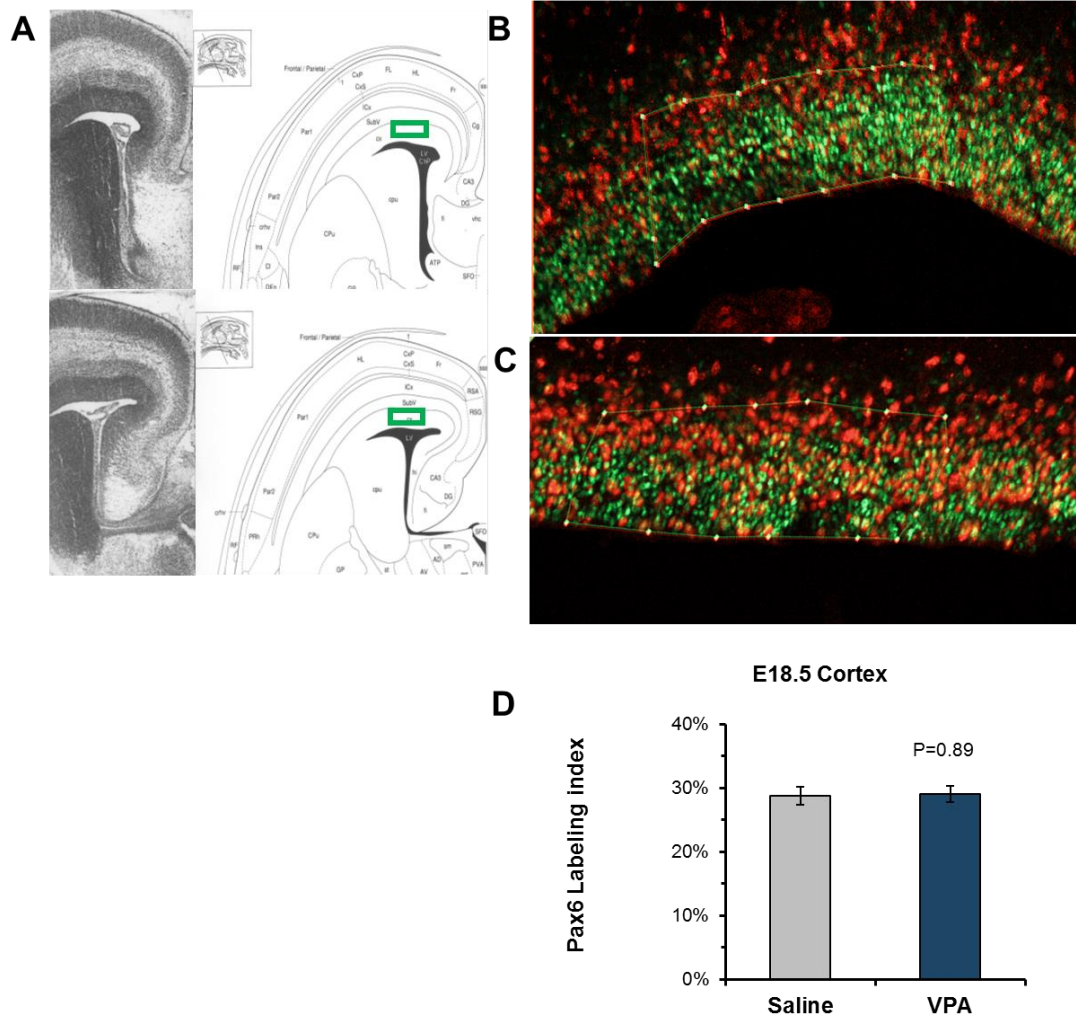
Figure 21 Pax6 labeling index in the E18.5 cortex +/- VPA: Pregnant dams were injected twice/ day for a total of five Saline or VPA (300mg/kg) exposures from E16.5 to E18.5, followed by 2h BrdU pulse and then sacrifice. (A) Diagram of Rostral/Caudal region of cortex analyzed, with dorsomedial region boxed in green. (B) Composite image of Saline exposed cortex Green=Pax6, Red=BrdU. (C) Composite image of VPA exposed cortex Green=Pax6, Red=BrdU. (D) Pax6 labeling index unchanged in VPA exposed embryonic cortices. N=3 expts per group, yielding 7 brains analyzed per condition.
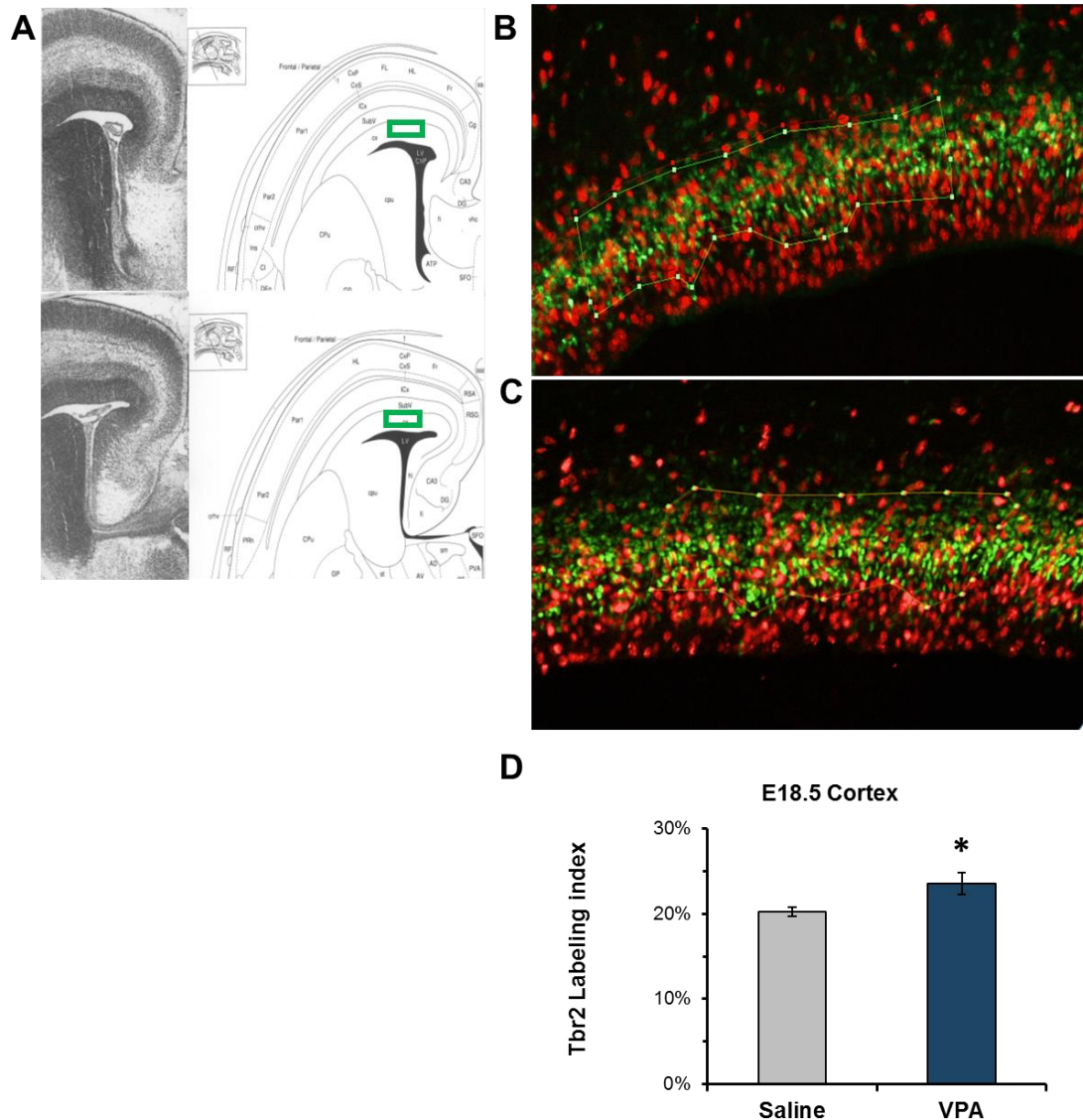
Figure 22 Increased Tbr2 labeling index in the E18.5 cortex after VPA injection series: Pregnant dams were injected twice/ day for a total of five Saline or VPA (300mg/kg) exposures from E16.5 to E18.5, followed by 2h BrdU pulse and then sacrifice. (A) Diagram of Rostral/Caudal region of cortex analyzed, with dorsomedial region boxed in green. (B) Composite image of Saline exposed cortex Green=Tbr2, Red=BrdU. (C) Composite image of VPA exposed cortex Green=Tbr2, Red=BrdU. (D) Tbr2 labeling index increased in VPA exposed embryonic cortices. N=3 expts, yielding a total of 7 Saline, and 6 VPA brains analyzed.

To ensure Pax6 labeling index was not equivalent due to altered Pax6 cell numbers, the estimated total population within this compartment was measured, and was found to be unchanged (Saline=25811 $\pm$3122 SEM N=7, VPA=21285 $\pm$3208 SEM P=0.33 N=7). The estimation of these cells double-

labeled for BrdU were also unchanged (Saline=7518 $\pm$1114 SEM N=7,

VPA=6187 $\pm$1032 SEM P=0.4 N=7). This suggested that the labeling index was

accurately represented for the given populations. Similar investigation was then

done on the average estimate of total Tbr2 cells within the Tbr2 compartment.

Interestingly, the Tbr2 total cell number was unchanged between saline and VPA

groups. Yet, within this Tbr2 compartment, the estimated number of cells

containing Tbr2 plus BrdU was trending to a significant increase (Saline=3186

$\pm$895 SEM N=7, VPA=4283 $\pm$338 SEM P=0.08 N=6) (Figure 23).
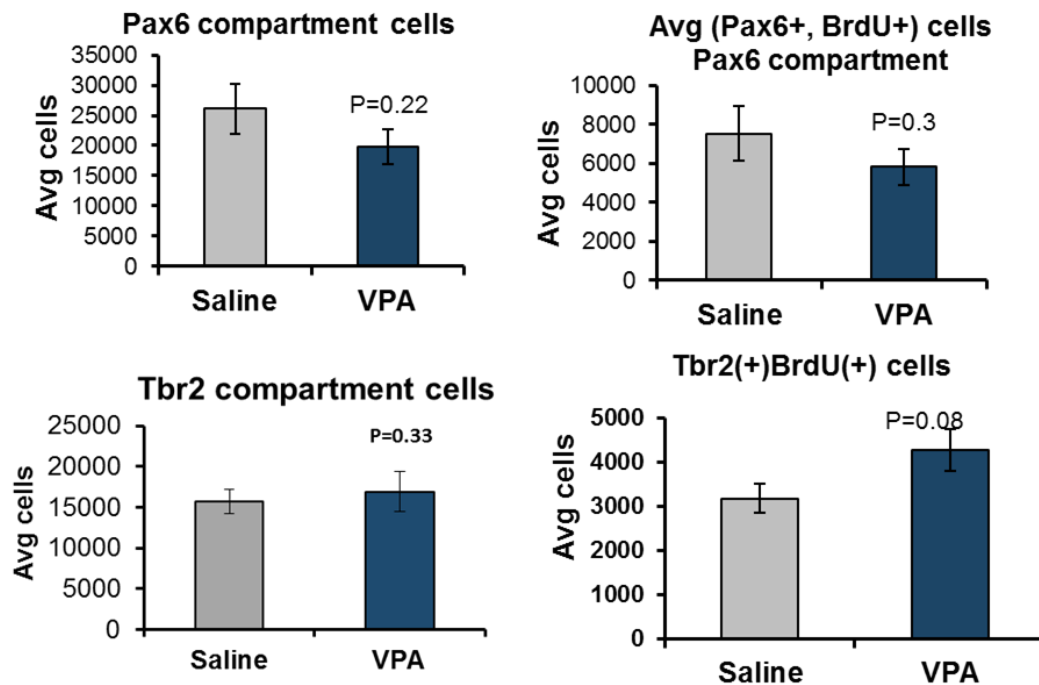
Figure 23 Average numbers of Pax6 and Tbr2 and compartment cells +/- BrdU:
Left: Estimated total numbers of Pax6 and Tbr2 positive cells within their respective
compartments. Right: Estimated total numbers of double positive cells within each
compartment. Analyses indicate there are no significant changes between total numbers of
Saline and VPA injected embryonic cortices. Pax6 N=3 expts per group, yielding 7 brains
analyzed per condition. Tbr2 N=3 expts, yielding a total of 7 Saline, and 6 VPA brains
analyzed.

In sum, these analyses confirm that labeling indexes are comparing equivalent numbers of cells, and indicate more Tbr2 cells are entering S phase.

An additional control was analyzed to ensure that labeling indexes were not obscured by changes in density of cells within the cortex, because alterations of this could artificially change the frequency of counting between saline and VPA brains. This measurement was a comparison of the total numbers of Dapi cells within a compartment normalized to the volume of Pax6 or Tbr2 regions. This revealed no significant changes between saline or VPA treated brains for Pax6 (Saline=0.0035 $\pm$0.0001 SEM N=7, VPA=0.0036 $\pm$0.0002 SEM P=0.4789 N=7) or Tbr2 (Saline=0.004 $\pm$0.0001 SEM N=7, VPA=0.004 $\pm$0.0001 SEM P=0.226 N=6) regions, indicating that cells were spaced equivalently and measured from similar total volumes(Figure 24a). The density to volume measures suggest that labeling indexes between saline and VPA brains are comparable, with equivalently spaced Dapi cells normalized to the region measured. Furthermore, estimations of absolute volumes (μm^3) between saline and VPA brains were also checked, revealing no significant changes. This suggests that Dapi estimations were a valid comparison measure, as saline and VPA compartment volumes analyzed were equivalent (Figure 24b).
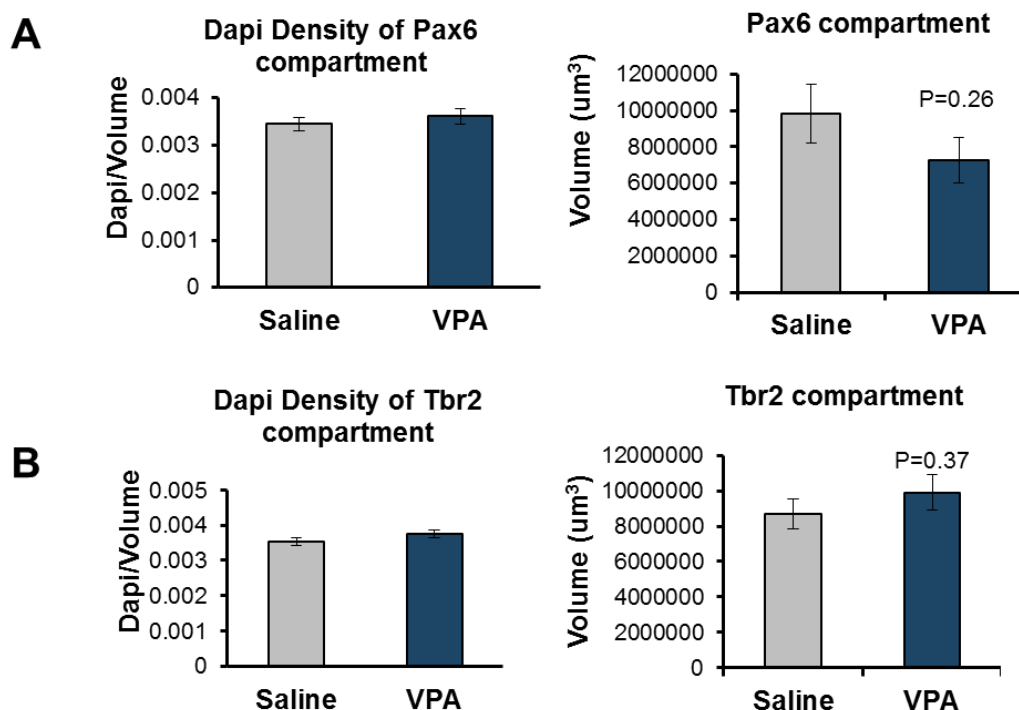
Figure 24 Density and volume measures for Pax6 and Tbr2 in the E18.5 cortex +/- VPA: (A) Left: estimated density of Dapi cells per volume for Pax6 compartments. Right: Estimated volume um^3 for Pax6 compartments. (B) Left: density of Dapi cells/ Volume in Tbr2 compartments. Right: Estimated volume um^3 for Tbr2 compartments. No changes observed in Dapi density or estimated volumes, indicating analyzed regions for Saline and VPA exposed brains are equivalent in numbers of cells and volume measured. Pax6 N=3 expts per group, yielding 7 brains analyzed per condition. Tbr2 N=3 expts, yielding a total of 7 Saline, and 6 VPA brains analyzed.

In sum these data suggest that VPA treated embryos have a higher percentage of Tbr2 cells in S-phase, with a trending increase in the total number of cells positive for both Tbr2 and BrdU. Given that Tbr2 cells are known to preferentially generate cells of upper cortical layers (161) , these findings could explain increased cux1 positive cells seen at P21.

A) Sex dependent VPA effects on Pax6 and Tbr2 proliferation

Studies have identified that VPA exposure can produce differential effects based on sex, with changes in rodent behavior (115, 123, 125), and brain development (115, 125). Additional studies are needed in order to make further

conclusions of how prenatal exposure can be differentially impacted by sex, as many studies do not identify sex of offspring, nor do they study behavior equally in both genders (115) . However, human studies have indicated that the incidence (14) and recurrence risk of ASD is lower in females than males (11), suggesting that females may have a protective effect. Therefore, I hypothesized that changes in the Tbr2 labeling index may be differential based on sex of embryos. To investigate this, I genotyped embryonic tissue from each brain analyzed with assistance from Transnetyx, and clustered stereology data by sex.
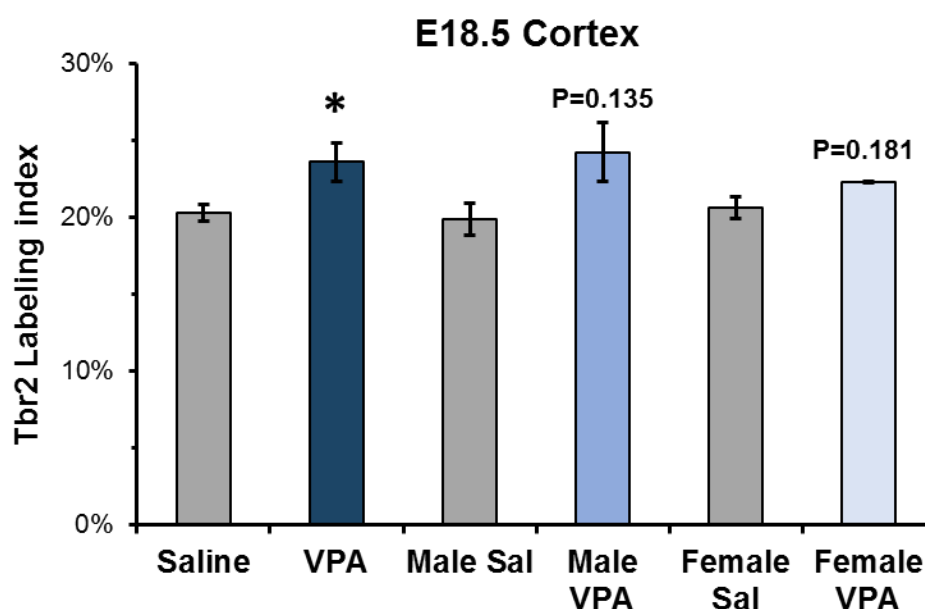
Figure 25 Sex dependent effect on Tbr2 labeling index +/- VPA at E18.5: Increased Tbr2 labeling index was observed after 5 prenatal VPA injection series as seen in blue bars. Results indicate almost significant increases in the Tbr2 labeling index for male embryos with a 22% increase from Saline, while female embryos only increase 8% from their sex matched saline controls. Tbr2 N=3 expts, yielding a total of 7 Saline, and 6 VPA brains analyzed. (Sal Male= 3, VPA Male=4, Sal Female=4, VPA Female=2).

I found a trending significant increase in the Tbr2 labeling index for male embryos prenatally exposed to VPA (Saline Male=19.9% +0.01% SEM N=3, VPA

Male=24.2% +0.019% N=4 P=0.135). Additionally, preliminary results observing

the labeling index for VPA exposed female embryos was markedly reduced with

a weaker trend in change from female saline controls (Saline Female=20.6%

+0.007% SEM N=4, VPA Female=22% +0.0001% N=2 P=0.181) (Figure 25).

The percent change in male labeling index was 22% while female was only 8.2%,

suggestive that there may be a sex dependent difference in Tbr2 proliferating

precursors.   Preliminary findings also indicate that Male VPA treated brains may

still have a trending increase in the average total cells containing both Tbr2 and

BrdU (Saline Male=3228 +513 SEM N=3, VPA Male=4659 +365 N=4 P=0.136).

Analysis of additional brains of each sex will explore trending effects in sex

differences of Tbr2 specific proliferative changes. Additionally, investigation into

sex dependent effects on the Pax6 labeling index revealed no changes between

Saline and VPA brains (Data not shown).   In sum, these potential differences in

the Tbr2 labeling index may suggest a protective effect from VPAs effects in

development of female cortical precursors.

Chapter 4: Altered neurogenesis due to the 16p11.2 CNV in Human NPCs

4.1) Rationale for neurogenesis study of 16p11.2 NPCs.

These studies complemented my investigation of altered neurogenesis due to the environmental ASD risk factor VPA, by investigating changes in neurogenesis due to a genetic risk factor for ASD, the CNV 16p11.2. Based on previous mouse studies, and human macrocephaly phenotypes, I hypothesized that 16p11.2 NPCs derived from ASD individuals may have increased proliferation. To test this I investigated DNA synthesis, cell counts and potential changes in G1 cyclins. I also hypothesized that these cells may have altered ERK 1 signaling, due to missing one copy of MAPK3. Therefore, I challenged these cells to mitogenic stimulation and investigated changes in DNA synthesis, and cell number. Further, I investigated potential signaling mechanisms that could be altered as a result of changes to ERK1. This was initially investigated without mitogenic stimulation, to further characterize anticipated changes in proliferation. These investigations will elucidate potential developmental changes due to alterations in this CNV.

While the first portion of my thesis investigated the effects of an environmental factor on neurogenesis, we now want to investigate changes in neurogenesis due to a genetic factor. The 16p11.2 CNV has been associated with 1% of ASD cases, suggesting that altering the dose of genes within this region can increase the risk for autism. Humans with this deletion often have

macrocephaly, while those containing the duplication tend to have microcephaly (162), suggesting growth phenotypes could play a role in the etiology. This CNV affects one copy of 27 (21) to 29 genes (109, 110), including the gene MAPK3 which encodes for ERK1. Extracellular factors can signal through ERK to stimulate proliferation and growth during development. Likewise, alterations in copies of ERK1 which can lead to ERK dysregulation, as seen in the 16P deletion mice, can impact brain development (21). Although 16P deletion mice exhibit similar behavioral characteristics to 16P del humans, they differ by having microcephalic brains, while duplication mice have macrocephaly. With rodents exhibiting opposite brain growth phenotypes from humans, it may suggest that using human cells may provide a more translatable understanding from biological outcomes. Fortunately, new models utilizing iPSC technology and human samples provide unique and valuable perspectives to model this CNV disorder. Studying iPCSC derived NPCs has been successfully utilized to characterize genetic (136, 139) and idiopathic models of autism (163, 164). Now through collaborative efforts, our lab has optimized similar techniques to study iPSC derived NPCs from idiopathic (186), and now 16p11.2 deletion autistic patients compared to unaffected control individuals.

In order to validate characteristics of 16p11.2 NPCs and respective controls, immunocytochemical (IHC) staining was conducted, to demonstrate typical NPC transcription factors were expressed in cells derived from each patient (Figure 26).
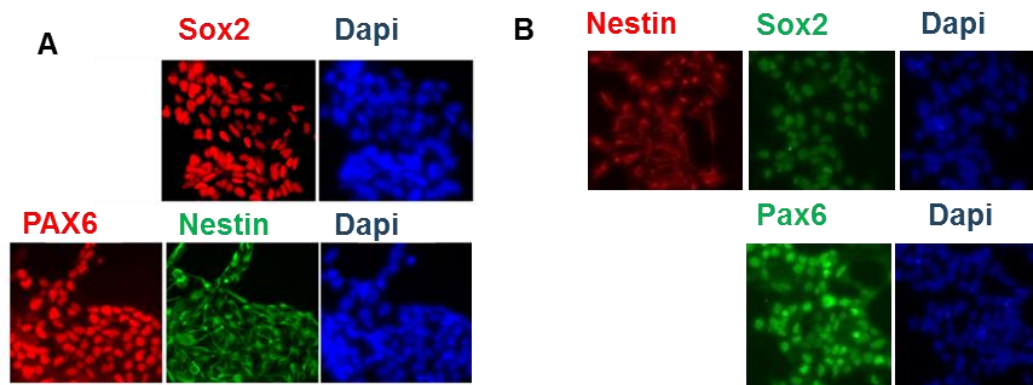
Figure 26 Examples of NPC markers: Pax6, Nestin and Sox2 markers are stained in Red and Green to indicate NPC characteristics. Nuclei are additionally stained by Dapi in blue. N≥1 expt per clone. A) Unaffected Control NPC marker staining, taken from Williams and Prem et al., 2017 (in press). B) 16p11.2 NPC marker staining.

To show NPCs pluripotency, unaffected control and 16p11.2 cells were also cultured for 10 days in differentiating medium, and then stained for markers indicative of early neuronal and glial cell type differentiations. As expected, NPC cells derived using our neural induction protocol can differentiate into neurons, astrocytes and oligodendrocytes. Because these cells exhibit expected differentiations, experiments characterizing the biology of these NPCs will be outlined below.

4.2) 16p11.2 NPC culture results

<u>A) 16p11.2 NPCs exhibit increased DNA synthesis</u>

Previous literature has identified multiple genes within the 16p11.2 region associated with proliferation, including MAPK3, MVP, and KCD13. Furthermore, one of the three patients within our cohort has macrocephaly as seen by head circumference in the 99th percentile. Because of this, I wanted to measure

proliferation rates of 16P NPCs in comparison to control individuals through 3H-thymidine incorporation studies using control media conditions. Studies aim to investigate three separate 16P patients and three control individuals from the larger Simons VIP cohort. For these ongoing studies, one clone of each 16P individual was analyzed compared to 5 clones comprised from the three control individuals.   With limitations of available female controls at the current time, the vast majority of analyses below will be conducted on the two 16p11.2 males as compared to the unaffected control individuals.

To explore proliferative changes in these human NPCs, I first measured the average level of DNA synthesis between the two male 16p11.2 NPCs compared to Unaffected Controls under 30% Expansion control media conditions. The male 16p11.2 NPCs exhibited a significant 30% increase in DNA synthesis compared to Unaffected NPCs (Average CPMA 16P=21055 $\pm$ 1263 SEM, Control=16140 $\pm$ 843 SEM, P= 0.002). Although there is not a sex matched control currently available for the 16P female, It was also worthy to note that averaging DNA Synthesis values for all three 16p11.2 deletion patients resulted in a 27% increase compared to that of Unaffected NPCs (Average CPMA 16P=20572 $\pm$ 1064 SEM, Control=16140 $\pm$ 843 SEM, P= 0.003). With an observable increase in DNA synthesis for the two 16P males, I then wanted to determine if there were passage specific changes. When only looking at earlier passages (P3-P5) the increase in DNA synthesis of two male 16P NPCS is actually 70% higher than passage matched Controls (Average CPMA 16P=26504 $\pm$2401; Control=15610 $\pm$1292 P$\leq$0.0001). Interestingly, at late

passages 16P NPCs had a 23% reduction in DNA synthesis compared to

Unaffected controls (Average CPMA 16P=12881 $\pm$849; Control=16770 $\pm$1027

P=0.04), suggesting they may have a differentiation and or death phenotype at

higher passages (Figure 27).
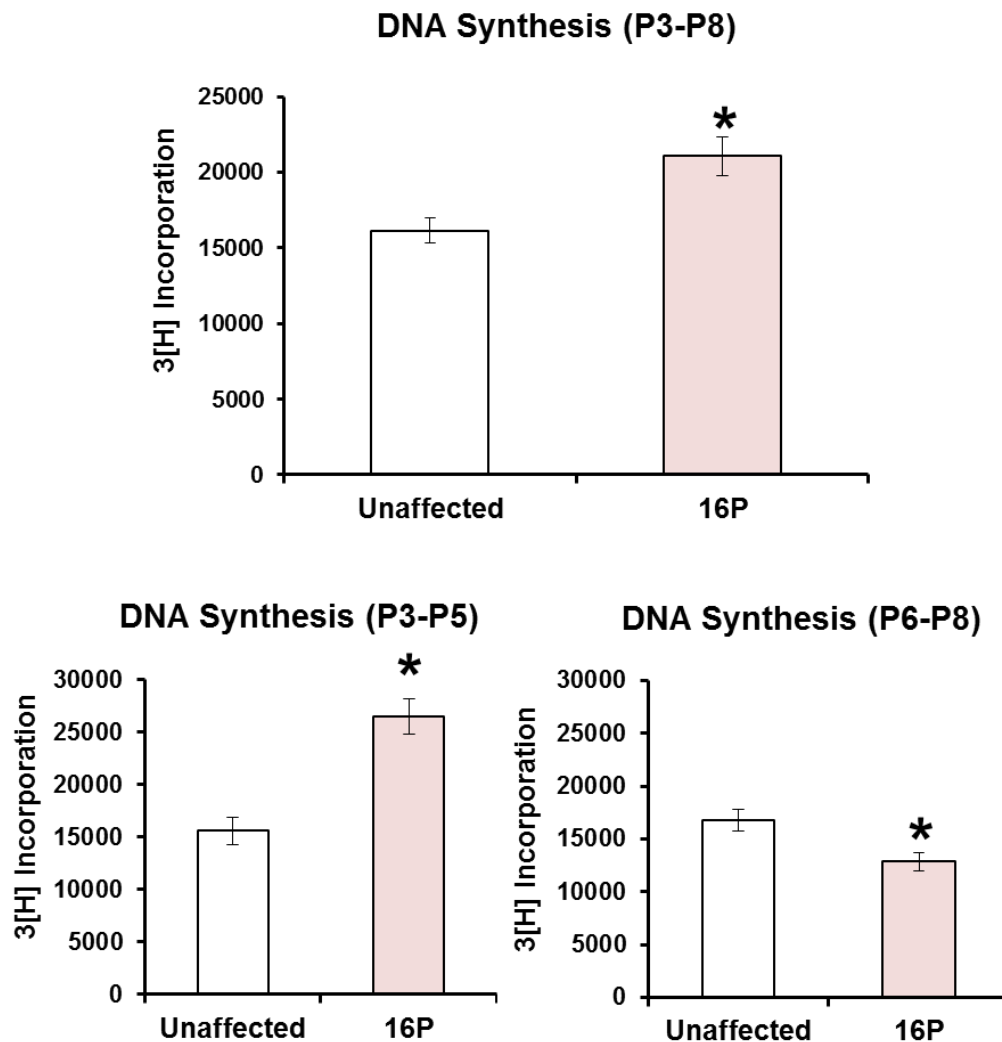
Figure 27 DNA synthesis for 16p11.2 and unaffected NPCs by passage: 16p11.2 NPCs (in pink) exhibit higher levels of DNA Synthesis compared to Unaffected NPCs (in white). However 16p NPCs have slower DNA synthesis at later passages. P3-P8 Unaffected N=1-3 clones per 3 individuals for 245 total wells. P3-P8 16P N=1 clone per 2 individuals for 90 total wells. P3-P5 Unaffected N=133 total wells. P3-P5 16P N=54 total wells. P6-P8 Unaffected N=112 total wells. P6-P8 16P N=36 total wells. Unaffected control values from 3 individuals, 1-3 clones per individual. 16P values from 2 individuals, 1 clone per individual.

Although preliminary, it was also noted that NPCs from the female 16P patient did not have a passage specific effect, maintaining a uniform level of DNA synthesis from P3-P8.

B) Blunted stimulation of DNA synthesis observed in 16p11.2 NPCs treated with FGF, with differential sensitivity to dose

As stated earlier, the MAPK3 gene is within the locus of 16p11.2 CNV and this gene encodes for ERK1. ERK 1 is a gene that plays roles in the ERK signaling pathway which regulates growth and proliferation. To assay if there is dysregulation of 16P DNA synthesis due to the ERK pathway, NPCs were cultured with Fibroblast Growth Factor (FGF), a stimulator of the ERK pathway. Average DNA synthesis counts for the two male 16P patients were not significantly different than average counts for unaffected control NPCs (Average CPMA 16P=36336 + 1905, Control=36405+ 1967, P= 0.95). To explore this further, raw DNA synthesis counts were separated out as just early passage (P3-P5), and then 16P NPCs had 29% more DNA synthesis increase in response to FGF over control NPC counts (Average CPMA 16P=44582 $\pm$ 1885, Control=34580$\pm$ 2948, P= 0.019). Conversely, at late passages, the male 16P NPCs exhibited a 46% reduction in DNA synthesis when stimulated with FGF, compared to the relatively unchanged Controls (Average CPMA 16P=20697 $\pm$ 1688, Control=38408$\pm$ 2562, P$\leq$ 0.001). A % control comparison was then made using average DNA synthesis values for control and FGF conditions. 16p11.2 NPCs consistently had a lower stimulation response after FGF treatment.
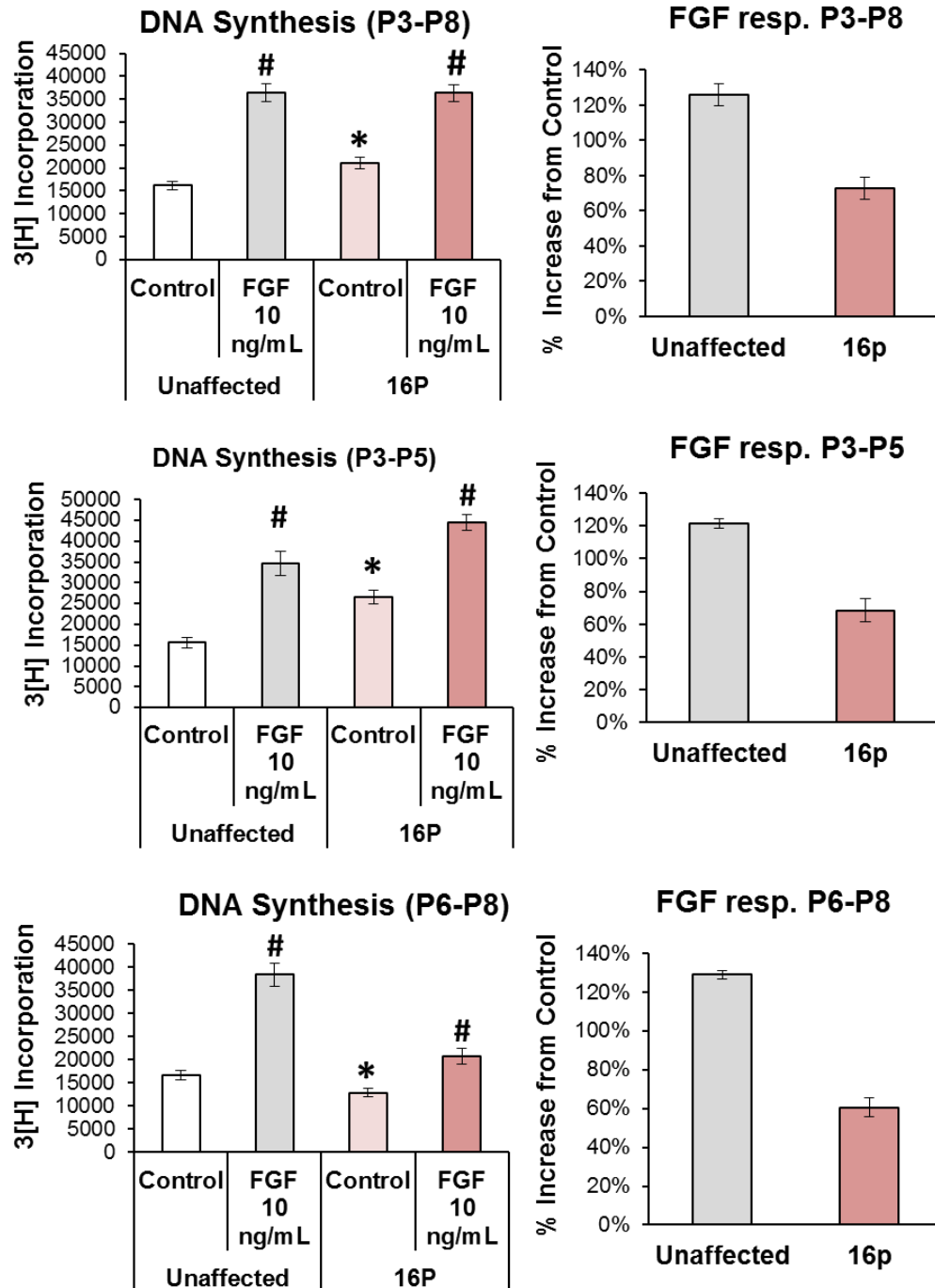
Figure 28 Increases in DNA synthesis due to FGF are blunted in 16p11.2 NPCs:
Left: Treatment with FGF produces greater increases in DNA synthesis for Unaffected
NPCs at all passages. Right: Calculation of blunted effect as seen by 3H counts
*= Significant difference between patients, #= Significant difference within groups. P3-P8
Unaffected N= 245 control media and 189 FGF media total wells. P3-P8 16P N=90 control
media and 81 FGF media total wells. P3-P5 Unaffected N=133 control media and 97 FGF
media total wells. P3-P5 16P N=54 control media and 55 FGF media total wells. P6-P8
Unaffected N=112 control media and 92 FGF media total wells. P6-P8 16P N=36 control
media and 29 FGF media total wells. Unaffected control values from 3 individuals, 1-3
clones per individual. 16P values from 2 individuals, 1 clone per individual.

Looking at all data, 16p11.2 males increased their DNA synthesis in response to FGF 73% over that of the control media, while Unaffected controls increased only 126%. Notably, at later passages (P6-P8) when 16p NPCs slowed down their absolute counts in DNA synthesis, the magnitude increase from control media was still blunted with respect to Unaffected controls (16P % increase: 61%, Unaffected control % increase=129%) (Figure 28). To explore this blunted response to FGF further, %increases were calculated for 16P and Unaffected controls, based on each experiments average CPMA in control media. Scatter plot of these data show that 16p11.2 NPCs are tighter in their spread, with a lower overall average % increase to that seen in unaffected controls (16P= 183.5% +4.87% SEM, Unaffected controls= 206.7% +5.06% SEM P=0.006) (Figure 29).
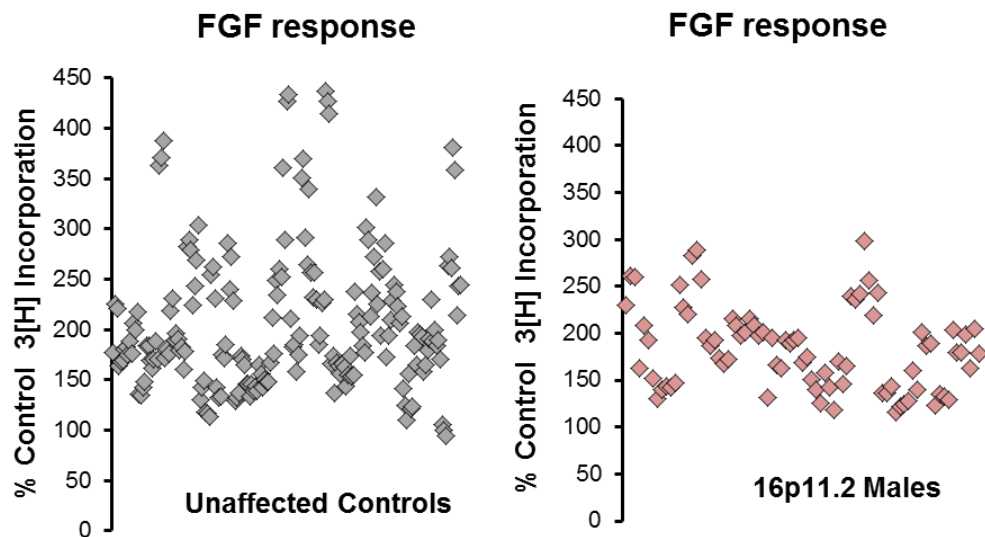
Figure 29 Scatter plots of Unaffected Control and 16p11.2 NPC responses to FGF as percent increases from control media: 16P males in red are observably blunted, with lower increases in 3[H] incorporation compared to levels seen for Unaffected individuals. The x axis represents individual expts by well. Unaffected N=189 wells, 16P N=81 wells

With a diminished response to FGF at 10ng/mL I next conducted an extensive dose response curve for 16P and controls followed by one way ANOVA on % control increases in DNA synthesis. The doses of FGF which elicited a significant increase in DNA synthesis for Unaffected control NPCs ranged from 0.3 ng/mL to 30ng/mL, with the highest percent increase seen at 3ng/mL (0.3 ng/mL= 179%, +7.63% SEM P=0.001, 1ng/mL=235% +12.55% SEM P=0.0001, 3ng/mL=273% +17.49 %SEM P=0.0001, 10ng/mL=264% +24.92% SEM P=0.0001, 30 ng/mL=251% +18.29% SEM P=0.0001). Examining the same dose response curve for the 16p11.2 males resulted in significant increases at the lower dose 0.1 ng/mL, extending up to 30ng/mL, while the highest percentage increase was seen at 1ng/mL (0.1ng/mL= 132% +8.17% SEM P=0.047, 0.3 ng/mL= 150%, +14.32% SEM P=0.0027, 1ng/mL=173% +10.48% SEM P=0.0001, 3ng/mL=166% +10.94 %SEM P=0.0001, 10ng/mL=150% +5.17% SEM P=0.0007, 30 ng/mL=144% +6.71% SEM P=0.0026). These data suggest that 16p11.2 may have a shifted dose response curve and potentially lower EC50 for FGF. When comparing the % increases for 16p11.2 as well as the Unaffected controls, the blunted response mentioned earlier occurred at FGF doses between 1ng/mL and 30 ng/mL (1 ng/mL FGF P=0.0039, 3ng/mL FGF P=0.0005, 10ng/mL FGF P=0.0022, 30ng/mL FGF P=0.0005) (Figure 30).

This T-test comparison indicates that 16P exhibits a reduced response at higher doses of FGF, suggesting that this pathway may have higher baseline activation

compared to Unaffected control NPCs.
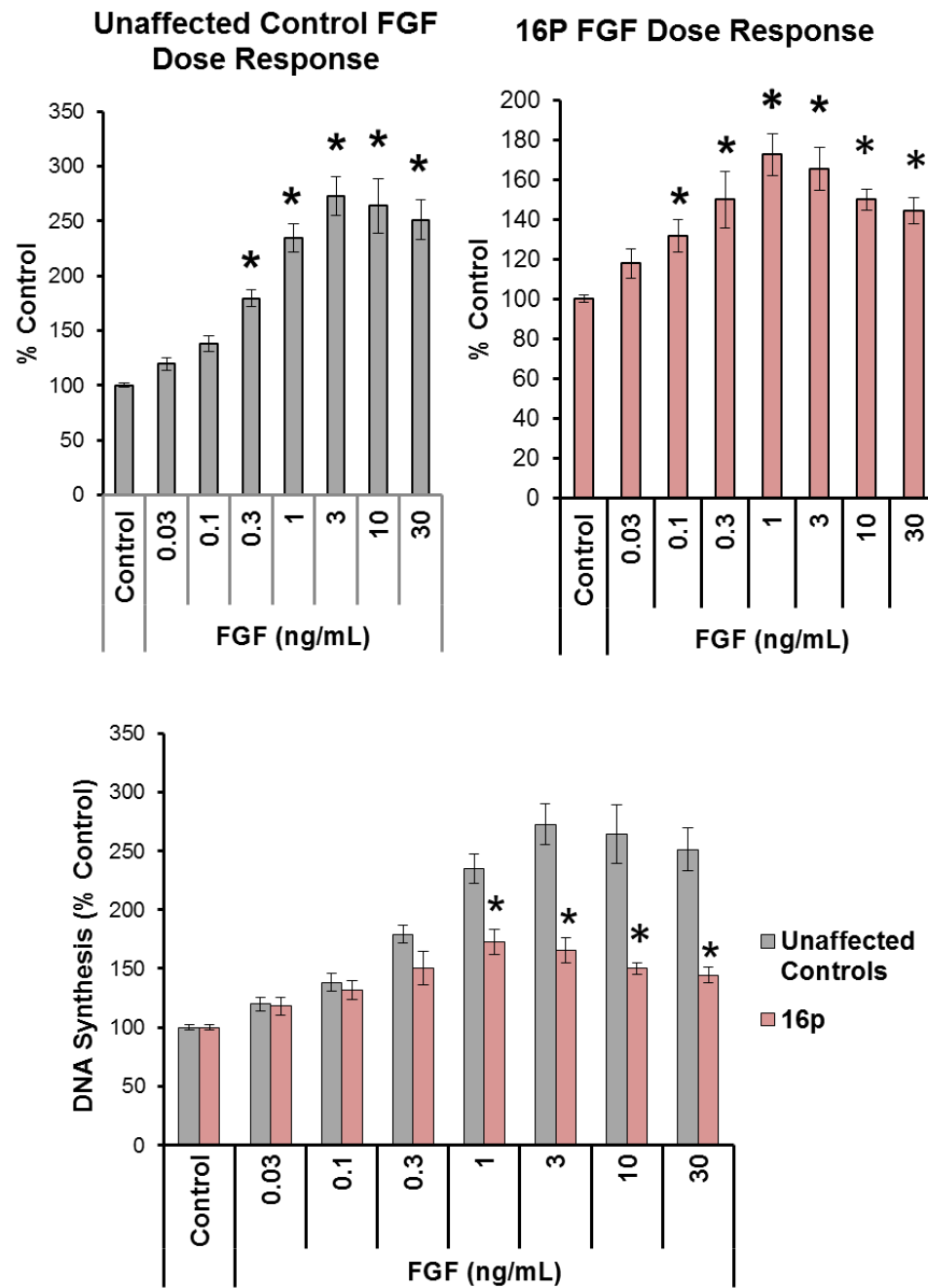
Figure 30 FGF dose responses of DNA synthesis for Unaffected control and 16p11.2 NPCs as percent control: 16P males in red exhibit a shifted EC50 peak at 1 ng/mL, responsiveness at lower doses, and respond less to FGF than unaffected controls, suggesting reductions in mitogenic activation by FGF or downstream signaling pathways. Unaffected N=3 expts, 16P N=2 expts. Unaffected values derived from 2 individuals, 1-2 clones per individual. 16P values derived from 2 individuals, 1 clone per individual.

C) Survival and Total Cell numbers are similar for Unaffected controls and 16p11.2

To better understand changes in DNA synthesis for 16P and Unaffected controls, I wanted to investigate cell survival and proliferation in a cell counting assay. This would also determine if changes in DNA synthesis could correlate with changes in total cells, I assayed total cell counts for 16P and unaffected controls after 2, 4, and 6 days of culture +/- FGF, plated at 50,000 cells/ml in 24 well plates with area of 1.9 cm^2 /well.

Total Cell counts for 16p11.2 and Unaffected controls are not significantly different in control media conditions

Measuring counts of total cells at 2, 4, and 6 days after plating revealed no significant changes between 16P and Control NPCs (Figure 29). At two days, cell number was highly similar between 16P and control cells (16P=41953 +3576, Control=42377 +4310 P=0.7). At four days 16P cells had a non significant 17% decrease compared to Controls (16P=64717 +5889 Control=77748 +5509 P=.28). By 6 days in culture, there was a non significant 15% increase in total cell counts for the 16P males compared to the 3 control individuals (Cell counts 16P=135078 +11680; Control=117429 +9936 P=.39)(Figure 31). However, preliminary results analyzing total cell counts at early passages, suggest trending significant differences by 6 days. At early passage (P3-5), the two 16P males exhibited a trending 40% increase in total cell counts over Control NPCs (Avg Total Cells 16P=141875 +12285,

Control=101514 $\pm$13442 P=0.09) (Figure 31a-b). These trending differences in total cell counts by day 6 at early passages are partially reflective of the increased DNA synthesis in 16P cells at 2 days, although alternate assays measuring cell cycle reentry may need to be explored in order to better understand proliferative changes in these cells.

<u>16p11.2 NPCs challenged with FGF do not exhibit significant changes in total cell numbers</u>

With total cell numbers being unchanged between 16P and Control NPCs under control conditions, and possible dysregulation of FGF responses seen through DNA synthesis, I also assayed total cell counts of NPCs in presence of FGF and as a % comparison to total cells under control media conditions. Analysis of total cell counts under FGF exposure revealed no differences between 16P males and Control NPCs after 2, 4, or 6 days of culture. However, the percent increase from total cells grown in control media was significantly increased by 22% for 16P NPCs by 4 days culture (16P % increase=203 $\pm$ 20%, Control=166$\pm$ 7.4%, P= 0.04). By day 6 there was a non significant 17% trending decrease in 16P NPCs compared to Controls, reflective of 3H 16P NPCs responding to FGF early but failing to effectively respond at later times comparatively to Control NPCs (Average %Increase 16P=248 $\pm$ 21%, Control=300$\pm$ 16%, P= 0.113) (Figure 31c).
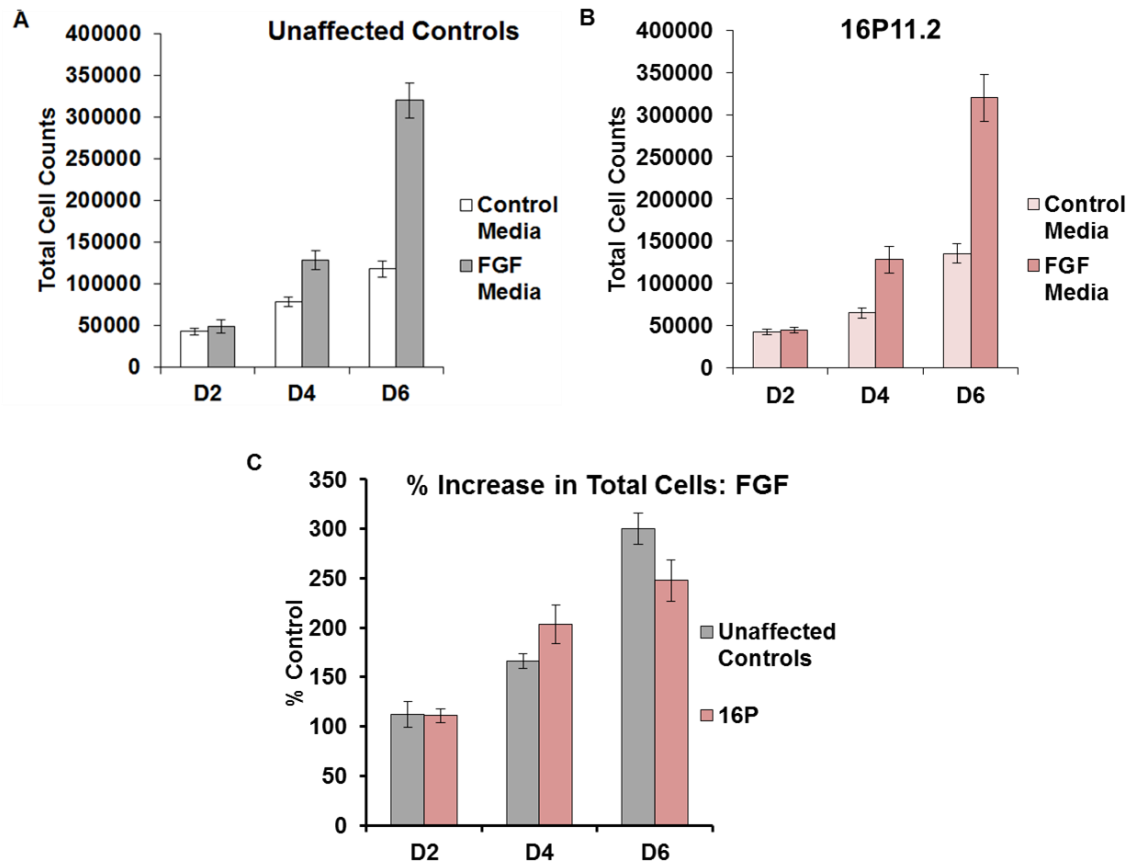
Figure 31 Total cell counts do not reveal significant changes between 16P and Unaffected controls: (A) Control media counts in white compared to FGF cell counts for Unaffected controls N=33 expts for control and N=30 expts for FGF. (B) Control media counts in pink vs FGF counts in red for 16P males. 16P N=8 expts for control and N=8 expts for FGF. (C) Calculated percent increase from control media counts for Unaffected and 16P. Subtle but non significant blunted effect may be seen by Day 6 in 16p male % increases. Days in culture denoted as D2, D4, and D6. % increase Unaffected % increase N=30 expts, 16P % increase N=8 expts. Unaffected control values from 3 individuals, 1-3 clones per individual. 16P values from 2 individuals, 1 clone per individual.

Analysis by early passages also failed to show changes in total cell counts, and the % increase values at day 6 for 16P males still exhibited a trending decrease comparative to Unaffected controls response (Average %Increase 16P=250 $\pm$ 24%, Control=300$\pm$ 19%, P= 0.14). These data suggest that proliferation is not largely changed under these conditions, and/or this assay is not sensitive enough to detect changes. It was observed that by Day 6, cells in

FGF treatment wells were highly confluent which could confound findings due to contact inhibition and limitations in area of the well.

D) 16p11.2 NPCs also have blunted increases in cell number after FGF stimulation in 35 mm dish culture

To further explore potential blunting effects of 16p11.2 NPCs, a collaborative effort was made between other lab members plating cells for assays in larger 35 mm dishes. Preliminary data measured cell counts by only counting non apoptotic cells within 1 cm stretches for both unaffected and 16p11.2 NPCs with and without FGF at 48hrs. Preliminary analysis of 16p11.2 NPCs under control media were not significantly different compared to unaffected NPCs (Total cells Unaffected=152 +12 SEM N=9 expts, 16p11.2=186 +15 SEM N=4 P=0.192) or when supplemented with FGF (Total cells Unaffected=302 +21 SEM N=9 expts, 16p11.2=278 +16 SEM N=4 P=0.576). However, when normalizing FGF number to its respective control media total cells, 16p11.2 NPCs have a significant decrease in response (% FGF Increase Unaffected=105.1% $\pm$15.12% SEM N=9 dishes, 16p11.2=49% $\pm$4.99% SEM N=4

dishes P=0.041) (Figure 32).
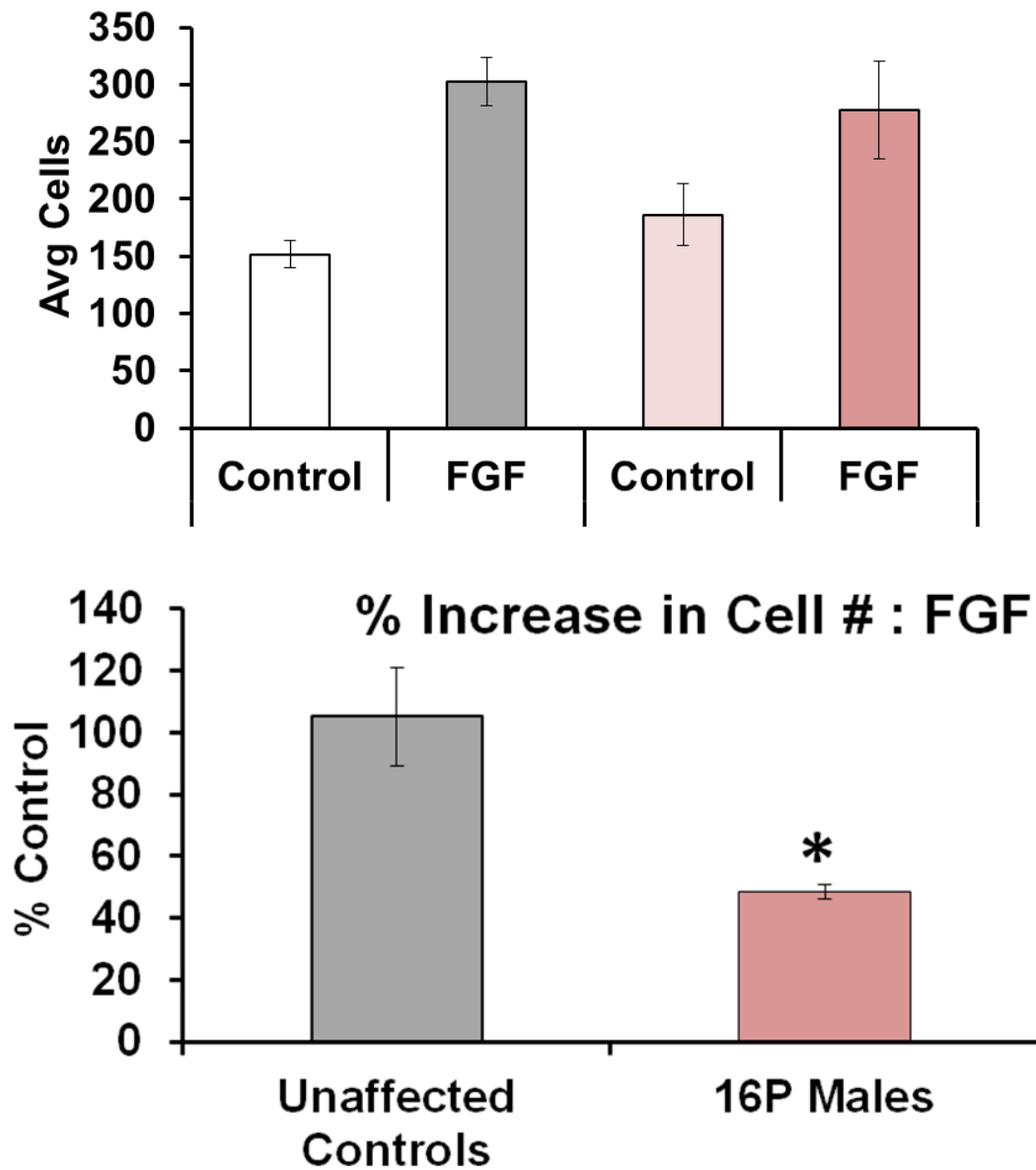
Figure 32 Blunted increases in 16P cell counts after FGF exposure: Top: Average cell counts +/- FGF for Unaffected controls and 16P NPCs after 48 h low density culture. Bottom: cell numbers as percent control indicate blunted increases for 16P NPCs compared to Unaffected controls. Unaffected controls N=9 expts derived from 1-2 clones from 3 individuals, 16P N=4 expts derived from 1 clone from 2 individuals. Unpublished data by Smrithi Prem

These data suggest that 16p11.2 NPCs under low density conditions may have less cells at 48hr in response to FGF. To further assess if this blunted effect is due to changes in cell death, IHC studies for cleaved caspase 3 can be investigated. Additionally, slower cell cycle could explain these changes, so cell cycle reentry could be measured by pulse of EDU followed by later fixation and analyses of co-labeled EDU and Ki67 NPCs. Finally, differentiation could be differential between unaffected controls and 16P, so IHC analyses could also stain for post mitotic neuronal markers, such as Tuj1 or Tbr1.

E) 16p11.2 NPCs exhibit increased signaling and cyclin protein expression in control media

16p11.2 NPCs may have a blunted response to FGF as seen by 3[H] incorporation and low density cultures, which could be due to a higher baseline activity, so it is possible that P-ERK could be increased. The mouse model of 16p11.2 have demonstrated there is a 50% protein reduction of total ERK1, as expected for cells missing one copy of MAPK3, as well as evidence of ERK1 hyperphosphorylation (21). To explore this possibility, I first validated the reduced protein levels in total ERK1 by western. 16p11.2 NPCs exhibited a significant decrease in total ERK1 protein close to 50%, validating the mouse genetic model (Unaffected=1 $\pm$0.049 SEM N=6, 16p11.2=0.685 $\pm$0.061 SEM N=7 P=0.0007). Additionally, levels of P-ERK1 showed a trending increase in 16p11.2 NPCs (Unaffected=1 $\pm$0.061 SEM N=6, 16p11.2=1.3 $\pm$0.198 SEM N=7 P=0.15) (Figure 33).
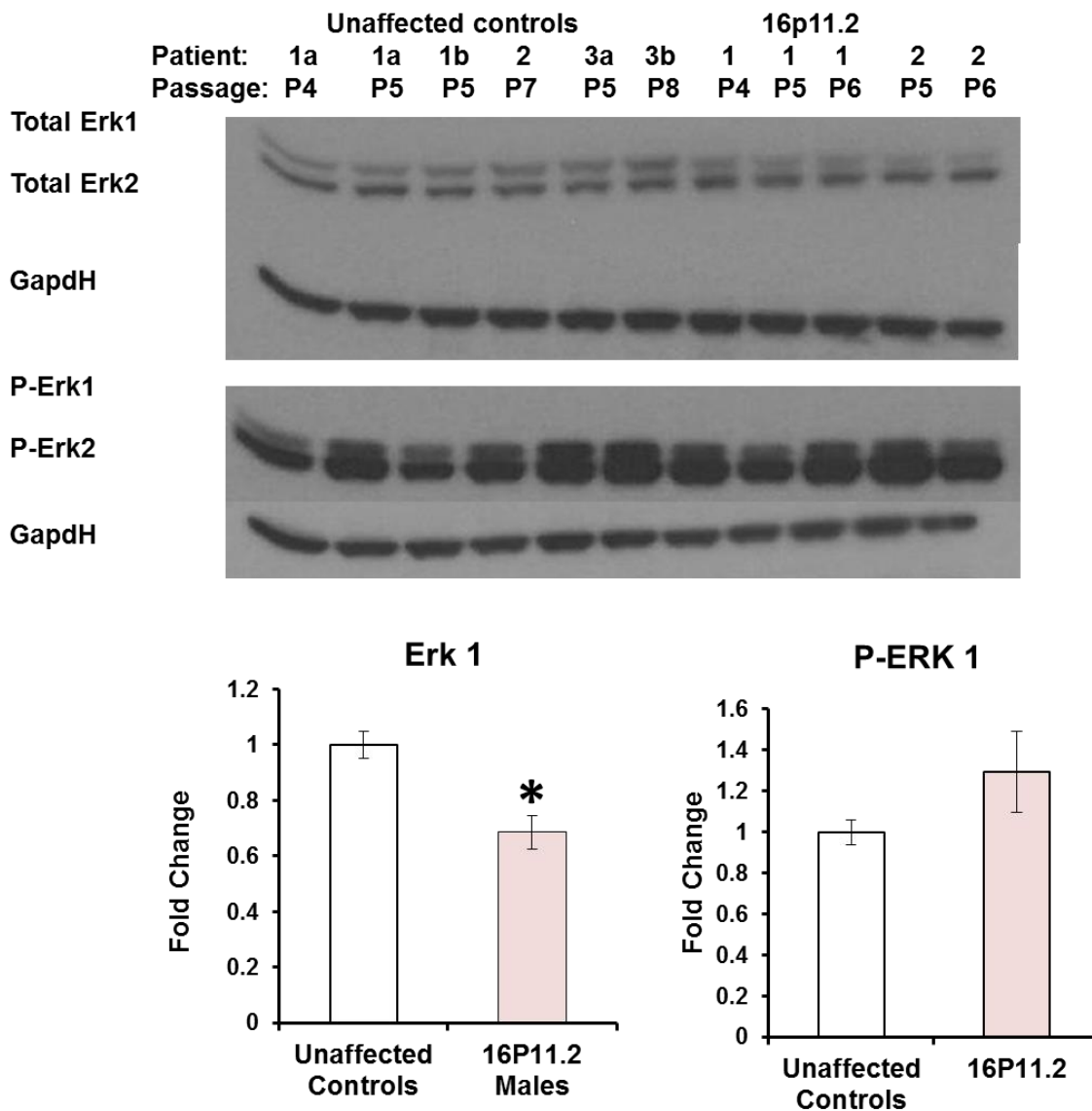
Figure 33 Alterations in total and phosphorylated Erk1 for 16P NPCs: 16p11.2 NPCs have reduced Total ERK1, as expected, yet have equivalent if not overactive P-ERK1 levels compared to Unaffected controls N= 6 expts, 16P N=7 expts. Total ERK1 was normalized to GapdH and then used to normalize P-ERK1 levels. Unaffected control values from 3 individuals, 1-2 clones per individual. 16P values from 2 individuals, 1 clone per individual.

These data suggest that although human 16p11.2 NPCs have 50% less ERK1, they are capable of responding equivalently to unaffected NPC levels, and potentially being more reactive.

With increased DNA synthesis in 16p11.2 NPCs, I looked for increases in

cyclin D1, which could support transition from G1 into S phase. Interestingly,

cyclin D1 was increased in the 16p11.2 NPCs (Unaffected=1 $\pm$0.085 SEM N=6,

16p11.2=1.32 $\pm$0.048 SEM N=7 P=0.007) (Figure 34).
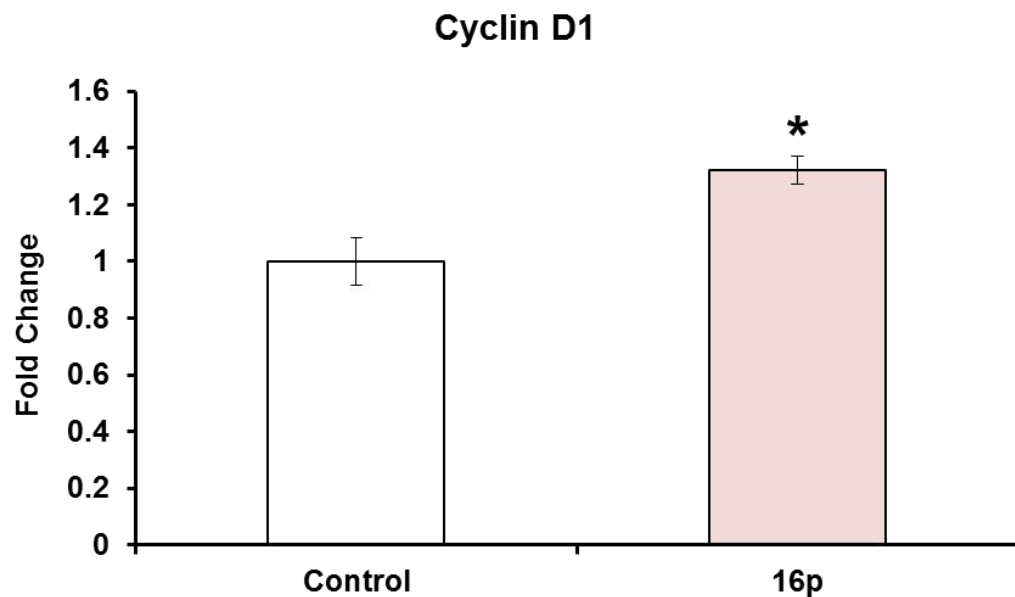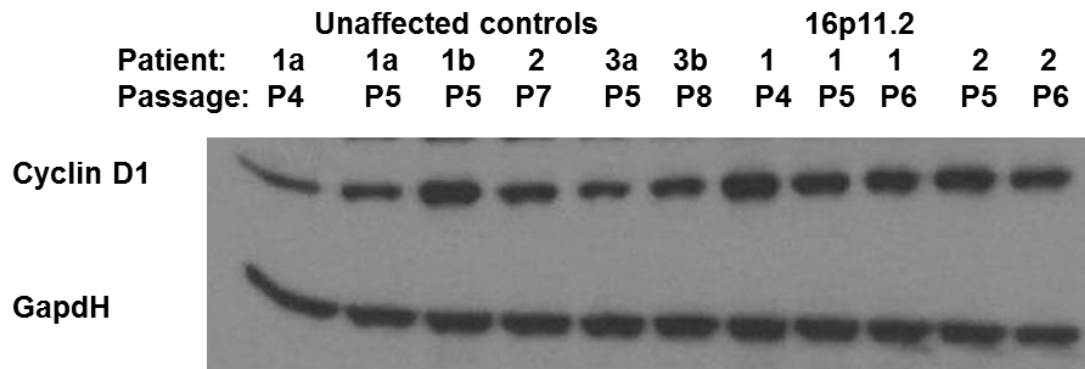
Figure 34 Increased cyclin D1 protein in 16P NPCs compared to Unaffected controls: N= 6 expts, 16P N=7 expts. This increase supports observed increases in DNA Synthesis for 16P NPCs. Unaffected control values from 3 individuals, 1-3 clones per individual. 16P values from 2 individuals, 1 clone per individual.

Studies have also shown that the ERK pathway is able to interact with the

mTOR pathway (77).

Additionally, through

observations of NPC cultures

under the microscope, the

somas of 16p11.2 cells appear

to be larger than the unaffected

controls (Figure 35).

Because of these

observations, as well as the

trending increase in PERK1

levels, I measured P-S6 levels,

and found a significant increase
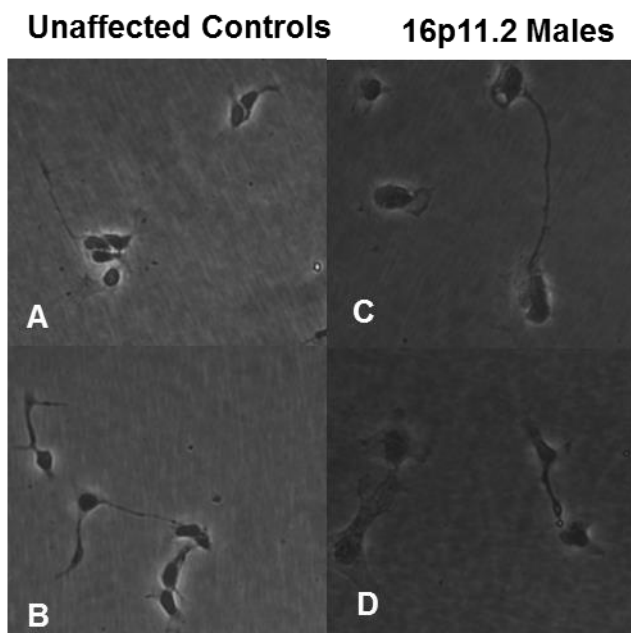
Figure 35 Visualization of Unaffected control and 16P NPCs by phase: Soma size appears enlarged for the two 16p11.2 males (C-D) in comparison to two Unaffected controls (A-B)

(Unaffected=1 $\pm$0.128 SEM N=6, 16p11.2=1.867 $\pm$0.229 SEM N=7 P=0.0128)

(Figure 36). In sum, these data suggest 16p11.2 NPCs exhibit elevated signaling

and cyclin protein expression which may contribute to their enhanced DNA

synthesis. These data also suggest there are signaling abnormalities in 16p11.2

NPCs which could support increased baseline activity, and dysregulated control

of cell proliferation.
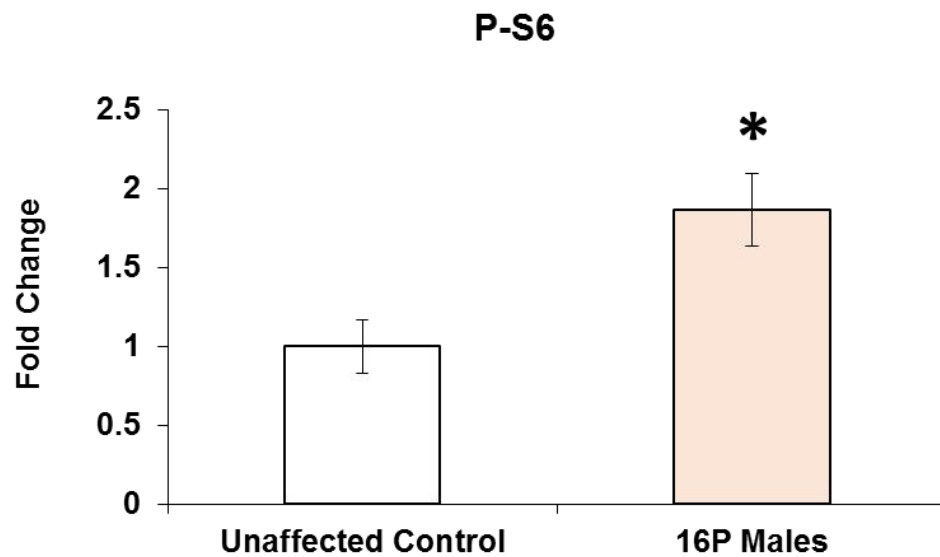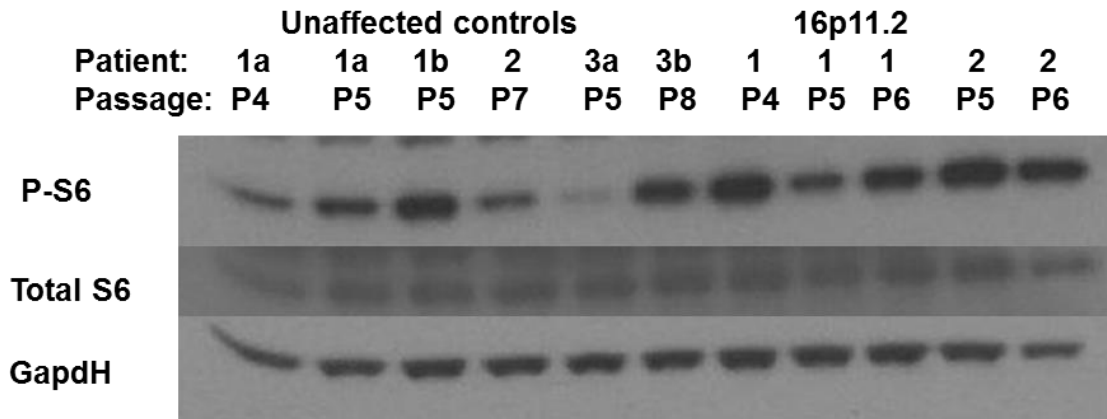
Figure 36 P-S6 is increased for 16p compared to Unaffected controls: Total S6 was normalized to GapdH prior to normalizing PS6 levels. Unaffected controls: N= 6 expts, 16P N=7 expts. This increase supports observed increase in DNA synthesis for 16P NPCs. Unaffected control values from 3 individuals, 1-3 clones per individual. 16P values from 2 individuals, 1 clone per individual.

Chapter 5: Discussion

5.1) Summary of findings

ASD is a complicated neurodevelopmental disease with a multitude of genes and environmental factors that contribute to its etiology, yet our understanding is far from complete. It is necessary to investigate genes and environmental factors which may cause ASD in order to identify both unique and converging phenotypes. Changes in proliferation and differentiation seem to be a common theme in neurodevelopmental diseases, and understanding mechanisms that impact these processes could further our understanding of the pathogenesis. Considering the fact that subsets of individuals with ASD exhibit overgrown brain regions and macrocephaly, it is possible that proliferation and or differentiation could be altered. Therefore, I sought to investigate how environmental and genetic risk factors for ASD can impact proliferation and differentiation during development.

A) Overview of Valproic acid findings

Previous lab results from studies of VPA, an environmental risk factor for ASD, have shown that cortical precursors exhibit increased DNA synthesis in vitro and in vivo following exposure. This was accompanied by rapid increases in cyclin and acetyl H3 proteins, ultimately giving rise to larger rodent brains by P21, including specific increases in upper layer neuronal types. In sum, these results suggested cortical precursors undergo a G1 to S-phase transition due to

elevated cyclins possibly through epigenetic mechanisms. Based on these data, I investigated if previous doses of VPA could still elicit increases in DNA synthesis in vitro. Although dose response of VPA was not identical to previous lab findings, I observed significant increases in DNA synthesis within the same range of VPA exposures. Further, I conducted preliminary studies exposing cortical cultures to a stimulatory dose of VPA for 4 hours, followed by western analyses. I observed increases in proteins cyclinE1 and acetyl H3, which was consistent with previous findings in our lab. To build on the existing story, I predicted that a rapid increase in cyclin proteins was due to increased transcription, through epigenetic mechanisms. I supported this hypothesis by providing evidence of broad HDAC messenger RNA expression in cortical tissue as well as protein expression of class I HDACs (1 and 2) in cortical precursors. Importantly, I was the first to demonstrate in primary rat cortical precursors that VPA can inhibit HDAC enzymatic activity in a dose dependent manner. This finding also correlates with a VPA doses range that also promotes G1 to S phase transition. Based on observed inhibition of HDAC activity, and rapid early increases in G1 cyclin proteins, I investigated if VPA could increase transcription of these cyclins. The primary function of cyclin regulation is degradation, yet I demonstrated early changes in G1 cyclin transcription, after brief exposure of cortical cultures to 1 mM VPA. This suggested that VPA can increase cyclin protein expression due to post transcriptional modifications to histone acetylation, through relaxation of histone/DNA interactions, thereby allowing for increased cyclin transcription. With these changes, I predicted that in vivo exposure to VPA

could elicit increased levels of cyclin G1 protein, acetylated Histone H3, and possibly increased expression of compartment specific progenitor markers in the embryonic cortex. I demonstrated *in vivo* that cyclin E1, acetylated histone H3, and Tbr2 but not Pax6 proteins were increased in E18.5 embryonic cortices which were prenatally exposed to VPA. With increased expression of cyclin E1 protein *in vitro*, and *in vivo*, and previous *in vivo* results demonstrating increased BrdU positive cells in the VZ/SVZ area, I predicted there would be an increase in compartment labeling indices for Pax6, and possibly Tbr2 cells by E18.5. My data partially supports my initial hypothesis. There was a significant increase in the labeling index of Tbr2, but not PAX6 positive cells. Additionally, there was almost a significant increase in the average total number of cells co expressing BrdU and Tbr2 within this region. The increased Tbr2 labeling index may also be sex dependent, with a 22% trending significant increase in VPA exposed males while females only increased by 8% compared to sex matched saline controls. These data suggest that VPA may alter the rate of symmetric division or differentiation in Tbr2 precursors, and female embryos may have a protective effect to this change. In sum, in vitro and in vivo results suggested that VPA altered cortical neurogenesis with increased G1-S transition among specific populations of cells, likely through enzymatic inhibition of HDACs.

B) Overview of 16p11.2 NPC findings

Additional results from human NPC culture compared cells derived from individuals with the copy number variant 16p11.2, a genetic risk factor for ASD,

and unaffected control individuals. The 16p11.2 CNV impacts one copy 27 (21) to 29 genes (109, 110) , and the functions of some genes within this region have been linked to growth and proliferation (21, 109) . Notably, several individuals with this CNV also have macrocephaly (108) . Because levels of these genes are altered and their dysregulation produces brain growth phenotypes, I predicted that 16p11.2 NPCs would exhibit altered neurogenesis and increased levels of DNA synthesis; my current results support this hypothesis. I demonstrated that 16p11.2 NPCs exhibit an increase in DNA synthesis at early passages. This increase is supported by the observed 30% increase In Cyclin D1 protein, which could promote G1 to S phase transition. However, total cell count assays have identified only trending significant increases in cell number by 6 days culture compared to unaffected control NPCs when observed only at early passages. Yet, trending increases were observed at day6 if analyses were limited to passages 3-5, when 16P NPCs exhibited the greatest increases in DNA synthesis under control media conditions. Interestingly, 16p11.2 NPCs exhibited equivalent or reduced DNA synthesis compared to control NPCs starting at passage 6. This data suggests that 16p11.2 cells may have early increased DNA synthesis followed by differentiation based on age of passage. Early passage increases in DNA synthesis and trending increased cell counts may be reflective of early brain overgrowth often seen in 16p11.2 patients and those with ASD.   I also demonstrated these cells have a significant reduction in total ERK1 proteins with a trending increase in phosphorylated ERK 1. Furthermore, I demonstrated altered signaling, as evident by a significant 1.8 fold

increase in phosphorylated S6. These signaling abnormalities suggested

potential explanations for the increased DNA synthesis for these cells.

I also presented evidence that 16p11.2 NPCs exhibited a reduced

response to FGF, a mitogen and activator of the ERK signaling pathway. Limited

increases in DNA synthesis and cell count for 16p11.2 NPCs after FGF

stimulation demonstrated a blunted response for these NPCs. Reduced DNA

synthesis was also visualized by scatterplot as percent control values, showing

16p11.2 NPCs had reduced stimulation compared to unaffected NPCs. MY FGF

dose response curve of DNA synthesis also provided evidence that 16p11.2

NPCs could have a shifted EC50 and as well as reduced sensitivity to several

FGF doses compared to unaffected controls. This blunted mitogenic effect of

FGF was also demonstrated by reduced increase in proliferation, yielding a 50%

reduction in cell numbers compared to unaffected controls within 35mm low

density cultures. These data suggested that 16p11.2 NPCs have reduced ability

to increase DNA synthesis and proliferate in response to this mitogenic signal, a

stimulator of the ERK pathway.

5.2) Effects of VPA on cortical neurogenesis, and relative findings

A) VPA promotes neurogenesis in cortical precursors

Cortical precursors exposed to VPA exhibit various alterations to

neurogenesis depending on experimental conditions. Studies observed both

mitogenic (119, 121) and antimitogenic effects on cortical development (122-

124). Often, this has been due to dose, and exposure time of VPA in culture.

Whether a dose of VPA acts mitogenically or not has also depended on culture composition. E14 cortical cultures exposed to 1 mM VPA resulted in antimitogenic effects when media was not supplemented with bovine serum albumen (BSA) (122), while studies in our lab used BSA in the media, resulting in NPCs with increased DNA synthesis after exposure to the same VPA dose. Furthermore, our lab previously shown that 10 fold lower doses of VPA elicited mitogenic effects without BSA in culture medium, which illustrated how seemingly disparate results could be due to media composition. Others have shown in primary astrocyte culture that acute exposure of VPA can be mitogenic at 0.6 mM but antimitogenic at 2 mM (119) . This fluctuation was due to VPAs ability to upregulate the CKIs p21 and p27 only at 2 mM, preventing G1 to S-phase transition (119). Duration of exposure has also impacted different signaling pathways. For example, chronic exposure of NSCs to 0.75 mM VPA over 3, 7 and 10 days promoted differentiation and increased levels of Wnt-3a and β-catenin (124). Therefore results observed after acute exposure compared to chronic will often indicate different mechanisms.

Other culture studies using neural progenitors demonstrated mitogenic effects of VPA on cortical precursors. NPC studies using FACS sorting after 18 hours exposure of 0.5 mM VPA, exhibited a reduction in G1 phase and increased S and G2/M phase (118). Previous data from our lab also supported G1 to S phase transition with elevated DNA synthesis after 1 mM VPA exposure in 24 hour culture, with direct changes to cyclins after acute 4 hour exposure, suggesting mechanism for such a transition. I demonstrated by VPA dose

response analysis, that elevated DNA synthesis could occur in E14.5 cortical progenitors with VPA doses as low as 0.3 mM, and as high as 1 mM. I also demonstrated that increases in DNA synthesis due to 0.5 mM VPA was comparable, to the 1 mM dose effect. With preliminary studies, I also provided preliminary evidence that this dose elicited elevations in cyclin E1 and acetyl H3 proteins, with static levels of cyclin D1 after 4 hours of culture. This finding was consistent with the model of increased G1 cyclins promoting G1 to S phase transition(165).

To frame results within the existing story of rapidly increased cyclin and acetylated H3 protein, and to provide mechanistic understanding for G1 to S phase transition *in vitro,* cultures were acutely exposed to 1 mM VPA, followed by analysis of cyclin cDNA levels. I demonstrated there was approximately a 2 fold increase in the cDNA for Cyclins D3 and E1 after 4h exposure of 1mM VPA. These findings were consistent with previous lab findings of rapid early increases in cyclin D3 and E1 proteins after VPA exposure. In addition, I showed that fold change findings at 4 h were highly similar to those seen at 2 h for all cyclin cDNAs, and continuous exposure with VPA resulted in persistent increases in cyclin E1message at the 8 and 17 hour time point that I measured. The early and constant elevations in Cyclin E1 and D3 message may also contribute to increased protein levels seen at 4 h and later time points. With such a rapid change in cyclin message, my data could suggest that VPA promoted post translational modifications of histones to alter transcription at these promoters. Previous data also identified that Cyclin D1 protein was unchanged by VPA, and

I demonstrated that Cyclin D1 message was actually 23% reduced after 4 hour culture with 1 mM VPA. The reduced D1 message suggested that VPA could be post translationally modifying histones which regulate this gene. Additionally, evidence of unchanged protein levels may suggest VPA could have regulated D1 protein degradation. Overall, this finding was still likely consistent with previous protein results, as cyclin D1 protein expression cycles at a slow rate, with prolonged expression through G2, M, and G1 phases of the cell cycle before decreasing in S phase (166). The ability of VPA to regulate gene expression was also consistent with other cortical culture studies indicating this drug can change expression of a vast number of genes (128). However, their analysis was on E17 cortical cultures after an 18 hour exposure with a higher VPA dose (5 mM) which could have been antimitogenic, while my data analyzed effects under a short exposure using a much lower dose. With acute VPA exposure using a lower, mitogenic dose, I have identified direct gene changes that provided supporting evidence for VPAs mitogenic response. . This was supported by the fact that this dose of VPA was able to inhibit HDAC activity and rapidly modulate gene expression. Additional studies in cell lines have shown that other HDAC inhibitors can upregulate mRNA of cyclin E through acetylation at Sp1 binding sites on the promoter (167), further supporting that VPAs ability to inhibit HDACs likely promoted the rapid increases in cyclin gene expression in my studies. Cell culture studies have also suggested that VPA most strongly inhibits HDAC1 (30). Other, studies have found that HDAC1 is bound at Sp1 sites for p21 which inhibits its expression, while HDAC inhibitors can upregulate its expression,

promoting growth arrest (168). This makes sense within the dose dependent mitogenic and antimitogenic effects of VPA seen in primary astrocyte cultures. Those studies have shown that low doses of VPA increased DNA synthesis, and cyclin D and E proteins, without p21 upregulation, however higher VPA doses decreased DNA synthesis and additionally upregulated p21 protein (119). This suggested that VPA may inhibit HDACs able to inhibit Sp1 sites at gene promoters, allowing for differential gene transcription, depending on VPA dose and the corresponding percentage of HDAC inhibition. Limitations to my above studies could include not measuring mRNA increases at both low and high doses of VPA and determining if there was altered expression of p21 mRNA within any of these doses. Ongoing studies could examine this potential mechanism further. However, current analysis of cyclin message supported early increases cyclin protein while also indicating that VPAs effects on cyclinD1 gene and protein expression can be differential. In sum, my data supported that VPA is capable of increasing cyclin mRNA levels through increased transcription, likely as a direct change of acetylation at the promoters of these genes. The increased cyclin message and protein, therefore promoted rapid G1 to S phase transition in cortical precursors, giving rise to more cells in the cerebral cortex.

B) HDAC message and protein is present in developing Rat cortex

The expression pattern of HDACs in the developing Rat cortex is currently incomplete. To date, in situ hybridization analyses in the murine brain only investigated expression for Class I (HDAC2) and II (HDAC 5, 6) developmental profiles [Allen Developing Mouse Brain Atlas]. Further, analysis of protein

expression within the developing rat cortex was only done for Class I HDACs (1 and 2), revealing distinct but overlapping expression in the VZ/SVZ (84). To expand on this current knowledge, I provided data observing cDNA of Class I, II, III and IV HDAC expression within the developing embryonic cortex, brain stem and basal ganglia. Multiple bands were present for HDAC 4, 6 and 11, suggesting alternative splicing. Studies have shown that HDAC protein activity can influence splice site selection of genes (169). Additional studies could investigate if HDAC inhibition by VPA could alter HDAC message splicing. When characterizing message, I also provided preliminary evidence by semi quantitative RT-PCR that HDAC cDNA levels were not drastically different among developing tissues. However, expression of several HDACs seemed to increase over the course of cortical development. These findings were consistent with in situ hybridization data for developmental HDAC expression. In addition, I observed that HDAC 1 and 2 proteins are expressed in rat cortical precursors, which is consistent with findings from previous studies. In sum these findings contribute to our understanding that broad HDAC expression from multiple classes could be expressed during brain development, and confirmed that HDAC protein is present in primary rat cortical cultures.

C) VPA inhibits endogenous HDACs in the developing cortex

HDACs regulate gene expression by deacetylating histones thus relaxing the DNA wrapped around them. Literature has shown that VPA is capable of inhibiting class I and II HDACs in cell lines with a specific IC50 for HDAC 1 between 0.4 mM (30) and 0.7 mM (30, 90). Valproic acid's IC50 for other

HDACs is also similar, with HDAC2 and 3 being 0.8 and 1 mM, in 293T cells (90). *In vitro* exposure to VPA can also increase acetylation levels of histones H3, (96, 118, 128) and H4 (96, 128, 170), further supporting its ability to inhibit HDAC activity. To now extend these findings to developing cerebral cortex, I provided supporting evidence that VPA increased Acetylated Histone H3 both in vitro and in vivo.

Although the scientific community assumed that VPA can inhibit HDACs, due to observable increases in acetylation of histone proteins, and cell line studies on HDAC activity, the enzymatic activity of Rat cortical HDACs has not yet been measured in the presence of VPA. I demonstrated for the first time that E14.5 rat cortical cells have HDAC enzymatic activity, and that VPA can inhibit this activity in a dose dependent manner. Inhibition of total HDACs was seen at all doses measured, and ranged from 11 to 50% activity. This inhibition was also reflective of VPA IC50 values for various HDACs. Further, I showed that increased DNA synthesis due to VPA treatment fell within VPA doses also seen to significantly inhibit HDAC enzymatic activity. With confirmation that VPA can inhibit HDAC activity within mitogenic dose range, this further supported the earlier proposed mechanism that rapid increases in cyclin E1 and D3 mRNAs and proteins was likely due to increased acetylated H3 protein, thereby allowing for increased cell cycle protein expression. I have also demonstrated that a 1mM exposure of VPA elevated G1 cyclin mRNAs and proteins, resulting in G1 to S-Phase transition. It should be noted that the degree of HDAC inhibition could be correlated to proliferative effects and ability for G1 to S transition. Studies using

C33a and Saos-2 cell lines suggest that exiting G1 of the cell cycle is regulated by a repressor complex including HDAC, hSWI/SNF nucleosome remodeling complex, and Rb (171). In these cell lines, it was observed that phosphorylation of Rb by cyclin D/cdk4 released HDAC from the complex, promoting transcription of cyclins E and A (171). Additionally the HAT p300 acetylates E2F1 to increase its transcriptional activity, and this deacetylation is reversed by HDAC1 (172). Therefore, inhibition of HDAC 1 could upregulate cyclin molecules through E2F transcriptional activity by multiple mechanisms. Because VPA inhibits HDACs, with strongest inhibition to HDAC1, it may directly open up cyclin promoter transcription, inhibit HDAC participation in the hSWI/SNF complex, and promote E2F1 transcriptional activity. All of these proposed mechanisms may work in concert to allow for the rapid increases in G1 cyclins we have observed *in vitro* and *in vivo*.

Studies which used primary mouse fibroblasts missing both HDAC 1 and 2 were stuck in G1, unable to proliferate (83). These cells exhibited elevated CKIs p21 and p57, while wildtype cells capable of proliferation exhibited HDAC 1 and 2 bound at these CKI promoters (83). When applying this information to proposed IC50 values for HDAC 1 +2, as well as my HDAC enzymatic assay inhibition levels in cortical precursors, it is likely that lower doses of VPA only partially upregulated these CKIs. This is further supported by our labs VPA dose response producing biphasic effects on DNA synthesis. Under low doses, VPA could promote G1 to S transition, while high VPA doses, appeared to inhibit this effect. My observed decreases in cyclin D1 mRNA seen after 1mM VPA

exposure could also be the beginning of antimitogenic impacts seen in VPA. It has also been shown that HDAC7 is expressed in embryonic development, and having too much or little of this HDAC downregulates cyclin D1 levels (172). The concept that higher HDAC inhibition could prevent proliferation by upregulating CKIs is consistent with a previous study showing mitogenic response after 0.6 mM VPA, but antimitogenic responses after2 mM VPA where increases in p21 and p27 were observed (119). Additionally, complete ablation of HDAC 1+2 genes within the developing brain caused defects in development, proliferation, and overall animal survival (86). Although, these animals had a temporary increase in BrdU at E14.5, it was immediately followed by increased cell death and drastic reduction in BrdU labeling index by E15.5 (86). These findings suggested that partial inhibition of HDAC1 and 2 can facilitate G1 to S phase transition, while complete inhibition also promotes apoptosis. Therefore having at least some HDAC activity may be necessary to maintain cell survival while minimal inhibition can facilitate G1-S transition. My in vitro analyses of HDAC inhibition, as well as increased DNA synthesis and cyclin proteins due to VPA exposure, suggested that minimal HDAC inhibition can facilitate G1 to S phase transition. In sum, the ability of VPA to inhibit HDAC enzymatic activity and increase acetylated H3 protein of rat cortical precursors was highly consistent with previous literature findings, and provided concrete foundations for a mechanism to our proliferative results.

Future studies are needed to further confirm if altered cyclin gene expression is due to VPA's inhibition of HDAC activity, and changes in histone

functions. In addition to regulating genes by HDAC inhibition, studies have shown that VPA can regulate microRNAs, potentially through multiple mechanisms. VPA can induce proteasome degradation of DICER, with key implications for the expression of several microRNAs (173). Furthermore, a recent study has shown the HDAC inhibitor SAHA can regulate levels of 24 miRNAs in skeletal muscle cells (174), providing implications that HDAC inhibition can also change miRNAs. The regulation of miRNAs may also provide insight into ASD etiology, as VPA can upregulate microRNA-132 in mouse brain which consequentially decreases MECP2 message (175). This alternate form of gene regulation could also play roles in proliferation, growth, and development. Others have shown VPA exposure can enlarge the amygdala in rats, while also increase microRNA-181C and microRNA-30d, thereby changing neurite outgrowth and branching (176). Although not currently linked to VPA or HDAC inhibition, microRNA-195 can also regulate expression of G1 cyclins D1 and E (177), suggesting that altered microRNA levels could directly impact the cell cycle. In sum, additional studies could identify if VPA could regulate microRNAs through HDAC inhibition or by other means; these studies could help uncover additional roles by which VPA could alter neurogenesis, and increase risk for ASD.

D) VPA promotes neurogenesis of specific cortical precursor populations *in vivo*

Subsets of ASD individuals have enlarged brains, and altered growth in brain regions including the cortex. This overgrowth is also seen in the cerebral cortex during early childhood (40). Further, studies have shown brain growth and

development is altered after prenatal VPA exposure, and my data supported this, as I have shown aberrant neurogenesis in the embryonic cortex, suggesting altered brain development.

After 5 prenatal injections of VPA from E16.5 to E18.5, I demonstrated that embryonic cortices had 1.58 fold more cyclin E1 protein, and 1.07 fold more Acetylated H3. Prenatal exposure to VPA has been shown to increase proliferation of cortical precursors in other animal studies (118, 121). My increases in cyclin E1 protein are consistent with these findings as well as previous lab data *in vitro* and *in vivo*. I also demonstrated that at this time, Tbr2 protein was increased 2.21 fold, while there was no significant change in Pax6 protein. Kim and colleagues observed an increase in cortical Tbr2 protein from E16 to E18 in response to a single VPA injection at E12. My findings may be consistent with these results. Yet at E18, Kim and colleagues also observed a decrease in Pax6 protein and message, suggesting Pax6 changes gave rise to later increases in Tbr2 intermediate progenitors (127). Further, they argued that changes in Pax6 may be regulating cell fate and the primary explanation for increased glutamatergic neurons. My data instead, suggested primary changes may be from direct changes in cyclins and increased SVZ cells in S phase expressing Tbr2, with no observed changes in Pax6. Considering injection duration and age of embryos during exposure of these studies, comparisons may not be directly comparable, but my findings may to provide alternate explanations by which VPA can increase glutamatergic neuronal cell numbers. Potential criticisms of my western analyses might be the limited *in vivo* increases in

acetylated Histone H3 protein after the VPA injection series. Although increased acetylated H3 in my studies was modest, it was significant. In mouse studies, increases in acetylated H3 were observed up to 6 hours after the VPA injection, and they noted it was a transient change (123). This could partially explain why acetylated H3 was only modestly increased in my studies, considering animals were sacrificed 5 hours after the last injection of VPA, yet these animals received multiple prior injections of VPA.

Using non-biased stereology, I demonstrated that there was a significant increase in the labeling index of Tbr2 but not Pax6 cell populations. This finding was consistent with, and could explain previous lab stereology data indicating that after prenatal VPA injection, postnatal day 21 rat pups exhibited more total cells in their brain with a specific increase in upper layer neuronal marker cux1 by 26.2%. Further, the increased number of Tbr2 cells in S phase could explain increased neuronal populations including cux1 because studies have indicated that Tbr2 expressing cells can contribute to generating all neuronal layers. Another mouse study identified that prenatal VPA promoted cortical dysgenesis, inhibited cell cycle exit of progenitor cells and increased numbers of superficial neurons (121). These findings are similarly consistent with my increased labeling index of Tbr2 precursors as these cells can give rise to upper layer neurons. Studies mutating Tbr2 also observed reduced upper layer neuronal markers Satb2, while most lower layer markers were unchanged (161). These data suggest that Tbr2 plays roles in maintaining cells within the cell cycle, as well as preferentially generating upper layer neurons. Although additional studies are

needed, my data may suggest that VPA exposure could increase cell cycle reentry. I have shown that prenatal VPA exposure causes increased levels of cyclin E1 protein. Additionally the CDK2-cyclin E complex can phosphorylate its CKI, p27 and promote its degradation (59). Cell cycle reentry only occurs when CKI levels are kept low enough and G1 cyclins are high. However if the CKI levels get too high, coupled with decreased Notch1 tone, cells will exit the cycle (3). Additionally, conditional inactivation of Tbr2 causes a reduction in cell cycle re-entry at E16 with more cells exiting the cell cycle (161). Although mechanisms remain to be defined, my data showing increased Tbr2 and cyclin E1 proteins may aid in cell cycle reentry, because Tbr2 loss promotes cell cycle exit, and cyclin E aids in reentry.

I have also provided data suggesting there were no significant changes in total numbers of Tbr2, Pax6, or cells co expressing Pax6 +BrdU, indicating that only the labeling index for Tbr2 cells has changed. This change was not due to a change in numbers of Tbr2 cells, therefore suggesting more cells are entering S-phase. However the estimated total number of co labeled Tbr2 + BrdU cells only had a trending significant increase. This could be due to variability in litters, and may become significant if an increased N was pursued. Because the labeling index for Tbr2 cells was significantly increased in VPA treated embryos, more Tbr2 cells were undergoing S phase, which could give rise to more neurons in the cerebral cortex.

I also provided preliminary evidence suggesting the increased TBR2 labeling index may be a sex dependent effect, being greater in males. Studies

have shown that females have a protective effect from developing autism (14). Others have identified that boys but not girls with ASD had abnormalities in generalized overgrowth of the birth, which could be predictive of reduced social and communication skills by 4 years old (178). Therefore, my findings were consistent with these studies.

One potential criticism in my stereological analysis is that previous lab results suggested there would be an overall increase in the BrdU/Dapi labeling index, yet this was not apparent in either the Pax6 or Tbr2 compartment analyzed in my studies. However, within the Tbr2 compartment, there was a trending increase in both the total number of BrdU+ cells as well as cells co expressing BrdU and Tbr2. The fact that there was not an overall increase in BrdU labeling index could have occurred if some litters were inaccurately time mated resulting in variation among embryonic litter ages and consequentially altering percentages of progenitor cells pools among groups. It is also possible that overall BrdU labeling index increases were not observed due to the rostral/caudal region analyzed, as I sampled from a more caudal point than previous studies within lab. Further, my analyses of Pax6 or Tbr2 compartments focused on the large majority of immunopositive cells but did exclude cells which did not have over 50% signal for any marker, while previous procedures conducted analyses on paraffin imbedded sections with visualization using DAB reaction, providing additional variation in signal to noise and exclusion criteria across both data sets.

In sum my in vivo data suggested that prenatal exposure to VPA impacted

proliferation of specific neuronal populations. The increased Tbr2 labeling index replicated previous lab results in part, and provided supporting evidence that prenatal VPA exposure can generate more upper layer neurons, consistent with other studies findings. The observed increases in cyclin E, Tbr2, and acetyl H3 proteins also supported previous results suggesting that epigenetic regulation could increase neurogenesis and promote G1 to S phase transition.

5.3) Findings outlining 16p11.2 deletion NPC altered neurogenesis

A) 16p11.2 NPCS have altered levels of DNA synthesis

Previous mouse studies have suggested that the 16p11.2 deletion favors enhanced proliferation due to increased ERK activation and cyclin D1, followed by early cell cycle exit due to p27 (21). Clinical descriptions of some humans with the 16P deletion indicated macrocephaly as a phenotype (162) suggesting alterations in brain development, and proliferation. Although there was some altered signaling due to loss of this CNV, additional research is needed to understand how increased proliferation occurs in these mice and humans. I presented data which supported the biology seen in the mouse. Specifically, I demonstrated 16p11.2 NPCs have elevated DNA synthesis at early passages, which then became dramatically slower compared to control NPCs at older passages. My data demonstrated that the two 16p11.2 males have a 30% increase in DNA synthesis overall, which increased to 70% if only looking at passages 3-5. From passage 6-8, the 16p11.2 males actually had a 20%

decrease in DNA synthesis with respect to control NPCs, suggesting that as NPCs become older, more of them could be differentiating. Although differentiation and S-phase markers for cell cycle exit need to be investigated, and additional clones need to be studied, my DNA synthesis data by passage was consistent with cellular biology seen in the mouse model for enhanced early proliferation, and early cell cycle exit.

B) 16p11.2 cell counts are similar to control NPCs under 30% expansion

One possible explanation for why 16p11.2 NPCs exhibited increased DNA synthesis after 48 hours could be increased cell number, due to alterations in proliferation. Mouse studies indicated proliferative changes were seen by overactive ERK1 and increased cyclin D1 (21). I presented preliminary evidence that 16p11.2 NPCs have a non significant 15% increase in total cell numbers by day 6 of culture. Further, by limiting experiments to P3-P5, a trending 40% increase was observed by day 6. Although additional experiments need to be conducted, this data may be consistent with observed increases in DNA synthesis after 48 hr culture. To address if cell survival was altered in 16p11.2 NPCs, I demonstrated that there were no significant difference in total cell numbers after 2 days culture. This shows that there was not a dramatic reduction in 16p11.2 NPC number compared to controls, which was consistent with the notion that survival of plated cells is equivalent. The mouse model also indicated no apparent differences in apoptosis between unaffected and affected rodents (21). Additional studies could investigate this further through cleaved caspase-3 staining. I also demonstrated that cell counts by day 6 were not

significantly different between 16P and control NPCs, however a trending

increase was observed for 16P if data were analyzed by early passage (P3-P5)

only. These data suggested that 16P NPCs do not have dramatically altered

survival or alterations in cell numbers compared to control NPCs under regular

media conditions. Thus the minimal increases in cell number with increased

DNA synthesis, trending increases in PERK and activated downstream effector

cyclin D1 suggested that these cells may have altered cell cycle length and

potentially altered size. This could be supported through overactive P-S6 which

is a downstream effector of mTORC1 (77).

C) 16p11.2 NPCs have reduced total ERK1, and evidence of altered signaling pathways

The increased proliferation seen in the 16p11.2 mouse was suggested to

be due to hyperphosphorylated ERK 1, as well as upregulation of its downstream

effector, cyclin D1 (21).   However, this finding has not yet been investigated in

non cancerous human cells. I first demonstrated that Total ERK 1 protein was

reduced close to 50% of unaffected controls, as expected for the CNV deletion.

With a reduction in total ERK1, studies suggested that mice with 16p11.2

exhibited dysregulation of ERK signaling (21). My data showed a trending 1.3

fold increase in PERK1, however there was variability across individuals. If

additional clones continue this trend to significance, my data would support P-

ERK1 hyperactivity, which is consistent with the mouse model findings.   ERK

signaling pathways are involved in regulation of proliferation (21, 69, 179).

Furthermore, Cyclin D1 transcription can occur through the RAF MKK1 ERK

signaling pathway (62). My western data demonstrated that 16p11.2 NPCs have a 1.32 fold increase in Cyclin D1 protein, which is consistent with the increased DNA synthesis, and could be increased through overactive ERK signaling, consistent with previous murine studies.

Considering there was elevated DNA synthesis and G1 cyclins, it would suggest that there could be more proliferation with increased cell numbers. With only a trending increase seen for this, I investigated P-S6 levels which could explain increased DNA synthesis without increasing cell numbers. I demonstrated that phosphorylated S6 was increased by 1.86 fold in 16p11.2 NPCs. Although normal activation of P-S6 can be explained by activation of the mTOR pathway, evidence has suggested interaction between mTOR and ERK (76, 77). The ERK pathway may indirectly upregulate P-S6 through RSK (180). Phosphorylated ERK ½ can phosphorylate the mTORC1 activating protein, Raptor in a Ras dependent mechanism using cell lines (181). The complex mTORC1 is also able to interact with S6, playing roles in translation initiation and elongation (77) . Therefore my findings could be consistent with other studies, and additional investigation into mTOR signaling within these cells should provide further understanding if crosstalk between these signaling pathways occurred in 16P NPCs or if these cells had activated mTOR activity. Although potential interactions between mTOR and ERK signaling pathways require additional research, there has also been correlative evidence of dysregulation of both cyclin D1 and P-S6 in hemimegalencephaly cases. It has been observed that cyclin D1 and P-S6 are co-expressed in hemimegalencephaly, and within

this phenotype, balloon cells and cytomegalic neurons are often observed (182).

However, this activation of cyclin D1 was proposed to be through activation of

beta-catenin signaling pathway (182). Others have suggested that there is

crosstalk between MAPK and beta-catenin pathways based on Wnt3a activation

of ERK pathway, and that inhibition of ERK is able to attenuate Wnt3a

transcription in cell lines (183). My data was also consistent with these findings,

as increases in cyclin D1 and P-S6 have been observed in 16p11.2 NPCs, and

by preliminary visual observation, these NPCs seem to have enlarged somas

compared to unaffected NPCs. Furthermore, the SFARI database indicated that

of these two 16p11.2 patients, one exhibited macrocephaly at 14.3 years, while

the other was within the 71 percentile at 1.5 years, suggesting slight increased

head circumference. Trending increases in PERK1, as well as increases in

Cyclin D1 and P-S6 provided explanations for increased DNA synthesis in 48

hour culture and the trending increases in total cell numbers by day 6. These

data also indicated that 16p11.2 NPCs have multiple alterations in growth and

altered signaling. Although P-S6 increases could be due to multiple signaling

pathways, the elevation corresponded with increased DNA synthesis and a

trending increase in PERK1. Additional studies would need to be done in order

to determine if some of these changes are due to crosstalk between ERK and

mTOR or beta-catenin signaling pathways. To better understand why increases

in cell number by day 6 are only trending, investigations into S phase length

could be elucidating. Increased symmetric division could promote a larger

population of cells and has been argued to have a longer s-phase due to greater

efforts in DNA repair and synthesis, while commitment to neural fates have

shorter s-phase (184). Based on signaling abnormalities, these cells could also

have altered cell cycle lengths, suggestive of proliferative or differentiating

phenotypes. In sum, these data suggested that 16p11.2 NPCs exhibit altered

signaling and protein expression in downstream effectors of ERK as well as

mTOR, which could explain increased DNA synthesis, and day6 cell count

findings.

D) 16p11.2 deletion NPCs have altered responses to mitogenic

stimulation

Mitogenic stimulation of the MAPK signaling cascade gives rise to

increased proliferation (69). Considering that recent evidence from 16p11.2

deletion mice suggest that there is ERK dysregulation in this system (21), it

would follow that mitogenic stimulation of this pathway could have altered

responses. The mitogenic factor, fibroblast growth factor (FGF), is known to

activate the ERK signaling pathway through tyrosine kinase receptors (179). I

demonstrated by scatter plot of percent control DNA synthesis values, that

unaffected NPCs have a higher FGF response than 16p11.2. This blunting was

also visibly observed from average DNA synthesis graphs where unaffected

NPCs exhibited a 122% increase in DNA synthesis after FGF, while 16P NPCs

only had 68% increase, mirroring the blunted response also seen by scatter plot.

I also demonstrated by FGF dose response, that 16p11.2 NPCs may have a

reduced EC50 at 1ng/mL, compared to 3 ng/mL for unaffected controls. Further,

I demonstrated that 16p11.2 percent control increases were significantly less

than unaffected control changes at doses between 1 ng/mL and 30 ng/mL.

Colleagues and I have also demonstrated through additional low density culture

assay that 16p11.2 NPCs increase in cell number after FGF treatment is

approximately 50% lower than increases seen for unaffected control NPCs,

replicating this blunted effect by alternative measures. However, higher density

cell counts do not appear to be dramatically different between 16P and

unaffected NPCs, yet still exhibited a trending decreased response by day 6

compared to unaffected NPCs. These findings are consistent with the mouse

studies indicating that 16p11.2 has ERK dysregulation. Currently, limitations to

this blunted observation are that we have not analyzed all patient clones, nor

have experiments been weighted equally across all passages, potentially

conflating the effect. Ongoing studies however will validate the magnitude of

difference in FGF response for 16p11.2 and unaffected NPCs. In sum, these

data suggested that 16p11.2 NPCs exhibited a blunted response to FGF mitogen

and this may indicate altered functional response in ERK signaling.

Chapter 6: Ongoing studies, Future directions, and Conclusions

6.1) Valproic acids impacts on neurogenesis

Currently, I have several studies which require additional investigation before findings are deemed complete. With respect to alteration in neurogenesis due to prenatal VPA exposure, I observed an increase in the Tbr2 labeling index, which may be sex dependent. Therefore I aim to examine additional embryonic brains which were injected with saline or VPA during late neurogenesis. After analyses of these additional brains, genotyping will be conducted, in order to conclude if a greater magnitude change in the Tbr2 labeling index is observed in male brains. Further, I expect the additional brains to result in significance for the average estimated total number of Tbr2 + BrdU+ cells, which likely was skewed due to sex specific changes in proliferation amongst these cells. It would be tremendously satisfying to conclude that sex dependent effects in neurogenesis are observed as a result of prenatal VPA exposure, as this would underscore the heterogeneity seen for this risk factor, and create interesting follow up questions into what mechanisms could sex regulate neurogenesis in the SVZ. I also plan to investigate the degree at which HDAC inhibition could be implicated in the SVZ. To do this, I plan to count the labeling index of HDAC2 positive cells. HDAC 2 is found within cells transitioning to become post mitotic, and has increased expression in neurons. Therefore if I see an increased labeling index in HDAC2 cells in VPA pretreated brains, this would suggest that

HDAC inhibition is preventing cells from differentiating, thus explaining why only this subset of cells is being impacted. With respect to in vitro studies investigating post translational modifications on histones, thereby increasing transcription of G1 cyclins, I would like to understand if CKIs are also increased. I would propose to expose cultures to a series of mitogenic doses of VPA for 4 h, and measure fold change increases in both cyclins and respective CKIs that HDACs may regulate. This could provide supporting evidence that lower doses of VPA can preferentially upregulate message for cyclins over CKIs.

6.2) 16p11.2 and its role in altering neurogenesis

In order to validate previous findings, all of the current findings must be replicated using additional clones for each patient. Current data suggests that most clones for a person agree in their biological responses, but some cases have shown large variability in signaling. To address discrepancies in signaling, I plan to run westerns using multiple clones for each patient on the same gel. This may further elucidate changes in P-ERK1 as I currently see a trending increase. In order for current studies in male 16p11.2 NPCs to be considered complete, each of the three unaffected controls as well as these two 16p11.2 NPCs should have studies repeated using 3 different clones. Unfortunately, some of these patients do not have this amount of clones currently available, so ongoing studies will be repeated as samples are received. I had also mentioned briefly that studies have investigated a female patient with the 16p11.2 CNV but did not have available sex matched controls. As of now, one clone is available to study, and is being expanded. I plan to conduct the same cassette of experiments on

this female control to determine if there are sex differences seen in neurogenesis within this genetic model for ASD.

My studies using the two male 16p11.2 NPCs indicated that there was an increase in P-S6 with cell somas being observably larger than unaffected controls. To investigate these things, I plan to measure volume of cell somas to determine if this could play a role in the enlarged brain phenotypes sometimes seen in 16P. Additionally, I am going to investigate the P-S6 signaling pathways in more detailed protein analyses. If there are no upstream increases in P-S6, I will look for feedback mechanisms and potential crosstalk with the ERK pathway. If after additional clones P-ERK1 levels become significant, I will also treat with an ERK inhibitor to determine if increased DNA Synthesis is due to hyperphosphorylation of the ERK pathway. I also plan to investigate proliferative changes in these cells further. It is possible that the current assay measuring total cell counts after 6 days is not sensitive enough. Therefore I may look into FACS sorting cell populations in order to get more accurate counts, and also plan to investigate total cell counts using more low density culture measures. Cell death will also be directly measured through cleaved caspase staining in order to identify if non significant increases in cell number is due to increased death in 16p11.2 NPCs. Other studies will investigate differentiation, by staining plated cells with early differentiated markers after 48 hr culture and analyses will be categorized by passage. This will help identify if passage specific changes in DNA synthesis are due to differentiation, or another mechanism.

6.3) Conclusions

These studies investigated alterations in neurogenesis due to environmental and genetic risk factors for ASD. Findings have indicated that neurogenesis is altered in both cases, but likely through different mechanisms that can stimulate G1 cyclins and DNA synthesis. Further, both exposures indicate there may be increased proliferation within precursor cells. VPA exposure may increase proliferation through HDAC inhibition, increasing G1 cyclins which specifically causes increased G1 to S transition in the SVZ. However, the CNV 16p11.2 may have increased early proliferation and overall increases in growth by altered P-ERK1, cyclin D1, and P-S6 signaling. These two ASD risk factors provide additional explanations for how altered brain growth in development can produce a bigger brain. Considering that accelerated brain growth is both observed in, and potentially an early diagnostic tool for ASD, my findings create a better understanding in how ASD may arise. Further, approximately 20% of ASD individuals exhibit macrocephaly, and I provide mechanistic evidence how alterations in neurogenesis can underpin a bigger brain. Understanding that these epigenetic and genetic changes could create a bigger brain, we can further study these signaling pathways, to learn how to prevent, and potentially treat brain overgrowth during development. Growing evidence suggests that increased neurogenesis is one way which ASD can arise, thus it is imperative that future studies delve further into these mechanisms.

References

1.   Breunig JJ, Haydar TF, Rakic P. Neural stem cells: historical perspective and future prospects. Neuron. 2011;70(4):614-25. doi: 10.1016/j.neuron.2011.05.005. PubMed PMID: 21609820; PubMed Central PMCID: PMC3225274.

2.   Tury A, Mairet-Coello G, DiCicco-Bloom E. The multiple roles of the cyclin-dependent kinase inhibitory protein p57(KIP2) in cerebral cortical neurogenesis. Developmental neurobiology. 2012;72(6):821-42. doi: 10.1002/dneu.20999. PubMed PMID: 22076965.

3.   Caviness VS, Jr., Nowakowski RS, Bhide PG. Neocortical neurogenesis: morphogenetic gradients and beyond. Trends in neurosciences. 2009;32(8):443-50. doi: 10.1016/j.tins.2009.05.003. PubMed PMID: 19635637; PubMed Central PMCID: PMC2725216.

4.   Kuo MH, Allis CD. Roles of histone acetyltransferases and deacetylases in gene regulation. BioEssays : news and reviews in molecular, cellular and developmental biology. 1998;20(8):615-26. doi: 10.1002/(SICI)1521-1878(199808)20:8<615::AID-BIES4>3.0.CO;2-H. PubMed PMID: 9780836.

5.   American Psychiatric A, American Psychiatric A, Force DSMT. Diagnostic and statistical manual of mental disorders : DSM-52013.

6.   American Psychiatric A, American Psychiatric A, Task Force on D-I. Diagnostic and statistical manual of mental disorders : DSM-IV-TR. Washington, DC: American Psychiatric Association; 2000.

7.   DiCicco-Bloom E, Lord C, Zwaigenbaum L, Courchesne E, Dager SR, Schmitz C, Schultz RT, Crawley J, Young LJ. The developmental neurobiology of autism spectrum disorder. The Journal of neuroscience : the official journal of the Society for Neuroscience. 2006;26(26):6897-906. doi: 10.1523/JNEUROSCI.1712-06.2006. PubMed PMID: 16807320.

8.   Developmental DMNSY, Investigators P. Prevalence of autism spectrum disorder among children aged 8 years-autism and developmental disabilities monitoring network, 11 sites, United States, 2012. Morbidity and mortality weekly report Surveillance summaries (Washington, DC: 2002). 2012;63(2):1.

9.   Harris SR. Early motor delays as diagnostic clues in autism spectrum disorder. European journal of pediatrics. 2017. doi: 10.1007/s00431-017-2951-7. PubMed PMID: 28660313.

10.   Jones W, Klin A. Attention to eyes is present but in decline in 2-6-month-old infants later diagnosed with autism. Nature. 2013;504(7480):427-31. doi: 10.1038/nature12715. PubMed PMID: 24196715; PubMed Central PMCID: PMC4035120.

11.   Estes A, Zwaigenbaum L, Gu H, St John T, Paterson S, Elison JT, Hazlett H, Botteron K, Dager SR, Schultz RT, Kostopoulos P, Evans A, Dawson G, Eliason J, Alvarez S, Piven J, network I. Behavioral, cognitive, and adaptive development in infants with autism spectrum disorder in the first 2 years of life. Journal of neurodevelopmental disorders. 2015;7(1):24. doi: 10.1186/s11689-015-9117-6. PubMed PMID: 26203305; PubMed Central PMCID: PMC4511527.

12.   Hogart A, Wu D, LaSalle JM, Schanen NC. The comorbidity of autism with the genomic disorders of chromosome 15q11.2-q13. Neurobiology of disease. 2010;38(2):181-91. doi: 10.1016/j.nbd.2008.08.011. PubMed PMID: 18840528; PubMed Central PMCID: PMC2884398.

13.   Bi X, Sun J, Ji AX, Baudry M. Potential therapeutic approaches for Angelman syndrome. Expert opinion on therapeutic targets. 2016;20(5):601-13. doi: 10.1517/14728222.2016.1115837. PubMed PMID: 26558806; PubMed Central PMCID: PMC4902328.

14.   Yin J, Schaaf CP. Autism genetics - an overview. Prenat Diagn. 2017;37(1):14-30. doi: 10.1002/pd.4942. PubMed PMID: 27743394.

15.   Khanzada NS, Butler MG, Manzardo AM. GeneAnalytics Pathway Analysis and Genetic Overlap among Autism Spectrum Disorder, Bipolar Disorder and Schizophrenia. International journal of molecular sciences. 2017;18(3). doi: 10.3390/ijms18030527. PubMed PMID: 28264500; PubMed Central PMCID: PMC5372543.

16.   Abrahams BS, Geschwind DH. Advances in autism genetics: on the threshold of a new neurobiology. Nature reviews Genetics. 2008;9(5):341-55. doi: 10.1038/nrg2346. PubMed PMID: 18414403; PubMed Central PMCID: PMC2756414.

17.   Ornoy A, Weinstein-Fudim L, Ergaz Z. Genetic Syndromes, Maternal Diseases and Antenatal Factors Associated with Autism Spectrum Disorders (ASD). Frontiers in neuroscience. 2016;10:316. doi: 10.3389/fnins.2016.00316. PubMed PMID: 27458336; PubMed Central PMCID: PMC4933715.

18.   Varghese M, Keshav N, Jacot-Descombes S, Warda T, Wicinski B, Dickstein DL, Harony-Nicolas H, De Rubeis S, Drapeau E, Buxbaum JD, Hof PR. Autism spectrum disorder: neuropathology and animal models. Acta neuropathologica. 2017. doi: 10.1007/s00401-017-1736-4. PubMed PMID: 28584888.

19.   Pinto D, Delaby E, Merico D, Barbosa M, Merikangas A, Klei L, Thiruvahindrapuram B, Xu X, Ziman R, Wang Z, Vorstman JA, Thompson A, Regan R, Pilorge M, Pellecchia G, Pagnamenta AT, Oliveira B, Marshall CR, Magalhaes TR, Lowe JK, Howe JL, Griswold AJ, Gilbert J, Duketis E, Dombroski BA, De Jonge MV, Cuccaro M, Crawford EL, Correia CT, Conroy J, Conceicao IC, Chiocchetti AG, Casey JP, Cai G, Cabrol C, Bolshakova N, Bacchelli E, Anney R, Gallinger S, Cotterchio M, Casey G, Zwaigenbaum L, Wittemeyer K, Wing K, Wallace S, van Engeland H, Tryfon A, Thomson S, Soorya L, Roge B, Roberts W, Poustka F, Mouga S, Minshew N, McInnes LA, McGrew SG, Lord C, Leboyer M, Le Couteur AS, Kolevzon A, Jimenez Gonzalez P, Jacob S, Holt R, Guter S, Green J, Green A, Gillberg C, Fernandez BA, Duque F, Delorme R, Dawson G, Chaste P, Cafe C, Brennan S, Bourgeron T, Bolton PF, Bolte S, Bernier R, Baird G, Bailey AJ, Anagnostou E, Almeida J, Wijsman EM, Vieland VJ, Vicente AM, Schellenberg GD, Pericak-Vance M, Paterson AD, Parr JR, Oliveira G, Nurnberger JI, Monaco AP, Maestrini E, Klauck SM, Hakonarson H, Haines JL, Geschwind DH, Freitag CM, Folstein SE, Ennis S, Coon H, Battaglia A, Szatmari P, Sutcliffe JS, Hallmayer J, Gill M, Cook EH, Buxbaum JD, Devlin B, Gallagher L, Betancur C, Scherer SW. Convergence of genes and cellular

pathways dysregulated in autism spectrum disorders. American journal of human genetics. 2014;94(5):677-94. doi: 10.1016/j.ajhg.2014.03.018. PubMed PMID: 24768552; PubMed Central PMCID: PMC4067558.

20.	Devlin B, Scherer SW. Genetic architecture in autism spectrum disorder. Current opinion in genetics & development. 2012;22(3):229-37. doi: 10.1016/j.gde.2012.03.002. PubMed PMID: 22463983.

21.	Pucilowska J, Vithayathil J, Tavares EJ, Kelly C, Karlo JC, Landreth GE. The 16p11.2 deletion mouse model of autism exhibits altered cortical progenitor proliferation and brain cytoarchitecture linked to the ERK MAPK pathway. The Journal of neuroscience : the official journal of the Society for Neuroscience. 2015;35(7):3190-200. doi: 10.1523/JNEUROSCI.4864-13.2015. PubMed PMID: 25698753.

22.	Hallmayer J, Cleveland S, Torres A, Phillips J, Cohen B, Torigoe T, Miller J, Fedele A, Collins J, Smith K, Lotspeich L, Croen LA, Ozonoff S, Lajonchere C, Grether JK, Risch N. Genetic heritability and shared environmental factors among twin pairs with autism. Archives of general psychiatry. 2011;68(11):1095-102. doi: 10.1001/archgenpsychiatry.2011.76. PubMed PMID: 21727249; PubMed Central PMCID: PMC4440679.

23.	Stromland K, Nordin V, Miller M, Akerstrom B, Gillberg C. Autism in thalidomide embryopathy: a population study. Developmental medicine and child neurology. 1994;36(4):351-6. PubMed PMID: 8157157.

24.	Wong H, Hoeffer C. Maternal IL-17A in autism. Experimental neurology. 2017. doi: 10.1016/j.expneurol.2017.04.010. PubMed PMID: 28455196.

25.	Kalkbrenner AE, Schmidt RJ, Penlesky AC. Environmental chemical exposures and autism spectrum disorders: a review of the epidemiological evidence. Current problems in pediatric and adolescent health care. 2014;44(10):277-318. doi: 10.1016/j.cppeds.2014.06.001. PubMed PMID: 25199954; PubMed Central PMCID: PMC4855851.

26.	Landrigan PJ. What causes autism? Exploring the environmental contribution. Current opinion in pediatrics. 2010;22(2):219-25. doi: 10.1097/MOP.0b013e328336eb9a. PubMed PMID: 20087185.

27.	Choi GB, Yim YS, Wong H, Kim S, Kim H, Kim SV, Hoeffer CA, Littman DR, Huh JR. The maternal interleukin-17a pathway in mice promotes autism-like phenotypes in offspring. Science. 2016;351(6276):933-9. doi: 10.1126/science.aad0314. PubMed PMID: 26822608; PubMed Central PMCID: PMC4782964.

28.	Kim YS, Leventhal BL. Genetic epidemiology and insights into interactive genetic and environmental effects in autism spectrum disorders. Biological psychiatry. 2015;77(1):66-74. doi: 10.1016/j.biopsych.2014.11.001. PubMed PMID: 25483344; PubMed Central PMCID: PMC4260177.

29.	Christensen J, Gronborg TK, Sorensen MJ, Schendel D, Parner ET, Pedersen LH, Vestergaard M. Prenatal valproate exposure and risk of autism spectrum disorders and childhood autism. JAMA : the journal of the American Medical Association. 2013;309(16):1696-703. doi: 10.1001/jama.2013.2270. PubMed PMID: 23613074.

30.   Phiel CJ, Zhang F, Huang EY, Guenther MG, Lazar MA, Klein PS. Histone deacetylase is a direct target of valproic acid, a potent anticonvulsant, mood stabilizer, and teratogen. The Journal of biological chemistry. 2001;276(39):36734-41. doi: 10.1074/jbc.M101287200. PubMed PMID: 11473107.

31.   Sacco R, Gabriele S, Persico AM. Head circumference and brain size in autism spectrum disorder: A systematic review and meta-analysis. Psychiatry research. 2015;234(2):239-51. doi: 10.1016/j.pscychresns.2015.08.016. PubMed PMID: 26456415.

32.   Courchesne E, Carper R, Akshoomoff N. Evidence of brain overgrowth in the first year of life in autism. JAMA : the journal of the American Medical Association. 2003;290(3):337-44. doi: 10.1001/jama.290.3.337. PubMed PMID: 12865374.

33.   Courchesne E, Pierce K. Brain overgrowth in autism during a critical time in development: implications for frontal pyramidal neuron and interneuron development and connectivity. International journal of developmental neuroscience : the official journal of the International Society for Developmental Neuroscience. 2005;23(2-3):153-70. doi: 10.1016/j.ijdevneu.2005.01.003. PubMed PMID: 15749242.

34.   Libero LE, Nordahl CW, Li DD, Ferrer E, Rogers SJ, Amaral DG. Persistence of megalencephaly in a subgroup of young boys with autism spectrum disorder. Autism research : official journal of the International Society for Autism Research. 2016;9(11):1169-82. doi: 10.1002/aur.1643. PubMed PMID: 27273931; PubMed Central PMCID: PMC5292980.

35.   Hazlett HC, Poe MD, Lightbody AA, Styner M, MacFall JR, Reiss AL, Piven J. Trajectories of early brain volume development in fragile X syndrome and autism. Journal of the American Academy of Child and Adolescent Psychiatry. 2012;51(9):921-33. doi: 10.1016/j.jaac.2012.07.003. PubMed PMID: 22917205; PubMed Central PMCID: PMC3428739.

36.   Hazlett HC, Gu H, Munsell BC, Kim SH, Styner M, Wolff JJ, Elison JT, Swanson MR, Zhu H, Botteron KN, Collins DL, Constantino JN, Dager SR, Estes AM, Evans AC, Fonov VS, Gerig G, Kostopoulos P, McKinstry RC, Pandey J, Paterson S, Pruett JR, Schultz RT, Shaw DW, Zwaigenbaum L, Piven J, Network I, Clinical S, Data Coordinating C, Image Processing C, Statistical A. Early brain development in infants at high risk for autism spectrum disorder. Nature. 2017;542(7641):348-51. doi: 10.1038/nature21369. PubMed PMID: 28202961; PubMed Central PMCID: PMC5336143.

37.   Amaral DG, Li D, Libero L, Solomon M, Van de Water J, Mastergeorge A, Naigles L, Rogers S, Wu Nordahl C. In pursuit of neurophenotypes: The consequences of having autism and a big brain. Autism research : official journal of the International Society for Autism Research. 2017;10(5):711-22. doi: 10.1002/aur.1755. PubMed PMID: 28239961; PubMed Central PMCID: PMC5520638.

38.   Schumann CM, Bloss CS, Barnes CC, Wideman GM, Carper RA, Akshoomoff N, Pierce K, Hagler D, Schork N, Lord C, Courchesne E. Longitudinal magnetic resonance imaging study of cortical development through

early childhood in autism. The Journal of neuroscience : the official journal of the Society for Neuroscience. 2010;30(12):4419-27. doi: 10.1523/JNEUROSCI.5714-09.2010. PubMed PMID: 20335478; PubMed Central PMCID: PMC2859218.

39.   Libero LE, Burge WK, Deshpande HD, Pestilli F, Kana RK. White Matter Diffusion of Major Fiber Tracts Implicated in Autism Spectrum Disorder. Brain connectivity. 2016;6(9):691-9. doi: 10.1089/brain.2016.0442. PubMed PMID: 27555361; PubMed Central PMCID: PMC5105348.

40.   Kaushik G, Zarbalis KS. Prenatal Neurogenesis in Autism Spectrum Disorders. Frontiers in chemistry. 2016;4:12. doi: 10.3389/fchem.2016.00012. PubMed PMID: 27014681; PubMed Central PMCID: PMC4791366.

41.   Sanders SJ. First glimpses of the neurobiology of autism spectrum disorder. Current opinion in genetics & development. 2015;33:80-92. doi: 10.1016/j.gde.2015.10.002. PubMed PMID: 26547130.

42.   Wolff JJ, Swanson MR, Elison JT, Gerig G, Pruett JR, Jr., Styner MA, Vachet C, Botteron KN, Dager SR, Estes AM, Hazlett HC, Schultz RT, Shen MD, Zwaigenbaum L, Piven J, Network I. Neural circuitry at age 6 months associated with later repetitive behavior and sensory responsiveness in autism. Molecular autism. 2017;8:8. doi: 10.1186/s13229-017-0126-z. PubMed PMID: 28316772; PubMed Central PMCID: PMC5351210.

43.   Casanova MF. Neuropathological and genetic findings in autism: the significance of a putative minicolumnopathy. The Neuroscientist : a review journal bringing neurobiology, neurology and psychiatry. 2006;12(5):435-41. doi: 10.1177/1073858406290375. PubMed PMID: 16957005.

44.   Wegiel J, Flory M, Kuchna I, Nowicki K, Ma SY, Imaki H, Wegiel J, Cohen IL, London E, Wisniewski T, Brown WT. Stereological study of the neuronal number and volume of 38 brain subdivisions of subjects diagnosed with autism reveals significant alterations restricted to the striatum, amygdala and cerebellum. Acta neuropathologica communications. 2014;2:141. doi: 10.1186/s40478-014-0141-7. PubMed PMID: 25231243; PubMed Central PMCID: PMC4177256.

45.   Courchesne E, Mouton PR, Calhoun ME, Semendeferi K, Ahrens-Barbeau C, Hallet MJ, Barnes CC, Pierce K. Neuron number and size in prefrontal cortex of children with autism. JAMA : the journal of the American Medical Association. 2011;306(18):2001-10. doi: 10.1001/jama.2011.1638. PubMed PMID: 22068992.

46.   Wegiel J, Flory M, Kuchna I, Nowicki K, Ma SY, Imaki H, Wegiel J, Cohen IL, London E, Brown WT, Wisniewski T. Brain-region-specific alterations of the trajectories of neuronal volume growth throughout the lifespan in autism. Acta neuropathologica communications. 2014;2:28. doi: 10.1186/2051-5960-2-28. PubMed PMID: 24612906; PubMed Central PMCID: PMC4007529.

47.   Wegiel J, Kuchna I, Nowicki K, Imaki H, Wegiel J, Marchi E, Ma SY, Chauhan A, Chauhan V, Bobrowicz TW, de Leon M, Louis LA, Cohen IL, London E, Brown WT, Wisniewski T. The neuropathology of autism: defects of neurogenesis and neuronal migration, and dysplastic changes. Acta neuropathologica. 2010;119(6):755-70. doi: 10.1007/s00401-010-0655-4. PubMed PMID: 20198484; PubMed Central PMCID: PMC2869041.

48.   Amaral DG, Schumann CM, Nordahl CW. Neuroanatomy of autism. Trends in neurosciences. 2008;31(3):137-45. doi: 10.1016/j.tins.2007.12.005. PubMed PMID: 18258309.
49.   Scott JA, Schumann CM, Goodlin-Jones BL, Amaral DG. A comprehensive volumetric analysis of the cerebellum in children and adolescents with autism spectrum disorder. Autism research : official journal of the International Society for Autism Research. 2009;2(5):246-57. doi: 10.1002/aur.97. PubMed PMID: 19885834; PubMed Central PMCID: PMC2999464.
50.   Kanner L. Autistic disturbances of affective contact. Acta paedopsychiatrica. 1968;35(4):100-36. PubMed PMID: 4880460.
51.   Spence SJ, Schneider MT. The role of epilepsy and epileptiform EEGs in autism spectrum disorders. Pediatric research. 2009;65(6):599-606. doi: 10.1203/PDR.0b013e31819e7168. PubMed PMID: 19454962; PubMed Central PMCID: PMC2692092.
52.   Chomiak T, Turner N, Hu B. What We Have Learned about Autism Spectrum Disorder from Valproic Acid. Pathology research international. 2013;2013:712758. doi: 10.1155/2013/712758. PubMed PMID: 24381784; PubMed Central PMCID: PMC3871912.
53.   Rausch A, Zhang W, Haak KV, Mennes M, Hermans EJ, van Oort E, van Wingen G, Beckmann CF, Buitelaar JK, Groen WB. Altered functional connectivity of the amygdaloid input nuclei in adolescents and young adults with autism spectrum disorder: a resting state fMRI study. Molecular autism. 2016;7:13. doi: 10.1186/s13229-015-0060-x. PubMed PMID: 26823966; PubMed Central PMCID: PMC4730628.
54.   Caviness VS, Jr., Takahashi T, Nowakowski RS. Numbers, time and neocortical neuronogenesis: a general developmental and evolutionary model. Trends in neurosciences. 1995;18(9):379-83. PubMed PMID: 7482802.
55.   Englund C, Fink A, Lau C, Pham D, Daza RA, Bulfone A, Kowalczyk T, Hevner RF. Pax6, Tbr2, and Tbr1 are expressed sequentially by radial glia, intermediate progenitor cells, and postmitotic neurons in developing neocortex. The Journal of neuroscience : the official journal of the Society for Neuroscience. 2005;25(1):247-51. doi: 10.1523/JNEUROSCI.2899-04.2005. PubMed PMID: 15634788.
56.   Noctor SC, Martinez-Cerdeno V, Ivic L, Kriegstein AR. Cortical neurons arise in symmetric and asymmetric division zones and migrate through specific phases. Nature neuroscience. 2004;7(2):136-44. doi: 10.1038/nn1172. PubMed PMID: 14703572.
57.   Sansom SN, Griffiths DS, Faedo A, Kleinjan DJ, Ruan Y, Smith J, van Heyningen V, Rubenstein JL, Livesey FJ. The level of the transcription factor Pax6 is essential for controlling the balance between neural stem cell self-renewal and neurogenesis. PLoS genetics. 2009;5(6):e1000511. doi: 10.1371/journal.pgen.1000511. PubMed PMID: 19521500; PubMed Central PMCID: PMC2686252.
58.   Sessa A, Mao CA, Colasante G, Nini A, Klein WH, Broccoli V. Tbr2-positive intermediate (basal) neuronal progenitors safeguard cerebral cortex

expansion by controlling amplification of pallial glutamatergic neurons and attraction of subpallial GABAergic interneurons. Genes & development. 2010;24(16):1816-26. doi: 10.1101/gad.575410. PubMed PMID: 20713522; PubMed Central PMCID: PMC2922508.

59.   Vermeulen K, Van Bockstaele DR, Berneman ZN. The cell cycle: a review of regulation, deregulation and therapeutic targets in cancer. Cell proliferation. 2003;36(3):131-49. PubMed PMID: 12814430.

60.   Sherr CJ. Mammalian G1 cyclins and cell cycle progression. Proceedings of the Association of American Physicians. 1995;107(2):181-6. PubMed PMID: 8624851.

61.   Sherr CJ, Roberts JM. Inhibitors of mammalian G1 cyclin-dependent kinases. Genes & development. 1995;9(10):1149-63. PubMed PMID: 7758941.

62.   Lavoie JN, L'Allemain G, Brunet A, Muller R, Pouyssegur J. Cyclin D1 expression is regulated positively by the p42/p44MAPK and negatively by the p38/HOGMAPK pathway. The Journal of biological chemistry. 1996;271(34):20608-16. PubMed PMID: 8702807.

63.   Pagano M. Cell Cycle Control: Springer Berlin Heidelberg; 2013.

64.   Schafer KA. The cell cycle: a review. Veterinary pathology. 1998;35(6):461-78. doi: 10.1177/030098589803500601. PubMed PMID: 9823588.

65.   Ohtani K, DeGregori J, Nevins JR. Regulation of the cyclin E gene by transcription factor E2F1. Proceedings of the National Academy of Sciences of the United States of America. 1995;92(26):12146-50. PubMed PMID: 8618861; PubMed Central PMCID: PMC40313.

66.   Subramanian M, Timmerman CK, Schwartz JL, Pham DL, Meffert MK. Characterizing autism spectrum disorders by key biochemical pathways. Frontiers in neuroscience. 2015;9:313. doi: 10.3389/fnins.2015.00313. PubMed PMID: 26483618; PubMed Central PMCID: PMC4586332.

67.   Kwan V, Unda BK, Singh KK. Wnt signaling networks in autism spectrum disorder and intellectual disability. Journal of neurodevelopmental disorders. 2016;8:45. doi: 10.1186/s11689-016-9176-3. PubMed PMID: 27980692; PubMed Central PMCID: PMCPMC5137220.

68.   Sun Y, Liu WZ, Liu T, Feng X, Yang N, Zhou HF. Signaling pathway of MAPK/ERK in cell proliferation, differentiation, migration, senescence and apoptosis. J Recept Signal Transduct Res. 2015;35(6):600-4. doi: 10.3109/10799893.2015.1030412. PubMed PMID: 26096166.

69.   Seger R, Krebs EG. The MAPK signaling cascade. FASEB journal : official publication of the Federation of American Societies for Experimental Biology. 1995;9(9):726-35. PubMed PMID: 7601337.

70.   Roux PP, Blenis J. ERK and p38 MAPK-activated protein kinases: a family of protein kinases with diverse biological functions. Microbiol Mol Biol Rev. 2004;68(2):320-44. doi: 10.1128/MMBR.68.2.320-344.2004. PubMed PMID: 15187187; PubMed Central PMCID: PMCPMC419926.

71.   Lillien L, Raphael H. BMP and FGF regulate the development of EGF-responsive neural progenitor cells. Development. 2000;127(22):4993-5005. PubMed PMID: 11044412.

72.   Li Z, Theus MH, Wei L. Role of ERK 1/2 signaling in neuronal differentiation of cultured embryonic stem cells. Dev Growth Differ. 2006;48(8):513-23. doi: 10.1111/j.1440-169X.2006.00889.x. PubMed PMID: 17026715.

73.   Duronio RJ, Xiong Y. Signaling pathways that control cell proliferation. Cold Spring Harbor perspectives in biology. 2013;5(3):a008904. doi: 10.1101/cshperspect.a008904. PubMed PMID: 23457258.

74.   Lee DY. Roles of mTOR Signaling in Brain Development. Experimental neurobiology. 2015;24(3):177-85. doi: 10.5607/en.2015.24.3.177. PubMed PMID: 26412966; PubMed Central PMCID: PMCPMC4580744.

75.   Qin L, Dai X, Yin Y. Valproic acid exposure sequentially activates Wnt and mTOR pathways in rats. Molecular and cellular neurosciences. 2016;75:27-35. doi: 10.1016/j.mcn.2016.06.004. PubMed PMID: 27343825.

76.   Dai J, Bercury KK, Macklin WB. Interaction of mTOR and Erk1/2 signaling to regulate oligodendrocyte differentiation. Glia. 2014;62(12):2096-109. doi: 10.1002/glia.22729. PubMed PMID: 25060812; PubMed Central PMCID: PMCPMC4406223.

77.   Mendoza MC, Er EE, Blenis J. The Ras-ERK and PI3K-mTOR pathways: cross-talk and compensation. Trends Biochem Sci. 2011;36(6):320-8. doi: 10.1016/j.tibs.2011.03.006. PubMed PMID: 21531565; PubMed Central PMCID: PMCPMC3112285.

78.   Rhim JH, Luo X, Gao D, Xu X, Zhou T, Li F, Wang P, Wong ST, Xia X. Cell type-dependent Erk-Akt pathway crosstalk regulates the proliferation of fetal neural progenitor cells. Scientific reports. 2016;6:26547. doi: 10.1038/srep26547. PubMed PMID: 27211495; PubMed Central PMCID: PMCPMC4876380.

79.   Toledo EM, Colombres M, Inestrosa NC. Wnt signaling in neuroprotection and stem cell differentiation. Progress in neurobiology. 2008;86(3):281-96. doi: 10.1016/j.pneurobio.2008.08.001. PubMed PMID: 18786602.

80.   Jobe EM, McQuate AL, Zhao X. Crosstalk among Epigenetic Pathways Regulates Neurogenesis. Frontiers in neuroscience. 2012;6:59. doi: 10.3389/fnins.2012.00059. PubMed PMID: 22586361; PubMed Central PMCID: PMC3347638.

81.   Dokmanovic M, Clarke C, Marks PA. Histone deacetylase inhibitors: overview and perspectives. Mol Cancer Res. 2007;5(10):981-9. doi: 10.1158/1541-7786.MCR-07-0324. PubMed PMID: 17951399.

82.   Brunmeir R, Lagger S, Seiser C. Histone deacetylase HDAC1/HDAC2-controlled embryonic development and cell differentiation. The International journal of developmental biology. 2009;53(2-3):275-89. doi: 10.1387/ijdb.082649rb. PubMed PMID: 19412887.

83.   Yamaguchi T, Cubizolles F, Zhang Y, Reichert N, Kohler H, Seiser C, Matthias P. Histone deacetylases 1 and 2 act in concert to promote the G1-to-S progression. Genes Dev. 2010;24(5):455-69. doi: 10.1101/gad.552310. PubMed PMID: 20194438; PubMed Central PMCID: PMCPMC2827841.

84.   MacDonald JL, Roskams AJ. Histone deacetylases 1 and 2 are expressed at distinct stages of neuro-glial development. Developmental dynamics : an

official publication of the American Association of Anatomists. 2008;237(8):2256-67. doi: 10.1002/dvdy.21626. PubMed PMID: 18651664.

85.   Kelly RD, Cowley SM. The physiological roles of histone deacetylase (HDAC) 1 and 2: complex co-stars with multiple leading parts. Biochemical Society transactions. 2013;41(3):741-9. doi: 10.1042/BST20130010. PubMed PMID: 23697933.

86.   Montgomery RL, Hsieh J, Barbosa AC, Richardson JA, Olson EN. Histone deacetylases 1 and 2 control the progression of neural precursors to neurons during brain development. Proceedings of the National Academy of Sciences of the United States of America. 2009;106(19):7876-81. doi: 10.1073/pnas.0902750106. PubMed PMID: 19380719; PubMed Central PMCID: PMCPMC2683090.

87.   Luo RX, Postigo AA, Dean DC. Rb interacts with histone deacetylase to repress transcription. Cell. 1998;92(4):463-73. PubMed PMID: 9491888.

88.   Morrison AJ, Sardet C, Herrera RE. Retinoblastoma protein transcriptional repression through histone deacetylation of a single nucleosome. Molecular and cellular biology. 2002;22(3):856-65. PubMed PMID: 11784861; PubMed Central PMCID: PMC133558.

89.   Robertson KD, Ait-Si-Ali S, Yokochi T, Wade PA, Jones PL, Wolffe AP. DNMT1 forms a complex with Rb, E2F1 and HDAC1 and represses transcription from E2F-responsive promoters. Nature genetics. 2000;25(3):338-42. doi: 10.1038/77124. PubMed PMID: 10888886.

90.   Gurvich N, Tsygankova OM, Meinkoth JL, Klein PS. Histone deacetylase is a target of valproic acid-mediated cellular differentiation. Cancer Res. 2004;64(3):1079-86. PubMed PMID: 14871841.

91.   Johannessen CU. Mechanisms of action of valproate: a commentatory. Neurochemistry international. 2000;37(2-3):103-10. PubMed PMID: 10812195.

92.   Monti B, Polazzi E, Contestabile A. Biochemical, molecular and epigenetic mechanisms of valproic acid neuroprotection. Current molecular pharmacology. 2009;2(1):95-109. PubMed PMID: 20021450.

93.   Meador KJ. Effects of in utero antiepileptic drug exposure. Epilepsy currents / American Epilepsy Society. 2008;8(6):143-7. doi: 10.1111/j.1535-7511.2008.00273.x. PubMed PMID: 19127305; PubMed Central PMCID: PMC2610228.

94.   Tomson T, Battino D. Pregnancy and epilepsy: what should we tell our patients? Journal of neurology. 2009;256(6):856-62. doi: 10.1007/s00415-009-5062-1. PubMed PMID: 19252776.

95.   McCorry D, Bromley R. Does in utero exposure of antiepileptic drugs lead to failure to reach full cognitive potential? Seizure : the journal of the British Epilepsy Association. 2015;28:51-6. doi: 10.1016/j.seizure.2015.01.019. PubMed PMID: 25819874.

96.   Gottlicher M, Minucci S, Zhu P, Kramer OH, Schimpf A, Giavara S, Sleeman JP, Lo Coco F, Nervi C, Pelicci PG, Heinzel T. Valproic acid defines a novel class of HDAC inhibitors inducing differentiation of transformed cells. The EMBO journal. 2001;20(24):6969-78. doi: 10.1093/emboj/20.24.6969. PubMed PMID: 11742974; PubMed Central PMCID: PMC125788.

97.	Hanson JW, Smith DW. The fetal hydantoin syndrome. The Journal of pediatrics. 1975;87(2):285-90. PubMed PMID: 50428.

98.	Robert E, Rosa F. Valproate and birth defects. Lancet. 1983;2(8359):1142. PubMed PMID: 6138672.

99.	DiLiberti JH, Farndon PA, Dennis NR, Curry CJ. The fetal valproate syndrome. American journal of medical genetics. 1984;19(3):473-81. doi: 10.1002/ajmg.1320190308. PubMed PMID: 6439041.

100.	Stadelmaier R, Nasri H, Deutsch CK, Bauman M, Hunt A, Stodgell CJ, Adams J, Holmes LB. Exposure to Sodium Valproate during Pregnancy: Facial Features and Signs of Autism. Birth defects research. 2017. doi: 10.1002/bdr2.1052. PubMed PMID: 28635121.

101.	Adab N, Kini U, Vinten J, Ayres J, Baker G, Clayton-Smith J, Coyle H, Fryer A, Gorry J, Gregg J, Mawer G, Nicolaides P, Pickering L, Tunnicliffe L, Chadwick DW. The longer term outcome of children born to mothers with epilepsy. Journal of neurology, neurosurgery, and psychiatry. 2004;75(11):1575-83. doi: 10.1136/jnnp.2003.029132. PubMed PMID: 15491979; PubMed Central PMCID: PMC1738809.

102.	Bromley RL, Baker GA, Meador KJ. Cognitive abilities and behaviour of children exposed to antiepileptic drugs in utero. Current opinion in neurology. 2009;22(2):162-6. doi: 10.1097/WCO.0b013e3283292401. PubMed PMID: 19532040; PubMed Central PMCID: PMC2743524.

103.	Williams G, King J, Cunningham M, Stephan M, Kerr B, Hersh JH. Fetal valproate syndrome and autism: additional evidence of an association. Developmental medicine and child neurology. 2001;43(3):202-6. PubMed PMID: 11263692.

104.	Moore SJ, Turnpenny P, Quinn A, Glover S, Lloyd DJ, Montgomery T, Dean JC. A clinical study of 57 children with fetal anticonvulsant syndromes. Journal of medical genetics. 2000;37(7):489-97. PubMed PMID: 10882750; PubMed Central PMCID: PMC1734633.

105.	Rasalam AD, Hailey H, Williams JH, Moore SJ, Turnpenny PD, Lloyd DJ, Dean JC. Characteristics of fetal anticonvulsant syndrome associated autistic disorder. Developmental medicine and child neurology. 2005;47(8):551-5. PubMed PMID: 16108456.

106.	Bromley RL, Mawer GE, Briggs M, Cheyne C, Clayton-Smith J, Garcia-Finana M, Kneen R, Lucas SB, Shallcross R, Baker GA, Liverpool, Manchester Neurodevelopment G. The prevalence of neurodevelopmental disorders in children prenatally exposed to antiepileptic drugs. Journal of neurology, neurosurgery, and psychiatry. 2013;84(6):637-43. doi: 10.1136/jnnp-2012-304270. PubMed PMID: 23370617; PubMed Central PMCID: PMC4115188.

107.	Weiss LA, Shen Y, Korn JM, Arking DE, Miller DT, Fossdal R, Saemundsen E, Stefansson H, Ferreira MA, Green T, Platt OS, Ruderfer DM, Walsh CA, Altshuler D, Chakravarti A, Tanzi RE, Stefansson K, Santangelo SL, Gusella JF, Sklar P, Wu BL, Daly MJ, Autism C. Association between microdeletion and microduplication at 16p11.2 and autism. The New England journal of medicine. 2008;358(7):667-75. doi: 10.1056/NEJMoa075974. PubMed PMID: 18184952.

108.   Shinawi M, Liu P, Kang SH, Shen J, Belmont JW, Scott DA, Probst FJ, Craigen WJ, Graham BH, Pursley A, Clark G, Lee J, Proud M, Stocco A, Rodriguez DL, Kozel BA, Sparagana S, Roeder ER, McGrew SG, Kurczynski TW, Allison LJ, Amato S, Savage S, Patel A, Stankiewicz P, Beaudet AL, Cheung SW, Lupski JR. Recurrent reciprocal 16p11.2 rearrangements associated with global developmental delay, behavioural problems, dysmorphism, epilepsy, and abnormal head size. Journal of medical genetics. 2010;47(5):332-41. doi: 10.1136/jmg.2009.073015. PubMed PMID: 19914906; PubMed Central PMCID: PMCPMC3158566.

109.   Golzio C, Willer J, Talkowski ME, Oh EC, Taniguchi Y, Jacquemont S, Reymond A, Sun M, Sawa A, Gusella JF, Kamiya A, Beckmann JS, Katsanis N. KCTD13 is a major driver of mirrored neuroanatomical phenotypes of the 16p11.2 copy number variant. Nature. 2012;485(7398):363-7. doi: 10.1038/nature11091. PubMed PMID: 22596160; PubMed Central PMCID: PMCPMC3366115.

110.   Torres F, Barbosa M, Maciel P. Recurrent copy number variations as risk factors for neurodevelopmental disorders: critical overview and analysis of clinical implications. Journal of medical genetics. 2016;53(2):73-90. doi: 10.1136/jmedgenet-2015-103366. PubMed PMID: 26502893.

111.   Ernst C. Proliferation and Differentiation Deficits are a Major Convergence Point for Neurodevelopmental Disorders. Trends in neurosciences. 2016;39(5):290-9. doi: 10.1016/j.tins.2016.03.001. PubMed PMID: 27032601.

112.   Estes ML, McAllister AK. Maternal immune activation: Implications for neuropsychiatric disorders. Science. 2016;353(6301):772-7. doi: 10.1126/science.aag3194. PubMed PMID: 27540164.

113.   Rodier PM, Ingram JL, Tisdale B, Croog VJ. Linking etiologies in humans and animal models: studies of autism. Reproductive toxicology. 1997;11(2-3):417-22. PubMed PMID: 9100317.

114.   Rodier PM, Ingram JL, Tisdale B, Nelson S, Romano J. Embryological origin for autism: developmental anomalies of the cranial nerve motor nuclei. The Journal of comparative neurology. 1996;370(2):247-61. doi: 10.1002/(SICI)1096-9861(19960624)370:2<247::AID-CNE8>3.0.CO;2-2. PubMed PMID: 8808733.

115.   Nicolini C, Fahnestock M. The valproic acid-induced rodent model of autism. Experimental neurology. 2017. doi: 10.1016/j.expneurol.2017.04.017. PubMed PMID: 28472621.

116.   Wang Z, Xu L, Zhu X, Cui W, Sun Y, Nishijo H, Peng Y, Li R. Demethylation of specific Wnt/beta-catenin pathway genes and its upregulation in rat brain induced by prenatal valproate exposure. Anatomical record. 2010;293(11):1947-53. doi: 10.1002/ar.21232. PubMed PMID: 20734317.

117.   Go HS, Seo JE, Kim KC, Han SM, Kim P, Kang YS, Han SH, Shin CY, Ko KH. Valproic acid inhibits neural progenitor cell death by activation of NF-kappaB signaling pathway and up-regulation of Bcl-XL. Journal of biomedical science. 2011;18(1):48. doi: 10.1186/1423-0127-18-48. PubMed PMID: 21722408; PubMed Central PMCID: PMC3158748.

118.   Go HS, Kim KC, Choi CS, Jeon SJ, Kwon KJ, Han SH, Lee J, Cheong JH, Ryu JH, Kim CH, Ko KH, Shin CY. Prenatal exposure to valproic acid increases the neural progenitor cell pool and induces macrocephaly in rat brain via a mechanism involving the GSK-3beta/beta-catenin pathway. Neuropharmacology. 2012;63(6):1028-41. doi: 10.1016/j.neuropharm.2012.07.028. PubMed PMID: 22841957.

119.   Lee HJ, Dreyfus C, DiCicco-Bloom E. Valproic acid stimulates proliferation of glial precursors during cortical gliogenesis in developing rat. Developmental neurobiology. 2016;76(7):780-98. doi: 10.1002/dneu.22359. PubMed PMID: 26505176.

120.   Mony TJ, Lee JW, Dreyfus C, DiCicco-Bloom E, Lee HJ. Valproic Acid Exposure during Early Postnatal Gliogenesis Leads to Autistic-like Behaviors in Rats. Clin Psychopharmacol Neurosci. 2016;14(4):338-44. doi: 10.9758/cpn.2016.14.4.338. PubMed PMID: 27776385; PubMed Central PMCID: PMCPMC5083944.

121.   Fujimura K, Mitsuhashi T, Shibata S, Shimozato S, Takahashi T. In Utero Exposure to Valproic Acid Induces Neocortical Dysgenesis via Dysregulation of Neural Progenitor Cell Proliferation/Differentiation. The Journal of neuroscience : the official journal of the Society for Neuroscience. 2016;36(42):10908-19. doi: 10.1523/JNEUROSCI.0229-16.2016. PubMed PMID: 27798144.

122.   Jung GA, Yoon JY, Moon BS, Yang DH, Kim HY, Lee SH, Bryja V, Arenas E, Choi KY. Valproic acid induces differentiation and inhibition of proliferation in neural progenitor cells via the beta-catenin-Ras-ERK-p21Cip/WAF1 pathway. BMC cell biology. 2008;9:66. doi: 10.1186/1471-2121-9-66. PubMed PMID: 19068119; PubMed Central PMCID: PMC2639384.

123.   Kataoka S, Takuma K, Hara Y, Maeda Y, Ago Y, Matsuda T. Autism-like behaviours with transient histone hyperacetylation in mice treated prenatally with valproic acid. Int J Neuropsychopharmacol. 2013;16(1):91-103. doi: 10.1017/S1461145711001714. PubMed PMID: 22093185.

124.   Wang L, Liu Y, Li S, Long ZY, Wu YM. Wnt signaling pathway participates in valproic acid-induced neuronal differentiation of neural stem cells. International journal of clinical and experimental pathology. 2015;8(1):578-85. PubMed PMID: 25755748; PubMed Central PMCID: PMC4348902.

125.   Favre MR, Barkat TR, Lamendola D, Khazen G, Markram H, Markram K. General developmental health in the VPA-rat model of autism. Frontiers in behavioral neuroscience. 2013;7:88. doi: 10.3389/fnbeh.2013.00088. PubMed PMID: 23898245; PubMed Central PMCID: PMC3721005.

126.   Fujiki R, Sato A, Fujitani M, Yamashita T. A proapoptotic effect of valproic acid on progenitors of embryonic stem cell-derived glutamatergic neurons. Cell death & disease. 2013;4:e677. doi: 10.1038/cddis.2013.205. PubMed PMID: 23788034; PubMed Central PMCID: PMC3702299.

127.   Kim KC, Lee DK, Go HS, Kim P, Choi CS, Kim JW, Jeon SJ, Song MR, Shin CY. Pax6-dependent cortical glutamatergic neuronal differentiation regulates autism-like behavior in prenatally valproic acid-exposed rat offspring. Molecular neurobiology. 2014;49(1):512-28. doi: 10.1007/s12035-013-8535-2. PubMed PMID: 24030726.

128. Fukuchi M, Nii T, Ishimaru N, Minamino A, Hara D, Takasaki I, Tabuchi A, Tsuda M. Valproic acid induces up- or down-regulation of gene expression responsible for the neuronal excitation and inhibition in rat cortical neurons through its epigenetic actions. Neuroscience research. 2009;65(1):35-43. doi: 10.1016/j.neures.2009.05.002. PubMed PMID: 19463867.

129. Hevner RF, Hodge RD, Daza RA, Englund C. Transcription factors in glutamatergic neurogenesis: conserved programs in neocortex, cerebellum, and adult hippocampus. Neuroscience research. 2006;55(3):223-33. doi: 10.1016/j.neures.2006.03.004. PubMed PMID: 16621079.

130. Marinova Z, Leng Y, Leeds P, Chuang DM. Histone deacetylase inhibition alters histone methylation associated with heat shock protein 70 promoter modifications in astrocytes and neurons. Neuropharmacology. 2011;60(7-8):1109-15. doi: 10.1016/j.neuropharm.2010.09.022. PubMed PMID: 20888352; PubMed Central PMCID: PMC3036778.

131. Marinova Z, Ren M, Wendland JR, Leng Y, Liang MH, Yasuda S, Leeds P, Chuang DM. Valproic acid induces functional heat-shock protein 70 via Class I histone deacetylase inhibition in cortical neurons: a potential role of Sp1 acetylation. Journal of neurochemistry. 2009;111(4):976-87. doi: 10.1111/j.1471-4159.2009.06385.x. PubMed PMID: 19765194; PubMed Central PMCID: PMC2766424.

132. Yasuda S, Liang MH, Marinova Z, Yahyavi A, Chuang DM. The mood stabilizers lithium and valproate selectively activate the promoter IV of brain-derived neurotrophic factor in neurons. Molecular psychiatry. 2009;14(1):51-9. doi: 10.1038/sj.mp.4002099. PubMed PMID: 17925795.

133. Dolmetsch R, Geschwind DH. The human brain in a dish: the promise of iPSC-derived neurons. Cell. 2011;145(6):831-4. doi: 10.1016/j.cell.2011.05.034. PubMed PMID: 21663789; PubMed Central PMCID: PMCPMC3691069.

134. Bilic J, Izpisua Belmonte JC. Concise review: Induced pluripotent stem cells versus embryonic stem cells: close enough or yet too far apart? Stem cells. 2012;30(1):33-41. doi: 10.1002/stem.700. PubMed PMID: 22213481.

135. Pasca SP, Panagiotakos G, Dolmetsch RE. Generating human neurons in vitro and using them to understand neuropsychiatric disease. Annual review of neuroscience. 2014;37:479-501. doi: 10.1146/annurev-neuro-062012-170328. PubMed PMID: 25002278.

136. Marchetto MC, Carromeu C, Acab A, Yu D, Yeo GW, Mu Y, Chen G, Gage FH, Muotri AR. A model for neural development and treatment of Rett syndrome using human induced pluripotent stem cells. Cell. 2010;143(4):527-39. doi: 10.1016/j.cell.2010.10.016. PubMed PMID: 21074045; PubMed Central PMCID: PMC3003590.

137. Sheridan SD, Theriault KM, Reis SA, Zhou F, Madison JM, Daheron L, Loring JF, Haggarty SJ. Epigenetic characterization of the FMR1 gene and aberrant neurodevelopment in human induced pluripotent stem cell models of fragile X syndrome. PloS one. 2011;6(10):e26203. doi: 10.1371/journal.pone.0026203. PubMed PMID: 22022567; PubMed Central PMCID: PMCPMC3192166.

138.   Marchetto MC, Belinson H, Tian Y, Freitas BC, Fu C, Vadodaria KC, Beltrao-Braga PC, Trujillo CA, Mendes AP, Padmanabhan K, Nunez Y, Ou J, Ghosh H, Wright R, Brennand KJ, Pierce K, Eichenfield L, Pramparo T, Eyler LT, Barnes CC, Courchesne E, Geschwind DH, Gage FH, Wynshaw-Boris A, Muotri AR. Altered proliferation and networks in neural cells derived from idiopathic autistic individuals. Molecular psychiatry. 2016. doi: 10.1038/mp.2016.95. PubMed PMID: 27378147.

139.   Pasca SP, Portmann T, Voineagu I, Yazawa M, Shcheglovitov A, Pasca AM, Cord B, Palmer TD, Chikahisa S, Nishino S, Bernstein JA, Hallmayer J, Geschwind DH, Dolmetsch RE. Using iPSC-derived neurons to uncover cellular phenotypes associated with Timothy syndrome. Nat Med. 2011;17(12):1657-62. doi: 10.1038/nm.2576. PubMed PMID: 22120178; PubMed Central PMCID: PMC3517299.

140.   Chen HM, DeLong CJ, Bame M, Rajapakse I, Herron TJ, McInnis MG, O'Shea KS. Transcripts involved in calcium signaling and telencephalic neuronal fate are altered in induced pluripotent stem cells from bipolar disorder patients. Translational psychiatry. 2014;4:e375. doi: 10.1038/tp.2014.12.

141.   Stern S, Santos R, Marchetto MC, Mendes AP, Rouleau GA, Biesmans S, Wang QW, Yao J, Charnay P, Bang AG, Alda M, Gage FH. Neurons derived from patients with bipolar disorder divide into intrinsically different sub-populations of neurons, predicting the patients' responsiveness to lithium. Molecular psychiatry. 2017. doi: 10.1038/mp.2016.260. PubMed PMID: 28242870.

142.   Brennand K, Savas JN, Kim Y, Tran N, Simone A, Hashimoto-Torii K, Beaumont KG, Kim HJ, Topol A, Ladran I, Abdelrahim M, Matikainen-Ankney B, Chao SH, Mrksich M, Rakic P, Fang G, Zhang B, Yates JR, 3rd, Gage FH. Phenotypic differences in hiPSC NPCs derived from patients with schizophrenia. Molecular psychiatry. 2015;20(3):361-8. doi: 10.1038/mp.2014.22. PubMed PMID: 24686136; PubMed Central PMCID: PMC4182344.

143.   Topol A, Zhu S, Tran N, Simone A, Fang G, Brennand KJ. Altered WNT Signaling in Human Induced Pluripotent Stem Cell Neural Progenitor Cells Derived from Four Schizophrenia Patients. Biological psychiatry. 2015;78(6):e29-34. doi: 10.1016/j.biopsych.2014.12.028. PubMed PMID: 25708228; PubMed Central PMCID: PMCPMC4520784.

144.   Handel AE, Chintawar S, Lalic T, Whiteley E, Vowles J, Giustacchini A, Argoud K, Sopp P, Nakanishi M, Bowden R, Cowley S, Newey S, Akerman C, Ponting CP, Cader MZ. Assessing similarity to primary tissue and cortical layer identity in induced pluripotent stem cell-derived cortical neurons through single-cell transcriptomics. Human molecular genetics. 2016;25(5):989-1000. doi: 10.1093/hmg/ddv637. PubMed PMID: 26740550; PubMed Central PMCID: PMCPMC4754051.

145.   Camp JG, Badsha F, Florio M, Kanton S, Gerber T, Wilsch-Brauninger M, Lewitus E, Sykes A, Hevers W, Lancaster M, Knoblich JA, Lachmann R, Paabo S, Huttner WB, Treutlein B. Human cerebral organoids recapitulate gene expression programs of fetal neocortex development. Proceedings of the National Academy of Sciences of the United States of America.

2015;112(51):15672-7. doi: 10.1073/pnas.1520760112. PubMed PMID: 26644564; PubMed Central PMCID: PMCPMC4697386.

146. Lu N, DiCicco-Bloom E. Pituitary adenylate cyclase-activating polypeptide is an autocrine inhibitor of mitosis in cultured cortical precursor cells. Proceedings of the National Academy of Sciences of the United States of America. 1997;94(7):3357-62. PubMed PMID: 9096398; PubMed Central PMCID: PMC20374.

147. Mairet-Coello G, Tury A, DiCicco-Bloom E. Insulin-like growth factor-1 promotes G(1)/S cell cycle progression through bidirectional regulation of cyclins and cyclin-dependent kinase inhibitors via the phosphatidylinositol 3-kinase/Akt pathway in developing rat cerebral cortex. The Journal of neuroscience : the official journal of the Society for Neuroscience. 2009;29(3):775-88. doi: 10.1523/JNEUROSCI.1700-08.2009. PubMed PMID: 19158303; PubMed Central PMCID: PMC3256126.

148. Burke K, Cheng Y, Li B, Petrov A, Joshi P, Berman RF, Reuhl KR, DiCicco-Bloom E. Methylmercury elicits rapid inhibition of cell proliferation in the developing brain and decreases cell cycle regulator, cyclin E. Neurotoxicology. 2006;27(6):970-81. doi: 10.1016/j.neuro.2006.09.001. PubMed PMID: 17056119; PubMed Central PMCID: PMC2013736.

149. Yan Y, Zhou X, Pan Z, Ma J, Waschek JA, DiCicco-Bloom E. Pro- and anti-mitogenic actions of pituitary adenylate cyclase-activating polypeptide in developing cerebral cortex: potential mediation by developmental switch of PAC1 receptor mRNA isoforms. The Journal of neuroscience : the official journal of the Society for Neuroscience. 2013;33(9):3865-78. doi: 10.1523/JNEUROSCI.1062-12.2013. PubMed PMID: 23447598; PubMed Central PMCID: PMC3652328.

150. DiCicco-Bloom E, Friedman WJ, Black IB. NT-3 stimulates sympathetic neuroblast proliferation by promoting precursor survival. Neuron. 1993;11(6):1101-11. PubMed PMID: 7903858.

151. Li B, DiCicco-Bloom E. Basic fibroblast growth factor exhibits dual and rapid regulation of cyclin D1 and p27 to stimulate proliferation of rat cerebral cortical precursors. Developmental neuroscience. 2004;26(2-4):197-207. doi: 10.1159/000082137. PubMed PMID: 15711060.

152. Carey RG, Li B, DiCicco-Bloom E. Pituitary adenylate cyclase activating polypeptide anti-mitogenic signaling in cerebral cortical progenitors is regulated by p57Kip2-dependent CDK2 activity. The Journal of neuroscience : the official journal of the Society for Neuroscience. 2002;22(5):1583-91. PubMed PMID: 11880488.

153. Mairet-Coello G, Tury A, Van Buskirk E, Robinson K, Genestine M, DiCicco-Bloom E. p57(KIP2) regulates radial glia and intermediate precursor cell cycle dynamics and lower layer neurogenesis in developing cerebral cortex. Development. 2012;139(3):475-87. doi: 10.1242/dev.067314. PubMed PMID: 22223678; PubMed Central PMCID: PMC3252351.

154. Tao Y, Black IB, DiCicco-Bloom E. Neurogenesis in neonatal rat brain is regulated by peripheral injection of basic fibroblast growth factor (bFGF). The Journal of comparative neurology. 1996;376(4):653-63. doi: 10.1002/(SICI)1096-

9861(19961223)376:4<653::AID-CNE11>3.0.CO;2-N. PubMed PMID: 8978476.

155.   Wagner GC, Reuhl KR, Cheh M, McRae P, Halladay AK. A new neurobehavioral model of autism in mice: pre- and postnatal exposure to sodium valproate. Journal of autism and developmental disorders. 2006;36(6):779-93. doi: 10.1007/s10803-006-0117-y. PubMed PMID: 16609825.

156.   Maity A, McKenna WG, Muschel RJ. Cyclin A message stability varies with the cell cycle. Cell growth & differentiation : the molecular biology journal of the American Association for Cancer Research. 1997;8(3):311-8. PubMed PMID: 9056673.

157.   Manuel M, Price DJ. Role of Pax6 in forebrain regionalization. Brain Res Bull. 2005;66(4-6):387-93. doi: 10.1016/j.brainresbull.2005.02.006. PubMed PMID: 16144620.

158.   Manuel M, Georgala PA, Carr CB, Chanas S, Kleinjan DA, Martynoga B, Mason JO, Molinek M, Pinson J, Pratt T, Quinn JC, Simpson TI, Tyas DA, van Heyningen V, West JD, Price DJ. Controlled overexpression of Pax6 in vivo negatively autoregulates the Pax6 locus, causing cell-autonomous defects of late cortical progenitor proliferation with little effect on cortical arealization. Development. 2007;134(3):545-55. doi: 10.1242/dev.02764. PubMed PMID: 17202185; PubMed Central PMCID: PMCPMC2386558.

159.   Talamillo A, Quinn JC, Collinson JM, Caric D, Price DJ, West JD, Hill RE. Pax6 regulates regional development and neuronal migration in the cerebral cortex. Developmental biology. 2003;255(1):151-63. PubMed PMID: 12618140.

160.   Elsen GE, Hodge RD, Bedogni F, Daza RA, Nelson BR, Shiba N, Reiner SL, Hevner RF. The protomap is propagated to cortical plate neurons through an Eomes-dependent intermediate map. Proceedings of the National Academy of Sciences of the United States of America. 2013;110(10):4081-6. doi: 10.1073/pnas.1209076110. PubMed PMID: 23431145; PubMed Central PMCID: PMCPMC3593833.

161.   Arnold SJ, Huang GJ, Cheung AF, Era T, Nishikawa S, Bikoff EK, Molnar Z, Robertson EJ, Groszer M. The T-box transcription factor Eomes/Tbr2 regulates neurogenesis in the cortical subventricular zone. Genes Dev. 2008;22(18):2479-84. doi: 10.1101/gad.475408. PubMed PMID: 18794345; PubMed Central PMCID: PMCPMC2546697.

162.   Steinman KJ, Spence SJ, Ramocki MB, Proud MB, Kessler SK, Marco EJ, Green Snyder L, D'Angelo D, Chen Q, Chung WK, Sherr EH, Simons VIPC. 16p11.2 deletion and duplication: Characterizing neurologic phenotypes in a large clinically ascertained cohort. American journal of medical genetics Part A. 2016;170(11):2943-55. doi: 10.1002/ajmg.a.37820. PubMed PMID: 27410714.

163.   Marchetto MC, Belinson H, Tian Y, Freitas BC, Fu C, Vadodaria K, Beltrao-Braga P, Trujillo CA, Mendes APD, Padmanabhan K, Nunez Y, Ou J, Ghosh H, Wright R, Brennand K, Pierce K, Eichenfield L, Pramparo T, Eyler L, Barnes CC, Courchesne E, Geschwind DH, Gage FH, Wynshaw-Boris A, Muotri AR. Altered proliferation and networks in neural cells derived from idiopathic autistic individuals. Molecular psychiatry. 2017;22(6):820-35. doi:

10.1038/mp.2016.95. PubMed PMID: 27378147; PubMed Central PMCID: PMCPMC5215991.

164.   Mariani J, Coppola G, Zhang P, Abyzov A, Provini L, Tomasini L, Amenduni M, Szekely A, Palejev D, Wilson M, Gerstein M, Grigorenko EL, Chawarska K, Pelphrey KA, Howe JR, Vaccarino FM. FOXG1-Dependent Dysregulation of GABA/Glutamate Neuron Differentiation in Autism Spectrum Disorders. Cell. 2015;162(2):375-90. doi: 10.1016/j.cell.2015.06.034. PubMed PMID: 26186191; PubMed Central PMCID: PMCPMC4519016.

165.   Nakayama KI, Hatakeyama S, Nakayama K. Regulation of the cell cycle at the G1-S transition by proteolysis of cyclin E and p27Kip1. Biochemical and biophysical research communications. 2001;282(4):853-60. doi: 10.1006/bbrc.2001.4627. PubMed PMID: 11352628.

166.   Stacey DW. Cyclin D1 serves as a cell cycle regulatory switch in actively proliferating cells. Curr Opin Cell Biol. 2003;15(2):158-63. PubMed PMID: 12648671.

167.   Kim S, Kang JK, Kim YK, Seo DW, Ahn SH, Lee JC, Lee CH, You JS, Cho EJ, Lee HW, Han JW. Histone deacetylase inhibitor apicidin induces cyclin E expression through Sp1 sites. Biochemical and biophysical research communications. 2006;342(4):1168-73. doi: 10.1016/j.bbrc.2006.02.081. PubMed PMID: 16516150.

168.   Ocker M, Schneider-Stock R. Histone deacetylase inhibitors: signalling towards p21cip1/waf1. Int J Biochem Cell Biol. 2007;39(7-8):1367-74. doi: 10.1016/j.biocel.2007.03.001. PubMed PMID: 17412634.

169.   Hnilicova J, Hozeifi S, Duskova E, Icha J, Tomankova T, Stanek D. Histone deacetylase activity modulates alternative splicing. PloS one. 2011;6(2):e16727. doi: 10.1371/journal.pone.0016727. PubMed PMID: 21311748; PubMed Central PMCID: PMCPMC3032741.

170.   Yu IT, Park JY, Kim SH, Lee JS, Kim YS, Son H. Valproic acid promotes neuronal differentiation by induction of proneural factors in association with H4 acetylation. Neuropharmacology. 2009;56(2):473-80. doi: 10.1016/j.neuropharm.2008.09.019. PubMed PMID: 19007798.

171.   Zhang HS, Gavin M, Dahiya A, Postigo AA, Ma D, Luo RX, Harbour JW, Dean DC. Exit from G1 and S phase of the cell cycle is regulated by repressor complexes containing HDAC-Rb-hSWI/SNF and Rb-hSWI/SNF. Cell. 2000;101(1):79-89. doi: 10.1016/S0092-8674(00)80625-X. PubMed PMID: 10778858.

172.   Telles E, Seto E. Modulation of cell cycle regulators by HDACs. Frontiers in bioscience. 2012;4:831-9. PubMed PMID: 22202094; PubMed Central PMCID: PMC3990255.

173.   Zhang Z, Convertini P, Shen M, Xu X, Lemoine F, de la Grange P, Andres DA, Stamm S. Valproic acid causes proteasomal degradation of DICER and influences miRNA expression. PloS one. 2013;8(12):e82895. doi: 10.1371/journal.pone.0082895. PubMed PMID: 24358235; PubMed Central PMCID: PMC3866160.

174.   Poddar S, Kesharwani D, Datta M. Histone deacetylase inhibition regulates miR-449a levels in skeletal muscle cells. Epigenetics : official journal of

the DNA Methylation Society. 2016;11(8):579-87. doi: 10.1080/15592294.2016.1188247. PubMed PMID: 27184529; PubMed Central PMCID: PMCPMC4990227.

175. Hara Y, Ago Y, Takano E, Hasebe S, Nakazawa T, Hashimoto H, Matsuda T, Takuma K. Prenatal exposure to valproic acid increases miR-132 levels in the mouse embryonic brain. Molecular autism. 2017;8:33. doi: 10.1186/s13229-017-0149-5. PubMed PMID: 28670439; PubMed Central PMCID: PMCPMC5490164.

176. Olde Loohuis NF, Kole K, Glennon JC, Karel P, Van der Borg G, Van Gemert Y, Van den Bosch D, Meinhardt J, Kos A, Shahabipour F, Tiesinga P, van Bokhoven H, Martens GJ, Kaplan BB, Homberg JR, Aschrafi A. Elevated microRNA-181c and microRNA-30d levels in the enlarged amygdala of the valproic acid rat model of autism. Neurobiology of disease. 2015;80:42-53. doi: 10.1016/j.nbd.2015.05.006. PubMed PMID: 25986729.

177. Hui W, Yuntao L, Lun L, WenSheng L, ChaoFeng L, HaiYong H, Yueyang B. MicroRNA-195 inhibits the proliferation of human glioma cells by directly targeting cyclin D1 and cyclin E1. PloS one. 2013;8(1):e54932. doi: 10.1371/journal.pone.0054932. PubMed PMID: 23383003; PubMed Central PMCID: PMCPMC3557299.

178. Campbell DJ, Chang J, Chawarska K. Early generalized overgrowth in autism spectrum disorder: prevalence rates, gender effects, and clinical outcomes. Journal of the American Academy of Child and Adolescent Psychiatry. 2014;53(10):1063-73 e5. doi: 10.1016/j.jaac.2014.07.008. PubMed PMID: 25245350; PubMed Central PMCID: PMCPMC4173120.

179. Samuels IS, Karlo JC, Faruzzi AN, Pickering K, Herrup K, Sweatt JD, Saitta SC, Landreth GE. Deletion of ERK2 mitogen-activated protein kinase identifies its key roles in cortical neurogenesis and cognitive function. The Journal of neuroscience : the official journal of the Society for Neuroscience. 2008;28(27):6983-95. doi: 10.1523/JNEUROSCI.0679-08.2008. PubMed PMID: 18596172; PubMed Central PMCID: PMCPMC4364995.

180. Roux PP, Shahbazian D, Vu H, Holz MK, Cohen MS, Taunton J, Sonenberg N, Blenis J. RAS/ERK signaling promotes site-specific ribosomal protein S6 phosphorylation via RSK and stimulates cap-dependent translation. The Journal of biological chemistry. 2007;282(19):14056-64. doi: 10.1074/jbc.M700906200. PubMed PMID: 17360704; PubMed Central PMCID: PMCPMC3618456.

181. Carriere A, Romeo Y, Acosta-Jaquez HA, Moreau J, Bonneil E, Thibault P, Fingar DC, Roux PP. ERK1/2 phosphorylate Raptor to promote Ras-dependent activation of mTOR complex 1 (mTORC1). The Journal of biological chemistry. 2011;286(1):567-77. doi: 10.1074/jbc.M110.159046. PubMed PMID: 21071439; PubMed Central PMCID: PMCPMC3013016.

182. Aronica E, Boer K, Baybis M, Yu J, Crino P. Co-expression of cyclin D1 and phosphorylated ribosomal S6 proteins in hemimegalencephaly. Acta neuropathologica. 2007;114(3):287-93. doi: 10.1007/s00401-007-0225-6. PubMed PMID: 17483958.

183.   Bikkavilli RK, Malbon CC. Mitogen-activated protein kinases and Wnt/beta-catenin signaling: Molecular conversations among signaling pathways. Commun Integr Biol. 2009;2(1):46-9. PubMed PMID: 19513264; PubMed Central PMCID: PMCPMC2649302.

184.   Arai Y, Pulvers JN, Haffner C, Schilling B, Nusslein I, Calegari F, Huttner WB. Neural stem and progenitor cells shorten S-phase on commitment to neuron production. Nature communications. 2011;2:154. doi: 10.1038/ncomms1155. PubMed PMID: 21224845; PubMed Central PMCID: PMC3105305.

185.   Paxinos, G., et al., Atlas of the Developing Rat Nervous System Second Edition. Academic Press 1994.

186.   Williams M, Prem S, Zhou X, Matteson P, Yeung L, Lu C.W., Pang Z, Flax J.F., Brzustowicz L, Millonig J.H, DiCicco-Bloom E. Rapid detection of neurodevelopmental phenotypes in human neural precursor cells (NPCs). Journal of Visualized Experiments (JOVE). Accepted with Revisions